Radboud Repository

Radboud University Nijmegen

PDF hosted at the Radboud Repository of the Radboud University Nijmegen

The following full text is a publisher's version.

For additional information about this publication click this link.
http://hdl.handle.net/2066/106936

Please be advised that this information was generated on 2017-12-06 and may be subject to change.

The 3-methylglutaconic acidurias - revisited

Saskia B. Wortmann

The 3–methylglutaconic acidurias - revisited

Saskia B. Wortmann

Colofon

The 3–methylglutaconic acidurias – revisited
Thesis Radboud University Nijmegen with a summary in Dutch

© 2013, S.B. Wortmann, Nijmegen, The Netherlands.

The research presented in this thesis was supported by the Sengers stipendium 2007 to S.B. Wortmann and the Dutch Brain foundation (grant 2011(1)-101 to E. Morava). Printing of the thesis was financially supported by the Radboud University Nijmegen Medical Centre.

ISBN: 978-94-6191-660-0

Cover foto (taken in Bhaktapur, Nepal, April 2010), cover design and layout by S.B.Wortmann.
Printed by Ipskamp Drukkers, Nijmegen.

The 3–methylglutaconic acidurias revisited

Proefschrift

ter verkrijging van de graad van doctor
aan de Radboud Universiteit Nijmegen
op gezag van de rector magnificus prof. mr. S.C.J.J. Kortmann,
volgens besluit van het college van decanen
in het openbaar te verdedigen op woensdag 03 april 2013
om 15.30 uur precies

door

Saskia Brigitte Wortmann

geboren op 28 februari 1978
te Hamm-Heessen, Duitsland

Promotoren
Prof. dr. R.A. Wevers
Prof. dr. E. Morava
Prof. dr. J.A.M. Smeitink

Co-promotor
Dr. R.J.T. Rodenburg

Manuscriptcommissie
Prof. dr. H.G. Brunner (voorzitter)
Prof. dr. M. A.A.P. Willemsen
Prof. dr. R.J. Wanders (Universiteit van Amsterdam)

Meinen Eltern

Contents

General introduction and outline of the thesis

Metabolic disorders can present with virtually any clinical symptom. Combining the biochemical and clinical findings, and recognizing a distinctive disease pattern is a powerful approach to solve the genetic background.

In the urine of healthy individuals the branched chain organic acid 3–methylglutaconic acid (3–MGA) is found only in trace amounts. Elevated urinary excretion of 3–MGA (3–MGA–uria) is a powerful diagnostic clue for several rare, but highly characteristic, neurometabolic syndromes like Barth syndrome (3–MGA–uria, cardiomyopathy, neutropenia; MIM #302060) or Costeff syndrome (3–MGA–uria, optic atrophy, ataxia, MIM #258501). On the other hand 3–MGA–uria is seen in a rapidly growing heterogeneous group of patients, mostly with progressive neurological signs and symptoms, designated type IV 3–MGA–uria.

The pathomechanism leading to 3–MGA–uria is poorly understood. Only in the rare case of 3–methylglutaconyl–CoA-hydratase deficiency (MIM #250950) 3–MGA is known to originate from leucine catabolism. In all other conditions the origin of 3–MGA is completely unknown but seems to be related to mitochondrial dysfunction.

This thesis describes the results of a thorough (re)-investigation of the 3–MGA–urias, the known, the unknown and the unknowable.

Chapter 1 presents the current knowledge on the different 3–MGA syndromes. The clinical and biochemical findings in patients with the known 3–MGA syndromes are reviewed. **Chapter 2** focuses on 3–methylglutaconyl–CoA-hydratase deficiency, which was thought to be a childhood onset disorder with non-specific symptoms or even a non-disease. We re-define 3–methylglutaconyl–CoA-hydratase deficiency as a clinically and radiologically highly characteristic syndrome with adult-onset of symptoms. From **Chapter 3** onwards we have a closer look on the rapidly expanding group of 3–MGA–uria type IV patients (MIM 250951). Chapter 3 presents a successful diagnostic strategy for the patient with 3–MGA–uria type IV based on the biochemical and clinical findings, which can spare children the invasive procedure of a muscle biopsy. **Chapter 4** shows that facial dysmorphic features may accompany these findings and may be helpful in diagnostics. **Chapter 5** describes the clinical, biochemical and radiological phenotype of a new and highly characteristic 3–MGA syndrome, the MEGDEL syndrome (MIM #614739). These patient present with mitochondrial dysfunction, dystonia, deafness and Leigh syndrome on MRI. In **Chapter 6** we elucidate the genetic background and its functional consequences. The gene involved is *SERAC1,* a gene of formerly unknown function, encoding a phospholipid remodeler at the crossroads of mitochondrial function and intracellular cholesterol trafficking. In **Chapter 7** we analyse nearly 400 patients with 3–MGA–uria referred to our centre, thereby showing in which disorders 3–MGA–uria can be found. Interestingly it did not only occur in patients with mitochondrial disorders but also in several other metabolic and non-metabolic disorders that had not been associated with 3–MGA–uria before. Additionally, this paper shows that 3–MGA–uria is a marker not only for mitochondrial dysfunction in general, but for specific mitochondrial disorders. Our findings on the

3-MGA-urias finally lead to a proper, pathomechanism based, classification of this group of disorders, which is presented in **Chapter 8.**

Chapter 1

The 3–methylglutaconic acidurias: what's new?

S. Wortmann[1], L. Kluijtmans[2], U. Engelke[2], R. Wevers[2], E. Morava[1]

[1]Nijmegen Centre for Mitochondrial Disorders at the Department of Pediatrics and the Institute of Genetic and Metabolic Disease (IGMD), [2]Department of Laboratory Medicine, Radboud University Nijmegen Medical Center, Radboud University Nijmegen Medical Centre, Nijmegen, The Netherlands.

J Inherit Metab Dis. 2012;35(1):13-22.

Abstract

The heterogeneous group of 3–methylglutaconic aciduria syndromes includes several inborn errors of metabolism biochemically characterized by increased urinary excretion of 3–methylglutaconic acid. Five distinct types have been recognized: 3–methylglutaconic aciduria type I is an inborn error of leucine catabolism; the additional four types all affect mitochondrial function through different pathomechanisms. We provide an overview of the expanding clinical spectrum of the 3–methylglutaconic aciduria types and provide the newest insights into the underlying pathomechanisms. A diagnostic approach to the patient with 3–methylglutaconic aciduria is presented, and we search for the connection between urinary 3–methylglutaconic acid excretion and mitochondrial dysfunction.

Branched-chain organic acid 3-methylglutaconic acid: the biochemical basis

The branched-chain organic acid 3-methylglutaconic acid (3-MGA) is an intermediate of the mitochondrial leucine catabolism. Figure 1 shows the metabolic pathway of leucine; 3-MGA, 3-methylglutaric acid (3-MG), and 3-hydroxyisovaleric acid (3-HIVA) accumulate when the conversion of 3-methylglutaconyl-coenzyme A (CoA) to 3-hydroxy-3-methyl-glutary-CoA (HMG-CoA) by the enzyme 3-methylglutaconyl-CoA hydratase (3-MGH, EC 4.2.1.18) is disturbed. This is the underlying cause in 3-MGA-uria type I. As we show in detail upon describing the different subtypes of 3-MGA-uria, there is no evidence that the 3-MGA-uria types II–V are caused by a disturbed leucine catabolism. Notably, subtypes II–V affect mitochondrial function through different pathomechanisms. But how can mitochondrial dysfunction lead to elevated urinary excretion of 3-MGA?

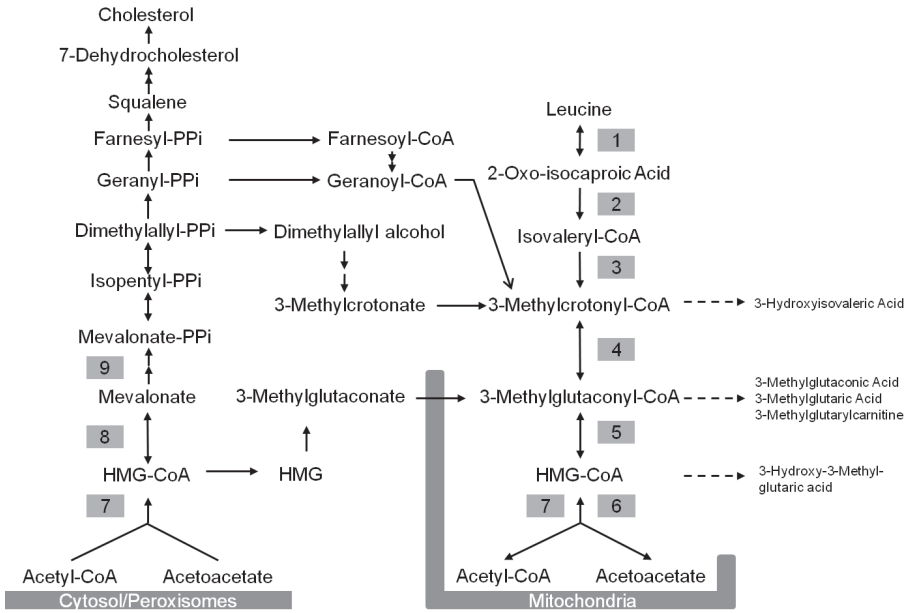

***Figure 1**. Leucine catabolism and possible shunts to cholesterol biosynthesis. 1 = Transaminase, 2 = branched-chain 2-oxo-acid dehydrogenase, 3 = isovaleryl-CoA dehydrogenase, 4 = 3-methylcrotonyl-CoA carboxylase, 5 = 3-methylglutaconyl-CoA-hydratase, 6 = 3-hydroxy-3-methylglutaryl-coenzyme A (HMG-CoA) lyase, 7 = HMG-CoA synthase, 8 = HMG-CoA-reductase. PPi pyrophosphate.*

In the urine of healthy individuals, 3-MGA is found only in traces (< 20 mmol/mol creatinine). In patients with 3-MGA-uria, concentrations can (intermittently) rise above 1000 mmol/mol creatinine. The urinary excretion of 3-MGA is generally higher in type I than in the other types[1-4]. Patients with 3- MGA-uria type I excrete even higher amounts of

urinary 3–MGA after a leucine-rich, or in general, a protein-rich meal[5, 6]. This is not the case in patients with the other types of 3–MGA–uria, which emphasizes that the excreted 3–MGA does not originate from leucine degradation (Barth syndrome[7, 8]; type IV[9]; Wortmann et al. unpublished data). Interestingly, in these patients, the excretion can be highly variable or intermittently absent, even within 24 h, seemingly unrelated to the clinical course or severity of the metabolic derangement[1, 3, 8, 10, 11].

Patients with 3–MGA–uria type II (Barth syndrome) have both increased 3–MGA and low cholesterol levels. Therefore, it was speculated that some of the idiopathic syndromes with 3–MGA–uria may be caused by defects of sterol or isoprenoid metabolism causing overflow of mevalonate carbon through the so-called mevalonate shunt (Figure 1[7, 12]). In this shunt, dimethylallyl pyrophosphate is dephosphorylated in two steps to the free alcohol, oxidized to 3-methylcrotonic acid, and then activated with CoA to form 3–methylcrotonyl–CoA, the precursor of 3–MGA-CoA in the regular leucine catabolic pathway[13]. Other links between the two pathways at the level of higher-order isoprenoids, such as geraniol and farnesol, have been described (Figure 1[13, 14]). Also, a direct shunt between mevalonate and 3–methylglutaconyl–CoA was hypothesized (Figure 1[13]). This is the only "mevalonate shunt" per se[15]. It seems that the shunt is more active in tissue of ectodermal origin (e.g., skin, placental tissue) than in tissue of mesodermal origin[13]. Physiologic evidence that the mevalonate shunt or a related shunt is significant in humans, at least in renal tissue, has been provided[16]. More data are available for rats, in which the liver is the main organ of mevalonate shunting[17]. Investigations in 35 patients with Smith-Lemli-Opitz syndrome (SLO, MIM 27400) showed a weak inverse correlation between low plasma cholesterol, its elevated precursor 7- dehydrocholesterol, and elevated plasma 3–MGA[12]. SLO patients with very low plasma cholesterol (< 200 µg/ml; seven of 35 patients) generally had plasma 3–MGA levels above the + 2 standard deviation (SD) range for age (five of seven patients; range 400– 5,000 nmol/l). The rise in cholesterol precursors (isoprenoids), which cannot be metabolized to cholesterol in patients with SLO, leads to overflow via the mevalonate shunt and a consequential increase in 3–MGA (Figure 1). The authors also hypothesized another mechanism. Low plasma cholesterol can induce HMG–CoA synthase, leading to increased HMG–CoA levels and an increased flux through the cholesterol biosynthesis pathway[18] . The HMG–CoA is then dehydrated to 3–MGA through 3–MGH (Figure 1[12]). The urine of some patients also contained high amounts of 3–MGA but no increased 3–HIVA levels, which is characteristic for 3–MGA–uria type I, suggesting that the 3–MGA does not originate from leucine catabolism. Still, the described shunt does not explain how mitochondrial dysfunction relates to excessive 3–MGA excretion. Several enzymes involved in leucine degradation as well as sterol biosynthesis are nicotinamide adenine dinucleotide phosphate (NADP)- NADP, reduced (NADPH) dependent. One could hypothesize that oxidative phosphorylation system (OXPHOS) dysfunction influences NADP-NADPH-dependent enzymes, such as the 3–MGA-hydratase by a disturbed NADP/NADPH ratio. However, excretion seems unrelated to clinical severity

or disease course. At the moment, 3- MGA is a biochemical marker for mitochondrial dysfunction of still unknown origin.

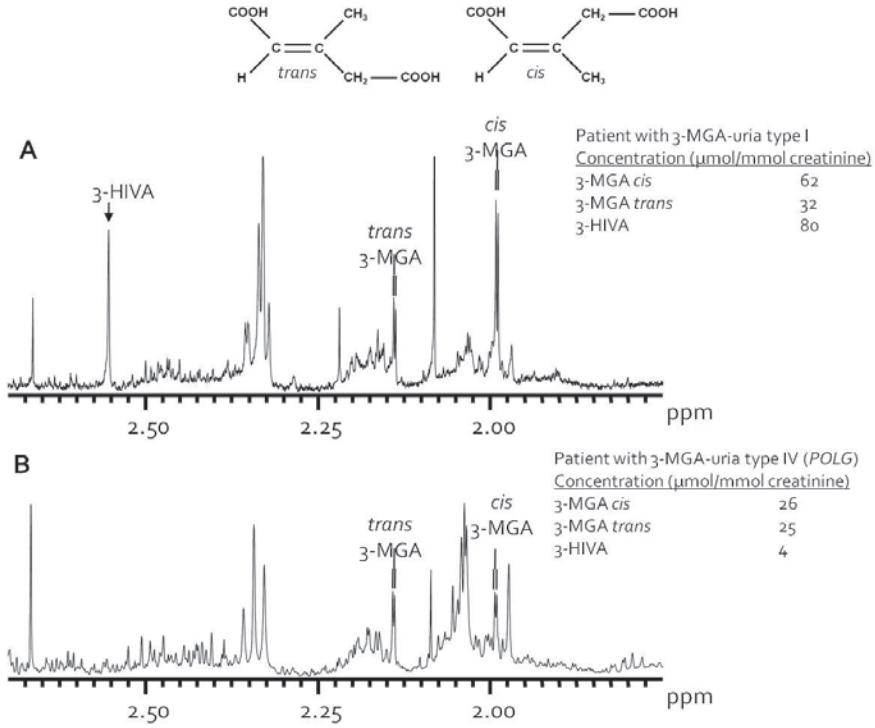

Figure 2. *[1H]-nuclear magnetic resonance (NMR) spectra of patients with 3–methylglutaconic aciduria (3–MGA–uria) types I and IV. One-dimensional [1H]- NMR spectra (500 MHz) of urine measured at pH 2.5. The region between 2.2. and 1.9 ppm is shown. A) 2:1 cis:trans ratio in the urine of a patient with 3- MGA-uria type I. B) 1:1 cis:trans ratio in the urine of a patient with 3–MGA–uria type IV.*

Measuring 3–MGA by gas chromatography/mass spectrometry (GC–MS) and one-dimensional [1H]-NMR spectroscopy

As part of the routine metabolic screening in our lab, urinary organic acid analysis is performed by gas chromatography/ mass spectrometry (GC–MS) after extraction of the urine sample with ethyl acetate and derivatization with N,N-bis(trimethylsilyl)trifluoroacetamide containing 1% trimethylchlorosilane. The concentration of 3–MGA is quantified by comparing the signals obtained with calibration curves of the pure compound, using a CP-Sil 8 CB column (Varian, Middelburg, The Netherlands) on a high performance (HP) 6890 Gas Chromatograph (Agilent, Amstelveen, The Netherlands). For research purposes, we additionally perform one-dimensional [1H]-nuclear magnetic resonance (NMR) spectroscopy of different body fluids (Figure 2[19]). Body fluid samples are measured at 500 MHz on a Bruker DRX 500 spectrometer with a triple-resonance inverse (TXI) 1H {15N, 13C}

probe head equipped with X,Y,Z gradient coils. 1H spectra are acquired as 128 transients in 32-K data points with a spectral width of 6,002 Hz. The water (H2O) resonance is presaturated by single-frequency irradiation during a relaxation delay of 10 s; a pulse width of 7 µs is used (corresponding to a 90° excitation pulse).

3–MGA–uria type I (MIM 250950)

For a long time, 3–MGA–uria type I was thought to be a classic organic aciduria. It is a rare autosomal recessive disorder of leucine catabolism characterized by markedly increased urinary excretion of 3–MGA and mildly elevated urinary 3–MG and 3–HIVA. The underlying cause of 3- MGA-uria type I is deficiency of 3–MGH, the enzyme that catalyzes the fifth step of leucine catabolism, the conversion of 3–methylglutaconyl–CoA to HMG–CoA (Figure 1). Murine 3–MGH is highly expressed in kidney, skeletal muscle, heart, and brain and was shown to be located in the mitochondria[20]. The activity of 3–MGH can be determined in fibroblasts or lymphocytes by use of an overall enzyme assay measuring three steps of leucine degradation, from 3–methylcrotonyl–CoA to acetoacetate[21, 22]. 3–MGH is encoded by the *AUH* gene, which was mapped to chromosome 9 and encompasses ten exons encoding for a protein with 339 amino acids[22, 23]. The ratio of *cis* and *trans* isoforms of 3–MGA in urine of 3–MGA–uria type I patients is 2:1, whereas in cerebrospinal fluid (CSF), only the *cis* isoform is detectable[19]. In the other 3–MGA–uria types, the urinary *cis:trans* ratio is approximately 1:1 (Figure 2; repetitive measurements in patients with 3–MGA–uria type I (n=5), II (n=5), III (n=6), and IV (n>80)[11]).

It is known that 3–methylcrotonyl–CoA carboxylase specifically forms the *trans* form of 3–methylglutaconyl–CoA[24]. The metabolic origin of *cis*–3–methylglutaconyl–CoA remains as yet unknown. Spontaneous *cis/trans* interconversion may play a role. A brainspecific isoform of 3–MGH or an enzyme converting the *trans* form into the *cis* form, thus taking care of local production of the *cis* form in the brain, may be an explanation[19].

3–MGA–uria was thought to present in childhood with nonspecific symptoms such as mental retardation or seizures. It was even speculated to be a nondisease[25]. Recently, we reported that it is, in fact, a slowly progressive leukoencephalopathy clinically presenting in adulthood[26]. Function abolishing mutations were reported in seven children with various nonspecific symptoms, such as mental retardation, seizures, hepatopathy[22, 23, 27, 28]. Recently, our group reported the biochemical details of the first patient with an adult onset of the disease, a Dutch woman[19, 26]. She presented with a progressive bilateral visual decline and optic atrophy at the age of 35 years. Over the following 16 years, dysarthria and mild limb ataxia with severe gait ataxia were observed. One additional late-presenting patient was reported with dementia and spasticity by a Japanese group[29]. Both had a slowly progressive leukoencephalopathy. The same clinical signs and symptoms and disease course was observed in a third adult patient who came to our attention[26]. This British man first presented at the age of 30 years with mild cerebellar ataxia and slowly worsened over 29 years, showing spastic paraparesis, nystagmus, and dementia. Magnetic resonance imaging (MRI) of our adult patients showed extensive and diffusively distributed

white-matter lesions restricted to the supratentorial region not affecting the cerebellum or the corpus callosum (for MRI/MR spectrometry (MRS), see[19]).
The Japanese patient also showed cerebellar involvement[29]. This led us to perform an MRI in a pediatric 3-MGA-uria type I patient who was detected upon metabolic screening for recurrent febrile seizures (in total, 15 up to age 7 years) at the age of four years[27]. He is ten years old at this writing and has developed completely normally. His MRI showed mild signal abnormalities in deep frontal white matter with sparing of the U-fibers. We propose that these abnormalities represent the earliest stages of the slowly progressive neurodegenerative disorder mainly affecting the white matter observed in the adult patients. Metabolite accumulation may contribute to the clinical signs and symptoms of this disease. A toxic effect of 3-MGA on the cerebral cortex has been demonstrated in rats[30]. There have also been speculations about the neurotoxicity of 3-HIVA[31]. The obvious accumulation of 3-HIVA in CSF and brain observed by MRS in the Dutch woman may be indicative for a central role of 3-HIVA accumulation in the natural course of brain damage in this disease[19]. As in other organic acidurias, accumulation of toxic metabolites may give rise to slow-onset excitotoxicity with cellular dysfunction and eventually cell death. If the natural-course scenario that we propose can be confirmed in a larger series of patients, leucine-restricted diet as a therapeutic approach from childhood onward must be reconsidered.

3-MGA-uria type II (Barth syndrome, MIM 302060)

The 3-MGA-uria type II or Barth syndrome is an X-linked recessive cardiomyopathy with (cyclic) neutropenia, skeletal myopathy, and mitochondrial respiratory chain dysfunction first described in a large Dutch family some 30 years ago[32, 33]. Ten years later, the 3-MGA-uria and decreased plasma cholesterol were added as consistent disease features[7]. Sudden unexpected death in early life has been reported[34]. The progression of cardiomyopathy (CM) is variable, sometimes slowly improving over the years, but mostly progressive and ending up at a point where heart transplantation is the only treatment option[8, 35, 36]. Cyclic neutropenia, ranging from mild to severe, is frequently seen; and fatal bacterial infections can occur in the neonatal period. Neutropenia and CM can develop simultaneously or in isolation. Onset ranges between birth and 49 years and peaks around puberty[37]. Chronic aphthous ulceration due to Candida infections is a common sequela. Treatment with granulocyte colony-stimulating factor (GCSF) seems to be successful and safe [38, 38]. Most patients show a degree of growth deficiency with height following the −2 SD percentile[37]. There is evidence that patients share distinct facial features (tall and broad forehead, round face with prominent chin and full cheeks, large ears, and deep-set eyes), which are most evident in infancy[39]. In early studies, normal mental functioning and intelligence is reported. Recent studies suggest a higher incidence of cognitive difficulties with regard to mathematics, visual spatial tasks, and short-term memory. Language ability is spared. In combination with the excess fatigue often seen in these patients, this should be given special attention[40].

The excretion of 3-MGA in urine can be highly variable, even within 24 h, and is often intermittent[3, 8]. The 3-MGA-uria is seemingly unrelated to the clinical course or severity of metabolic derangement. Even patients without 3-MGA-uria have been described[10]. Other characteristic findings in the urine are increased levels of 3-MG and 2-ethylhydracrylic acid, the latter a consequence of the isoleucine breakdown. Neither prolonged fasting nor leucin loading tests leads to changes in 3-MGA excretion, suggesting an alternative source of 3-MGA in affected patients[7, 8]. Moderately decreased plasma total cholesterol, mostly belonging to the low-density lipoprotein (LDL) pool, is a consistent finding [7]. This led to the hypothesis that 3-MGA results from overflow via the mevalonate shunt (Figure 1[7, 12]). Cells from patients with Barth syndrome show a characteristic abnormal cardiolipin profile, which is the basis for the diagnosis (for review, see[41]).

Total cardiolipin levels are lower, especially of the tetralineoyl subclasses, and the acyl chain composition is shifted toward less unsaturated species with markedly elevated monolysocardiolipin[42]. Cardiolipin is primarily found in the inner mitochondrial membrane and to a lesser extent in the outer mitochondrial membrane. Several proteins of the respiratory chain have been reported to bind to cardiolipin or require cardiolipin for optimal activity (as reviewed in[43]). Furthermore, cardiolipin is reported to function in the stabilization of the individual respiratory chain complexes in a larger so-called supercomplex, enabling efficient channelling of electrons through the complexes. Barth syndrome is caused by mutations in the *TAZ* gene located at Xq28, encoding the protein tafazzin, named after the masochistic comic character from an Italian TV sport show[44]. The function of this mitochondrial cardiolipin transacylase and its different splice variants (129–292 amino acids long) in the remodelling of cardiolipin remains elusive. A role in apoptosis has been suggested, but how this causes CM and neutropenia is unknown[43].

3-MGA-uria type III (Costeff syndrome, MIM 258501)

The 3-MGA-uria type III, or Costeff syndrome, is an autosomal recessive disorder with infantile bilateral optic atrophy, extrapyramidal signs, spasticity, ataxia, dysarthria, and cognitive deficit in decreasing order of frequency. It was first described in 19 Israeli patients in 1989[45]. The excretion of 3-MGA and 3-MG is, as in the other 3-MGA-uria types, quite variable[1]. All patients of Iraqi Jewish origin are homozygous for a splice site founder mutation in *OPA3* (mapped to 19q13.2-q13.3[46]). Several patients have been reported since then, almost exclusively of Iraqi Jewish origin, with the exception of one Turkish Kurdish and one Indian patient harboring different mutations[47-49]. Two other *OPA3* mutations result in a rare dominant disorder (ADOAC; MIM 165300) involving optic atrophy, cataracts, and extrapyramidal signs without 3-MGA-uria[50, 51]. The *OPA3* gene was first thought to consist of two exons; recently, it was proven to compromise three exons, resulting in two gene transcripts—*OPA3A* and *OPA3B*[46, 52]. Both transcripts contain exon 1, which is spliced to exon 2 in OPA3A (179 amino acids) and exon 3 in OPA3B (180 amino acids). OPA3A is expressed and conserved from fungi to primates, whereas OPA3B is uniquely found in mammals. In contrast to OPA3A, OPA3B is not identified in the proteomic database and is

considerably less frequently expressed in wild-type cells[52]. Recently, the prediction of a mitochondrial localization of the OPA3A protein could be confirmed. It is an integral protein of the mitochondrial outer membrane. The authors also reported an integral role for OPA3A in mitochondrial fission and apoptosis[53]. Very recently, a zebrafish model of Costeff syndrome has been described. Herein mitochondrial OPA3 is shown to protect the electron transport chain against inhibitory compounds[54].

3-MGA-uria type IV (MIM 250951)

Although about 100 patients with 3-MGA-uria not being classified as type I, II, III, or V have been described, OMIM refers to only one case report from 1992 for 3-MGA-uria type IV. This was a young man with severe psychomotor retardation, poor growth, subvalvular aortic stenosis, and CM. He later developed seizures, spasticity, and sensorineural hearing loss [9]. Since then, the spectrum has expanded rapidly. The underlying etiology has not been elucidated as yet but is certainly heterogeneous [55].

The majority of patients described so far presented with CM[56-62]. A subgroup presented with a severe early-onset phenotype with hypertrophic CM, and the unique features of early cataract, hypotonia/developmental delay, and lactic acidosis[63]. Recently, the underlying genetic defect in a subgroup of patients of Gypsy origin presenting with hypertrophic CM, hypotonia, hepatomegaly, facial dysmorphism, and microcephaly was found. Mutations in *TMEM70* encoding a mitochondrial protein proposed to be an ancillary factor involved in the biosynthesis and assembly of adenosine triphosphate (ATP) synthase (complex V of the respiratory chain) cause an isolated deficiency of ATP synthase. Half of the patients died, mostly within the first weeks of life; survivors showed psychomotor and various degrees of mental retardation[56, 61, 64, 65]. Interestingly, ATP synthase deficiency has been reported twice more in association with 3-MGA-uria. Recently, a young woman with mild mental retardation and peripheral neuropathy was described. She harbored a mutation in the *ATP5E* gene encoding the F1 epsilon subunit of the ATP synthase. This subunit is supposed to be involved in the incorporation of subunit c to the rotor structure of mammalian ATP synthase[66]. Some time ago, a girl with a syndromic phenotype mimicking cerebrooculo-facio-skeletal syndrome (but without microphthalmia/cataracts) was reported. She had hypoplastic kidneys, dysgenesis of the corpus callosum, and progressive brain atrophy involving the basal ganglia. She died aged 14 months after a course with intercurrent infections and seizures. She was found to have a mutation in the *ATP12* gene, which encodes an ATP synthase assembly factor[67]. How these nuclear-encoded mitochondrial disorders involved in ATP synthesis or ATP synthase assembly lead to 3-MGA-uria remains elusive.

In 2006, we reported four patients with a distinct clinical phenotype called MEGDEL association[68]. These patients presented with neuroradiological evidence of Leigh disease, sensorineural hearing loss, recurrent lactic academia, severe neonatal infections, and hypoglycemia. The 3-MGA in urine was moderately elevated, and all patients had complex I deficiency. In the mean time, we found three additional patients from other countries.

Genetic investigations are pending. Furthermore, patients with mitochondrial DNA (mtDNA) depletion or deletion syndromes, and m.3243A>G mutation, have been described in literature (*POLG1* mutations[69]; unspecified mtDNA depletion[70, 71]; Pearson syndrome[72-74]; m.3243A>G[60]). Recently, we presented a diagnostic strategy that enabled us to elucidate the underlying genetic defect in 11 out of 18 children with 3- MGA type IV by delineating patient groups (encephalomyopathic: *SUCLA2*; hepatocerebral: *POLG1*, cardiomyopathic: *TMEM70*, myopathic: *RYR1*) on clinical and biochemical grounds (for details, see[11]).

The 3–MGA–uria type IV is definitely the most intriguing type of the 3–MGA–urias, with a rapidly broadening spectrum. In contrast to the well-defined, distinct phenotypes 3–MGA–uria I, II, III and V, 3–MGA–uria type IV is most frequently associated with progressive neurological impairment, variable organ dysfunction, and biochemical features of a dysfunctional OXPHOS. Urinary 3–MGA seems to be a biochemical marker for mitochondrial dysfunction.

Clinical feature in the patient with 3–MGA–uria	Type	Next diagnostic step	Genetic confirmation[b]
Leukoencephalopathy	I	UOA: 3–MGA *cis:trans* isoforms (2:1), no ↑3–HIVA 3–MGH activity in leucocytes/fibroblasts	*AUH*
Optic atrophy	I	UOA: 3–MGA *cis:trans* isoforms (2:1), no ↑3–HIVA 3–MGH activity in leucocytes/fibroblasts	*AUH*
	III	+ Iraqi Jewish origin: proceed to genetic testing	*OPA3*
Ataxia/spasticity	I	UOA: 3–MGA *cis:trans* isoforms (2:1), no ↑3–HIVA 3–MGH activity in leucocytes/fibroblasts	*AUH*
	III	+ Optic atrophy: proceed to genetic testing	*OPA3*
Sensorineural deafness	IV	OXPHOS measurements in muscle/fibroblasts[a]	*SUCLA2*
Encephalopathy (epilepsy, psychosis, depression)	IV	OXPHOS measurements in muscle/fibroblasts[a]	*POLG1, SUCLA2*
Cardiomyopathy (± cataracts)	II	Cardiolipin profile + Neutropenia: proceed to genetic testing	*TAZ*
	IV	OXPHOS measurements in muscle/fibroblasts[a]	*m.3243A>G*
	IV	+ Gypsy origin: proceed to genetic testing	*TMEM70*
	V	+ Canadian-Hutterite origin: proceed to genetic testing	*DNAJC19*
Liver failure	IV	OXPHOS measurements in muscle/fibroblasts[a] Typical case of Alpers syndrome: proceed to genetic testing	*POLG1*
Bone marrow failure, exocrine pancreas insufficiency	IV	Proceed to genetic testing	*mtDNA deletions*

***Table 1**. A diagnostic approach to the patient with 3-MGA-uria. 3–MGA = 3–methylglutaconic acid, 3–MGA–uria = 3–methylglutaconic aciduria, 3–MGH = 3–methylglutaconyl–CoA hydratase, OXPHOS = oxidative phosphorylation system, UOA = urine organic acid analysis. [a]In case of suspicion of a mitochondrial disorder (e.g., combined with lactic acidosis, elevated alanine, clinical or biochemical signs, and symptoms of multisystem disease), [b]Current knowledge, the underlying genetic defect is not always known.*

3–MGA–uria type V (MIM 610198)

The 3–MGA–uria type V, or dilated cardiomyopathy with ataxia (DCMA) syndrome, is a novel autosomal recessive condition with early-onset dilated CM with conduction defects

and nonprogressive cerebellar ataxia in 18 patients of the Canadian Dariusleut Hutterite population, further characterized by testicular dysgenesis and growth failure[75]. Affected patients consistently showed five- to tenfold increases in both plasma and urine 3-MGA and 3-MG. Homozygosity mapping revealed the underlying splice-site mutation in the *DNAJC19* gene. Proteins containing a DNAJ domain are typically involved in molecular chaperone systems. Based upon the predicted tertiary structure of DNAJ19 it could be located in the inner mitochondrial membrane. Because of the similarity with the yeast Tim14 protein, a defect of protein import via the inner mitochondrial membrane, as seen in Mohr-Tranebjaerg syndrome, is suggested[76].

Other causes of 3-MGA-uria

Elevated urinary excretion of 3-MGA, parallel with increased excretion of 3-HIVA, 3-MG, 3-methylglutarylcarnitin, and 3- hydroxy-3-methylglutaconic acid, can be found in patients with HMG-CoA lyase deficiency (MIM 246450, [77]).This mitochondrial enzyme catalyses the last step of leucine breakdown (Figure 1) but is also required for ketogenesis. Patients present with a Reye-like picture with hypoketotic acidosis, metabolic acidosis, and liver failure. The prognosis is good if no damage from the initial presentation remains. The excretion pattern of HMG-CoA lyase deficiency is characteristic and distinguishes it from the other 3-MGA-uria types. Two patients with the late-onset form of multiple acyl-CoA dehydrogenase deficiency (MADD, or glutaric aciduria II, MIM 231680) also excreted 3-MGA[78]. Deficient electron transfer from the flavin adenine dinucleotide (FAD)-dependent dehydrogenases to the respiratory chain due to genetic defects of electron transfer flavoproteins (ETF) not only affects fatty acid oxidation but also dehydrogenases involved in the metabolism of amino acids (e.g., leucine), which could explain the 3-MGA-uria. The diagnosis is difficult to establish but worth elucidating, as treatment with riboflavin or coenzyme Q10 shows dramatic improvement in some patients.

The 3-MGA-uria can occur secondarily in patients with SLO because of abnormal isoprenoid/cholesterol biosynthesis, as well as in patients with glycogen storage disease Ib (MIM 232220) and IX (MIM306000), where it is speculated that an imbalance between gluconeogenesis and de novo cholesterol synthesis result in secondarily increased 3-MGA excretion ([12, 79]; Wortmann et al. unpublished data). These patients may present with elevated lactate levels and hypoglycemia. However, the clinical picture is distinct enough to allow correct diagnosis.

In the 1990s a letter to the Lancet suggested that 3-MGA-uria seen in pregnant mothers could be indicative for a metabolic disorder or in general a congenital defect in the offspring[80]. Investigations in a larger cohort of pregnant women revealed that 3-MGA-uria is frequently seen in healthy pregnant women (13/18 patients reported by[81], and no correlation to an underlying disease in the mother or child could be established[81]. It is speculated that the 3-MGA-uria occurs due to increased flux via the mevalonate shunt, as this is possible in tissue of ectodermal origin such as the placenta[15]. Interestingly, patients with congenital adrenal hyperplasia and thereby elevated production of sterol precursors

do not show 3–MGA–uria. The authors concluded that this is due to increased steroid flux occurring in the adrenal cortex, which is of mesodermal origin and where the mevalonate shunt is not supposed to function[15].

Gene	Type	Protein	Predicted function in	patients[a]
AUH	I	3–methylglutaconyl–CoA hydratase	Leucine catabolism	10
TAZ	II	Tafazzin, a mitochondrial cardiolipin transacylase	Cardiolipin remodelling	>100
OPA3	III	OPA3A and OPA3B protein	Mitochondrial (mt) fisson, apoptosis	>36
TMEM70	IV	Transmembrane protein 70	Biosynthesis and assembly of ATP synthase	53
ATP5E	IV	ATP synthase, epsilon subunit	Biosynthesis and assembly of ATP synthase	1
ATP12	IV	ATP 12 protein	Biosynthesis and assembly of ATP synthase	1
POLG1	IV	Polymerase gamma	mtDNA replication	3
m.3243A>G	IV	tRNA leucine	mtDNA translation	1
mtDNA deletions	IV	Not applicable	mtDNA replication and translation	6
mtDNA depletion	IV	Not applicable	mtDNA replication and translation	5
SUCLA2	IV	Succinate-CoA ligase	Tricarboxylic acid cycle	3
RYR1	IV	Ryanodine receptor	Calcium channel of sarcoplasmatic reticulum	1
DNAJC19	V	Translocase of inner mitochondrial membrane 14	Mitochondrial protein import	16

Table 2. *Genes, their translational products, and predicted function associated with 3–MGA–uria. ATP = adenosine triphosphate. Mt = mitochondrial.* [a]*Genetically confirmed, in association with 3–MGA–uria.*

Conclusion and approach to the patient with unexplained 3–MGA–uria

In this review, we present to the reader the fascinating spectrum of the 3–MGA–uria syndromes. 3–MGA–uria is an important biochemical marker that should stimulate the physician to proceed with investigations. Therefore, we would end our review by providing an approach to the patient with unexplained 3–MGA–uria. 3–MGA–uria can be seen in two conditions: as a consistent feature in the well-defined 3–MGA–uria subtypes I, II, III, V, and as a marker for mitochondrial dysfunction. It is often necessary to repeat (but certainly worth doing so) the urine organic acid analysis, as the 3–MGA–uria can occur intermittently. Table 1 gives an overview of which diagnostic steps should be taken in patients with 3- MGA-uria and unexplained signs and symptoms, such as optic atrophy or CM. Table 2 provides an overview of all known genes and their translational products that are involved in the 3–MGA–urias.

Chapter 2

3–methylglutaconic aciduria type I redefined - A syndrome with late-onset leukoencephalopathy

S. Wortmann[1], B. Kremer[2], A. Graham[3], M. Willemsen[4], F. Loupatty[5], S. Hogg[6], U. Engelke[7],L. Kluijtmans[7], R. Wanders[8], S. Illsinger[9], B. Wilcken[10], J. Cruysberg[11], A. Das[9], E. Morava[1]*, R. Wevers[7]*

Departments of [1]Pediatrics, [4]Neurology, [7]Laboratory Medicine and [11]Ophthalmology, Radboud University Nijmegen Medical Centre, Nijmegen;[2]Department of Neurology, University Medical Centre Groningen, Groningen, the Netherlands; [3]Department of Neurology, Ipswich Hospital, Ipswich, UK; [5]Department of Clinical Chemistry, Onze Lieve Vrouwe Gasthuis Amsterdam, the Netherlands; [6]Biochemical Genetics Unit, Addenbrooke's Hospital, Cambridge University Hospitals NHS Foundation Trust, Cambridge, UK; [8]Department of Clinical Chemistry, Academic Medical Center, Amsterdam, the Netherlands; [9]Department of Pediatric Kidney, Liver and Metabolic Diseases, Children's Hospital, Hannover Medical School, Hannover, Germany; and [10]Department of Biochemical Genetics, Children's Hospital at Westmead, Sydney, Australia. *Equal contribution.

Neurology. 2010;75(12):1079-83.

Abstract

Objective: 3–methylglutaconic aciduria type I is a rare inborn error of leucine catabolism. It is thought to present in childhood with nonspecific symptoms; it was even speculated to be a nondisease. The natural course of disease is unknown. *Methods:* This is a study on ten patients with 3–methylglutaconic aciduria type I. We present the clinical, neuroradiologic, biochemical, and genetic details on 2 new adult-onset patients and follow-up data on two patients from the literature. *Results:* Two unrelated patients with the characteristic biochemical findings of 3–methylglutaconic aciduria type I presented in adulthood with progressive ataxia. One patient additionally had optic atrophy, the other spasticity and dementia. Three novel mutations were found in conserved regions of the *AUH* gene. In both patients, MRI revealed extensive white matter disease. Follow-up MRI in a ten-year-old boy, who presented earlier with isolated febrile seizures, showed mild abnormalities in deep white matter. *Conclusion:* We define 3–methylglutaconic aciduria type I as an inborn error of metabolism with slowly progressive leukoencephalopathy clinically presenting in adulthood. In contrast to the nonspecific findings in pediatric cases, the clinical and neuroradiologic pattern in adult patients is highly characteristic. White matter abnormalities may already develop in the first decades of life. The variable features found in affected children may be coincidental. Long-term follow-up in children is essential to learn more about the natural course of this presumably slowly progressive disease. Dietary treatment with leucine restriction may be considered.

Introduction

3–methylglutaconic aciduria type I (3–MGA–uria I; MIM 250950) is a rare autosomal recessive disorder of leucine catabolism, characterized by markedly increased urinary excretion of 3–methylglutaconic acid (3–MGA), and mildly elevated urinary 3–methylglutaric acid (3–MG) and 3–hydroxyisovaleric acid (3–HIVA). This disorder is caused by a deficiency of 3–methylglutaconyl–CoA hydratase (3–MGH), which catalyzes the conversion of 3–methylglutaconyl–CoA to 3-hydroxy-3-methylglutaryl-CoA. 3–MGH is encoded by *AUH* and function-abolishing mutations were reported in 7 children with various unspecific symptoms (Table 1)[22, 23, 27, 28]. There is no firm evidence that 3–MGA–uria I causes clinical signs and symptoms in early childhood. Recently our group reported the biochemical details on the first patient with an adult onset of the disease[19]. One additional late-presenting patient was reported[29]. Both had a slowly progressive leukoencephalopathy with ataxia. Additionally, optic atrophy occurred in one patient while the other had dementia and spasticity.

Here we present the clinical, neuroradiologic, biochemical, and genetic details of two patients with adult presentation of 3–MGA–uria I. The clinical findings are compared with the spectrum seen in the eight patients reported in literature. Our data shed new light on the natural course of the disease. 3–MGA–uria I may remain asymptomatic in childhood but seems to present with a slowly progressive leukoencephalopathy in adulthood.

Methods and results

Patient characteristics

Detailed patient characteristics are available in appendix e-1 and summarized in Table 1. Patient 1, a Dutch woman, had experienced a progressive visual decline with bilateral optic atrophy from 35 years of age. Over the following 16 years, dysarthria and mild limb ataxia with severe gait ataxia were observed. Patient 2, a British man, first presented at the age of 30 years with mild cerebellar ataxia. Over 29 years, the condition slowly worsened, and spastic paraparesis, nystagmus, and dementia occurred.

To study the natural course of the disorder, follow-up on two patients was obtained (Table 1; patients 4 and 8).

MRI characteristics

Extensive, confluent white matter signal abnormalities (high on T2-weighted images) were seen in patients 1 and 2 (Figure 1, A–D). The lesions were restricted to the supratentorial region with predominant involvement of the deep and subcortical white matter. Notably, the cerebellum and the corpus callosum were spared. In patient 1 (at age 61 years), a periventricular rim was clearly spared. In patient 2 (at age 50 years), the subcortical U-fibers were less extensively involved, while there was a smaller periventricular rim with normal signal intensities in the parietooc cipital regions. Magnetic resonance spectroscopy in patient 1 was suggestive of 3–HIVA accumulation in brain[19].

Characteristics/ findings	Patient 1	Patient 2	Patient 3	Patient 4	Patient 5	Patient 6	Patient 7	Patient 8	Patient 9	Patient 10
Patient age at onset, y/gender	35/F	30/M	52/F	0/M[a]	4 mo/M	1/M	1/F	1/M	1/M[b]	<7/M[b]
Reference	This article, [19]	This article	[29]	[23] (pat. 1)	[28c]	[22] (pat. 1), [23] (pat. 4), [5c]	[23] (pat. 5), [82] (pat. 1)[c]	[27]	[23] (pat. 2)[c]	[22] (pat. 2), [23] (pat. 3)[c]
Ancestry (consanguinity)	Dutch (-)	British (+)	NA (NA)	Lebanese (+)	Japanese (NA)	Afghan (+)	NA (+)	German (-)	Moroccan (-)	Moroccan (-)
Mutation	c.559G>A/ c.650G>A	c.991A>T/ c.991A>T	IVS8–1G>A/ IVS8–1G>A	c.80delG/ c.80delG	IVS1–2A>G/ IVS1–2A>G	IVS8–1G>A/ IVS8–1G>A	c.719C>T/ c.613_614ins A	IVS9–2A>G/ IVS9–2A>G	c.589C>T/ c.589C>T	c.589C>T/ c.589C>T
Urinary 3-MGA[e]	94–141	78	108	1500–2900	168	400	249–953	570	765–934	521–844
Dementia	-	+	+	-	-	-	-	-	-	-
Ataxia	+	+	+	-	-	-	-	-	-	-
Spasticity	+	+	-	-	-	-	-	-	-	-
Cerebellar syndrome	-	+	-	-	-	-	-	-	-	-
Optic atrophy	+	-	-	-	-	-	-	-	-	-
Speech/mental retardation	-	-	-	-	+	+	-	-	+	+
Motor delay	-	-	-	-	+	+	-	-	+	+
Other clinical features					Quadriplegia, athetoid movements		Vomiting, selfmutilation, insomnia, crying fits, hepatomegaly	Febrile seizures, hyperkinesias, attention deficit		Shortened attention span, fasting hypoglycemia
Age at MRI, y	61	50	Adult	NA	Pediatric	Pediatric	Pediatric[d]	10	NA	NA
MRI: white matter changes	+++	+++	+++	NA	-	-	NA[d]	+	NA	NA
MRI: additional findings	-	-	-	NA	Atrophy basal ganglia	-	NA[d]	-	NA	NA

Table 1. *Clinical, biochemical, and neuroradiologic findings in patients with 3-MGA-uria I and mutations in AUH. Abbreviations:+ = Mild; +++ = severe; 3-MGA-uria I = 3-methylglutaconic aciduria type I; NA = not available. [a]Detected by newborn screening, [b]brothers, [c]patients also reported elsewhere: see appendix e1, [d]CT at unknown age reported as normal, [e]µmol/mmol creatinine.*

Biochemical and genetic characteristics

See appendix e-1 and Figure e-1 for details. Urine proton nuclear magnetic resonance spectroscopy in both patients revealed markedly elevated 3–MGA and mildly elevated 3–MG and 3–HIVA (Table e-1). As described pathognomic for 3–MGA–uria I, both patients presented *cis* and *trans* isoforms of 3–MGA in the characteristic 2:1 ratio in urine, and only *cis* isoform in CSF[19]. In both, 3–MGH activity was virtually undetectable in fibroblasts and lymphocytes.

Sequence analysis of *AUH* on genomic DNA identified compound heterozygosity for c.559G_A (G187S) and c.650 G_A (G217D) mutations in patient 1, which are predicted to abolish the enzymatic activity by altering trimer formation and catalytic activity. Patient 2 harbors a novel homozygous c.991A_T (K331X) mutation, which leads to the production of an aberrant protein, in which only eight terminal amino acid residues are missing. As crystal structure analysis suggests that the terminal part of the protein is not only a constituent of the active-site pocket, but is also necessary for subunit interaction and trimer stabilization, this could well explain the complete deficiency of 3–MGH activity in our patient (Figure e-1).

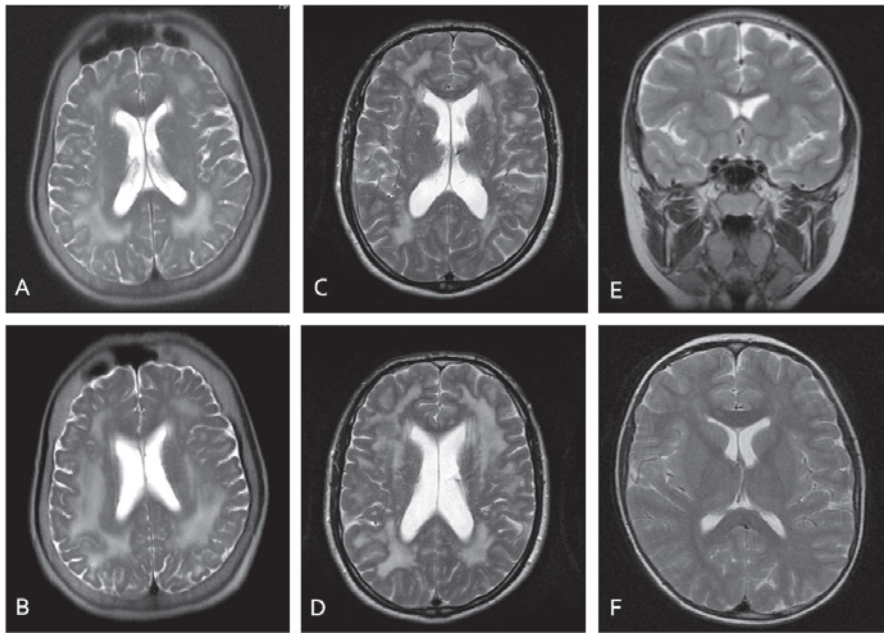

Figure 1: *Neuroradiologic findings in patients with 3–methylglutaconic aciduria type I (3–MGA–uria I). Cerebral MRI (T2-weighted) in three patients with 3–MGA–uria I. Images of patient 1 at age 61 years (A, B) and patient 2 at age 50 years (C, D) show extensive, confluent white matter lesions, almost completely sparing the corpus callosum as well as a periventricular rim especially in patient 1. The lesions spread until the U-fibers in patient 1 and to a lesser extent also in patient 2. Images of patient 8 (E, F) at age 10 years show mild abnormalities in deep frontalwhite matter sparing the corpus callosum and the U-fibers.*

Follow-up of pediatric patients from the literature

A summary of all reported patients is shown in Table 1. Patient 4, son of Lebanese consanguineous parents, was diagnosed by newborn screening (elevated C5- OH-carnitine: 2.5 µmol/L, normal 1.5 µmol/L)[23]. He had the characteristic 3–MGA–uria I urine profile while 3–HIVA was normal. 3–MGH deficiency was confirmed in fibroblasts; mutation analysis revealed a homozygous c.80delG mutation in *AUH*. He is now nine years of age, has developed normally, and formal neuropsychological testing showed functioning within the normal range. The patient's sister, now aged 6.5 years, had similar findings on newborn screening (no genetic testing). She also developed age appropriately and does well at school. So far, no cerebral imaging has been undertaken in the patients; physical examination was unremarkable.

Patient 8, a son of German nonconsanguineous parents, was diagnosed upon metabolic screening for recurrent febrile seizures (in total 15 up to age seven) at the age of four years[27]. Now he is ten years old and has developed normally. He attends regular school but exhibits attention-deficit/hyperactivity disorder. Physical examination was unrevealing. A recent MRI (Figure 1, E and F) showed mild signal abnormalities in deep frontal white matter with sparing of the U-fibers.

Discussion

Currently, eight patients from seven families have been reported with *AUH* mutations and 3–MGA–uria I (Table 1)[19, 22, 23, 27-29]. We identified three novel missense mutations in two patients presenting in adulthood. The homozygous mutation in patient 4 is predicted not to leave any residual enzyme activity. In spite of this, the patient and his sister (not shown in Table 1) are both healthy at the age of nine and 6.5 years[23]. The adult patient 3 with late-onset ataxia, dementia, and spasticity has the same homozygous mutation as the pediatric patient 6 with motor and speech delay[22, 29]. Comparing all patients, there seems to be no genotype–phenotype correlation. Only four pediatric patients (5, 6, 9, 10) share one particular symptom: the common and nonspecific finding of psychomotor retardation. In contrast, the adult patients show a distinct clinical pattern with adult onset of ataxia and spasticity[29].

In the pediatric group, findings on cerebral imaging have been reported in only three patients (patient 5: MRI with basal ganglia lesions and cerebral atrophy; patient 6: normal MRI; patient 7: normal CT; ages at imaging not reported)[5, 28, 82]. The MRI of the adult patients 1–3 showed extensive and diffusively distributed white matter lesions restricted to the supratentorial region not affecting the cerebellum or the corpus callosum (Figure 1). Patient 3 also showed cerebellar involvement[29]. This led us to perform an MRI in the pediatric patient 8 (aged ten) which showed mild abnormalities in deep supratentorial white matter. We propose that these abnormalities represent the earliest stages of the slowly progressive neurodegenerative disorder mainly affecting the white matter observed in the adult patients.

3–MGA, 3–MG, and 3–HIVA accumulate in the body fluids of patients with 3–MGA–uria I. Metabolite accumulation may contribute to the clinical signs and symptoms of the disease. A toxic effect of 3–MGA on the cerebral cortex has been demonstrated in rats[30]. The same is speculated for 3–HIVA[31]. The obvious accumulation of 3–HIVA in CSF and brain (as detected by MRS in patient 1) provides further evidence for the potentially toxic effects of this metabolite on the brain[19]. As in other organic acidurias, accumulating toxic metabolites may give rise to slow onset excitotoxicity with cellular dysfunction and eventually cell death. Patients may have a normal life expectancy, and the ultimate phenotype of the disease may turn out to be a progressive leukoencephalopathy with incapacitating neurologic deficits. In view of the healthy boy found by newborn screening and the mild and nonspecific phenotypes in other published pediatric patients with 3–MGA–uria I, it has been suggested that complete absence of 3–MGH causes clinical problems in childhood only in association with other, as yet undefined genetic or external factors[23, 27]. Ascertainment bias seems unlikely, owing to the rarity of this condition found in newborn screening[83]. At least three of the seven reported pediatric patients have consanguineous parents (patients 4, 6, and 7); the four other children harbor homozygous mutations (patients 5, 8–10), which may hint toward unknown or unreported consanguinity or a genetic founder effect. Such consanguinity could explain the high incidence of a second "genetic hit" which leads to the reported nonspecific symptoms in children that in fact are unrelated to 3–MGA–uria I (Table 1, Figure e-1).

Urinary organic acid analysis should be carried out in adult patients with unexplained slowly progressive leukoencephalopathy, as the diagnosis may be easily overlooked. We further advise performing regular MRIs of affected patients in the first decades of life to learn more about the natural course in these early stages of the disease. If the natural course scenario that we propose can be confirmed in a larger series of patients, leucine-restricted diet as a therapeutic approach from childhood onwards must be reconsidered.

Supplementary data

Appendix e-1

Supplementary patient characteristics

Patient 1, a Dutch woman, daughter of non-consanguineous parents, had experienced a progressive visual decline from 35 years of age, in the beginning with recurrent episodes of rapid deterioration and subsequent improvement. Initial ophthalmological examinations, two years later, revealed a best corrected visual acuity of 0.6 (20/33) in the right eye and 0.8 (20/25) in the left. Examination of the ocular fundus showed bilateral optic disc pallor and atrophy. Visual evoked potentials (with bilateral absence of occipital response) and color vision tests (with bilateral dichromatic red-green defect) indicated optic neuropathy of both eyes. Electroretinography indicated normal cone function and subnormal rod function. Over the years, her visual acuity gradually deteriorated with fluctuations. Repeated Goldmann perimetry showed progressive concentric constriction of the visual fields. Ophthalmological evaluation at age 61, revealed best corrected visual acuity of 0.05 (20/400) in the right eye and 0.02 (20/1000) in the left eye, bilateral optic disc atrophy, and pendular nystagmus. At initial neurological evaluation aged 37 years slight gait and limb ataxia and bilateral extensor responses of the toes were seen. Ataxia and pyramidal abnormalities increased slightly, while orobucal dyskinesia was noted three years later. By the age of 61 years, minimal dysarthria, mild limb ataxia with severe gait ataxia and frequent falls despite preserved ambulation were observed. Increased tendon reflexes with absent ankle tendon reflexes and extensor responses of the toes were seen. Nerve conduction studies at that age remained normal. Biochemical details on this patient have been reported previously.[19]

Patient 2, a British male, son of consanguineous parents, first presented to neurology services at the age of 30 years, complaining of progressive unsteadiness on walking. Examination showed a mild cerebellar ataxia with a spastic increase in tone of both legs, brisk reflexes throughout, and bilateral extensor plantar responses. The previous medical history was unremarkable except for "pigeon-toed" walking and clumsiness at school sport with plain lumbar radiographs showing a spina bifida occulta. No definite diagnosis was made. He re-presented to neurology at the age of 45 complaining of worsening unsteadiness. Examination showed similar findings as before, with a marked spastic paraparesis and mild/moderate cerebellar ataxia. Eye movement examination showed broken pursuit movements in all directions of gaze and bilateral first degree horizontal nystagmus in lateral gaze. At age 50 his best corrected visual acuity was 6/6 (20/20) bilaterally with normal appearing optic discs. Visual evoked potentials showed no abnormalities. The P100 latency on the right was at the upper limit of normal but overall there was no evidence of optic nerve demyelination.

At the age of 52 years, his wife complained that her husband's thinking was slowing down; this lead to definite concern about his performance at work. Cognitive assessment showed moderate global impairment and he was subsequently retired on medical grounds.

Physical examination showed a spastic ataxic paraparesis as before. At the most recent presentation (59 years) he had also developed a sleep disorder with excessive daytime sleepiness and involuntary jerky leg movements at night. Polysomnography was unremarkable.

	Urine (µmol/mmol creatinine)			CSF (µmol/L)		
	Pat. 1	Pat. 2	Reference	Pat. 1	Pat. 2	Ref.
3–methylglutaconic acid (total)	94-141	78	1.0-6.5	125	122	<10
- *cis* isoform	62-90	54	1.0-6.5	125	122	<10
- *trans* isoform	32-51	24		<10	<10	
3–methylglutaric acid	12-15	<10	0.3-0.7	<10	<10	<10
3–hydroxyisovaleric acid	61-63	58	<15	172	122	<10

Supplemental Table e-1. *Biochemical findings in patients with 3–MGA–uria I. Biochemical details of our patients detected in different body fluids by proton NMR spectroscopy with a 500 MHz Bruker spectrometer. Ref. = Reference range*[19]*.*

Supplementary biochemical and genetic characteristics

In both patients reported here routine blood clinical chemistry analysis was normal, both showed slight increases of plasma C5-hydroxy-carnitine (patient 1: 0.10 µmol/L; patient 2: 0.09 µmol/L; N: < 0.06 µmol/L). CSF cell count, lactate, glucose and total protein, were normal. No intrathecal immunoglobulin synthesis nor abnormal IgG bands were detected. 3–MGH-activity was virtually undetectable in both patients (reference values fibroblasts 2.1 ± 0.7 nmol/min/mg protein, lymphocytes 1.8 ± 0.2 nmol/min/mg protein)[84]. 3–MGA–uria type III was excluded in patient 1 by sequence analysis of the *OPA3* gene[46]. Both patients were not suspected of 3–MGA–uria type IV, which is known to be associated with mitochondrial dysfunction, as they both had normal lactate and alanine and low mitochochondrial disease scores[11, 85].

Sequence analysis of the *AUH* gene on genomic DNA identified compound heterozygosity for c.559G>A (G187S) and c.650G>A (G217D) missense mutations in patient 1 (Figure e-1). These mutations predict the substitution of the neutral amino acid glycine for a polar residue (serine or aspartic acid). Both glycine residues are conserved between different species, including Mus musculus (mouse), Rattus norvegicus (rat), Bos taurus (cow), Canis lupus familiaris (dog), Pan troglodytes (chimpanzee), Caenorhabditis elegans (nematode), Drosophila melanogaster (fruitfly) and Danio rerio (zebra fish). This suggests that these glycines are critical for enzyme function. Hydration of an enoyl-CoA substrate by 3–MGH proceeds through an intermediate which is stabilized via hydrogen bond interactions with two peptide NH-groups[86]. These amino groups are positioned in two distinct, but conserved regions that are an intrinsic part of the active site pocket. Glycine 187 of 3–MGH is located in one of these regions. Mutagenesis studies of this region in human short-chain enoyl-CoA hydratase revealed that substitution of glycine with proline resulted in a 106-fold decrease in hydratase activity, whereas the overall protein production of this mutant

remained unaffected[87]. The three-dimensional structure of 3–methylglutaconyl–CoA hydratase is a dimer of trimers[88]. Glycine 217 is located in a short flexible region (seven nucleotides) which is surrounded by two α-helices; one helix contains a catalytic glutamate residue, whereas the other is involved in subunit interactions to form the trimers.
Both the catalytic activity and trimer formation depend on hydrogen bond interactions. Substitution of glycine 217 with the charged amino acid residue aspartate could alter the conformation of the flexible region thereby disrupting the distance required for optimal hydrogen bond interaction. As a result, trimer formation and catalytic activity could be hindered which may abolish the enzymatic activity.

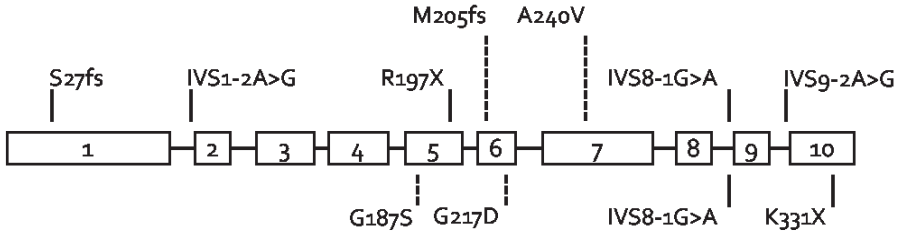

Mutation (DNA level)	Mutation (amino acid level)	Effect	Observed in patient
c.80delG	S27fs	Frameshift and truncated protein after 7 amino acids	4
IVS1-2A>G	-	Skipping of exon 2	5
c.559G>A	G187S	Predicted to affect the active site pocket	1
c.589C>T	R197X	Truncated protein	9, 10
c.613_614insA	M205fs	Frameshift and truncated protein after four amino acids.	7
c.650G>A	G217D	Predicted to alter protein conformation	1
c.719C>T	A240V	Not investigated	7
IVS8-1G>A	-	Skipping of exon 9	3, 6
IVS9-2A>G	-	Expected to delete exon 9*	8
c.991A>T	K331X	Truncated protein with last 8 amino acids missing, predicted to disrupt the active site pocket and alter protein conformation	2

Supplementary Figure e-1: *Overview of mutations in the AUH gene and functional consequences. Schematic representation of the AUH gene, including all mutations known from literature and from the current paper. Note that mutations found in pediatric patients are shown in the upper part and mutations found in the adult patients are shown in the lower part. The table gives an overview of all reported mutations on c.DNA and protein level and their (predicted) effects. * personal communication Prof. J. Zschocke, Innsbruck, Austria.*

In patient 2 a novel homozygous c.991A>T (K331X) mutation (Figure e-1), consistent with parental consanguinity, was identified. This nonsense mutation leads to the production of an aberrant protein, if any, in which only eight terminal amino acid residues are missing. Crystal structure analysis suggests that the terminal part of the protein is a constituent of the active-site pocket, but is also necessary for subunit interaction and trimer stabilization. Indeed, the importance of the terminal part of the mature protein is illustrated by the complete deficiency of 3–methylglutaconyl–CoA hydratase activity in our patient. The

mutations identified were not found in the NCBI single nucleotide polymorphism (SNP) database (www.ncbi.nlm.nih.gov/SNP/) and were not present in 50 Caucasian control alleles.

Supplementary details of patients reported in literature (see Figure e-1)

Currently eight patients from seven families are reported with *AUH* mutations and 3–MGA–uria I.[5, 19, 21-23, 25, 27-29, 82, 89, 90] Several patients are reported more than once. In the main text we only cite the articles in which the mutation and the neuroradiological details are reported. For more details: patient 5[28, 89], patient 6 (patient 1 in[22], patient 4 in[5, 23]), patient 7 (patient 5 in[23], patient 1 in[82], patient EVR in[25]), patient 9 (patient 2 in[23], patient 2 in[21], patient 2 in[90]) and patient 10 (patient 2 in[22,] patient 3 in[23] patient 1 in[21], patient 1 in[90]). All patient details are summarized in Table 1.

Seven different mutations were found in patients diagnosed in the first decade of life (patients 4-10): three splice site mutations (patients 3, 5, 6, 8), one deletion (patient 4), one insertion and two missense mutations (patient 7, 9, 10). Three mutations lead to a premature stop codon (patients 4, 7, 9, 10). We identified three novel missense mutations in two patients presenting in adulthood. Nine patients were homozygous for the reported mutations (patients 2-6, 8-10) while consanguinity was reported in four patients (patients 2, 4, 6, 7).

The homozygous mutation in patient 4 is of particular interest as it leads to seven abnormal aminoacids from serine 27 onwards and hereafter the protein is truncated. This mutation is therefore unlikely to leave any residual enzymatic activity. This patient was identified by newborn screening. In spite of the severe homozygous truncating mutation he and his sister (not shown in Table 1; no genetic testing but identical newborn screening result), who presumably share the same defect, are both healthy at the age of nine and 6.5 years.

Interestingly patient 3 with the late-onset presentation with ataxia, dementia and spasticity has the same homozygous mutation as the pediatric patient 6 with motor and speech delay.[29] Comparing all patients, there seems no genotype-phenotype correlation. The pediatric patients presented between the day of newborn screening and before seven years of age with diverse symptoms such as quadriplegia, athetoid movements, vomiting, hepatomegaly, self mutilation, febrile seizures or shortened attention span and fasting hypoglycemia (see Table 1 for details). Only four patients (patients 5, 6, 9, 10) share one particular symptom: the common and nonspecific finding of psychomotor retardation. In contrast, the adult patients show a distinct clinical pattern with late presentation of ataxia and spasticity, two also had dementia.[29] Patient 1 had optic atrophy as the presenting symptom and was misdiagnosed for a long time as having multiple sclerosis, *OPA3* mutations were excluded.

Chapter 3

Biochemical and genetic analysis of 3–methylglutaconic aciduria type IV:
a diagnostic strategy

S. Wortmann[1], R. Rodenburg[2], A. Jonckheere[1], M. de Vries[1], M. Huizing[3], K. Heldt[4], L. van den Heuvel[2], U. Wendel[4], L. Kluijtmans[2], U. Engelke[2], R. Wevers[2*], J. Smeitink[1], E. Morava[1*]

[1]Nijmegen Center for Mitochondrial Disorders, Department of Paediatrics, [2]Laboratory of Paediatrics and Neurology, Radboud University Medical Center Nijmegen, The Netherlands; [3]National Human Genome Research Institute, National Institutes of Health, Bethesda, USA; [4]Department of General Paediatrics, University Children's Hospital, Düsseldorf, Germany. *Equal contribution.

Brain. 2009;132(Pt 1):136-46.

Abstract

The heterogeneous group of 3–methylglutaconic aciduria type IV consists of patients with various organ involvement and mostly progressive neurological impairment in combination with 3-methyl-glutaconic aciduria and biochemical features of dysfunctional oxidative phosphorylation. Here we describe the clinical and biochemical phenotype in 18 children and define four clinical subgroups (encephalomyopathic, hepatocerebral, cardiomyopathic, myopathic). In the encephalomyopathic group with neurodegenerative symptoms and respiratory chain complex I deficiency, two of the children, presenting with mild Methylmalonic aciduria, Leigh-like encephalomyopathy, dystonia and deafness, harboured *SUCLA2* mutations. In children with a hepatocerebral phenotype most patients presented with complex I deficiency and mtDNA-depletion, three of which carried *POLG1*-mutations. In the cardiomyopathic subgroup most patients had complex V deficiency and an overlapping phenotype with that previously described in isolated complex V deficiency, in three patients a TMEM70 mutation was confirmed. In one male with a pure myopathic form and severe combined respiratory chain disorder, based on the pathogenomic histology of central core disease, *RYR1* mutations were detected. In our patient group the presence of the biochemical marker 3–methylglutaconic acid was indicative for nuclear coded respiratory chain disorders. By delineating patient-groups we elucidated the genetic defect in 10 out of 18 children. Depending on the clinical and biochemical phenotype we suggest *POLG1*, *SUCLA2*, *TMEM70* and *RYR1* sequence analysis and mtDNA-depletion studies in children with 3–methylglutaconic aciduria type IV.

Introduction

The heterogeneous group of 3–methylglutaconic aciduria (3–MGA–uria) syndromes includes several different inborn errors biochemically characterized by increased urinary excretion of 3-methyl-glutaconic acid (3–MGA) and 3–methylglutaric acid. At the present time five distinct types have been recognized. 3–MGA–uria type I (MIM 250950) is an inborn error of leucine catabolism with either an acute, life threatening presentation or a late onset form, caused by the deficiency of 3-methylglutaconyl- CoA hydratase (3–MGH; EC 4.2.1.18). The additional four types of 3–MGA–uria all affect mitochondrial function through different pathomechanisms. Type II (Barth syndrome; MIM 302060) occurs due to mutations of the *TAZ* gene and abnormal cardiolipin metabolism, presenting in males with cardiomyopathy (CM), cyclic neutropenia, muscle hypotonia, and (in the classical form) with normal cognitive function. In type III (Costeff syndrome, MIM 258501) patients present with bilateral optic atrophy and progressive extrapyramidal symptoms. The underlying mutations are in the mitochondrial *OPA3* gene, whose function is not fully understood.
3–MGA–uria type V (MIM 610198)[75] is a novel autosomal recessive condition with early onset dilated CM with conduction defects and non-progressive cerebellar ataxia (DCMA) in the Canadian Dariusleut Hutterite population, further characterized by testicular dysgenesis and growth failure. It is speculated that the underlying mutation in the *DNAJC19* gene leads to a defective mitochondrial protein import.
The diagnosis of 3–MGA–uria type IV ('unspecified' MIM 250951) is based on the exclusion of the other, well-defined clinical subtypes. The underlying aetiology is not yet elucidated but certainly heterogeneous[55]. 3–MGA–uria can occur secondarily in patients with Smith-Lemli-Opitz syndrome, a defect of cholesterol biosynthesis, because of abnormal isoprenoid/cholesterol biosynthesis[12] as well as in patients with glycogen storage disease Ib[79], where it is speculated that imbalanced gluconeogenesis and *de novo* cholesterol synthesis result in secondarily increased 3–MGA excretion.
However, 3–MGA–uria type IV is frequently associated with progressive neurological impairment, variable organ dysfunction and the common finding of biochemical features of a dysfunctional oxidative phosphorylation (OXPHOS). In some 3–MGA type IV patients the underlying genetic defect has been elucidated, mostly in patients with multiple complex deficiencies, like in mitochondrial DNA depletion syndromes[69-71], mitochondrial DNA deletion syndromes[72-74] or MELAS syndrome[60]. Furthermore there are several reports about patients with CM, mitochondrial dysfunction and 3–MGA–uria type IV[57-59, 61-63]. Di Rosa et al. described five patients presenting with a severe early-onset phenotype with hypertrophic cardiomyopathy (HCM), cataract,hypotonia/developmental delay and lactic acidosis[63]. Another distinct phenotype has been defined in 14 cases with an isolated deficiency of the mitochondrial complex V of nuclear genetic origin presenting with HCM, hypotonia, hepatomegaly, facial dysmorphism and microcephaly. Half of the patients died, mostly within the first weeks of live; the survivors showed psychomotor and various degrees of mental retardation[61].

Recently we performed biochemical and genetic investigations in four children with 3–MGA–uria presenting with neuro-radiological evidence of Leigh disease, hearing loss, recurrent lactic academia and hypoglycemia, and defined a new mitochondrial phenotype within 3–MGA–uria type IV (MEGDEL association: 3–MGA–uria with sensori-neural deafness, encephalopathy and Leigh-like syndrome)[68].
In this study we evaluated 18 children sequentially diagnosed with 3–MGA–uria type IV to assess the occurrence of associated symptoms, malformations, minor anomalies and biochemical features in order to define distinct phenotypes and elucidate the underlying genetic etiology in 3–MGA–uria type IV syndrome.

Methods

We evaluated the clinical data, collected by the same clinical investigator, of 17 out of 262 children evaluated by muscle biopsy in the period of 2002–2006 at our centre who were consecutively diagnosed with a mitochondrial disorder and 3–MGA–uria. We additionally included one child related to the index patients with overlapping clinical features, who underwent a skin biopsy. All children were referred under suspicion of an OXPHOS disorder and underwent a standard diagnostic protocol including organ function, imaging and laboratory studies[91].

Urine organic acid analysis/in vitro NMR spectroscopy
Organic acids in urine were analysed by gas chromatography/mass spectrometry (GC–MS) after extraction of the urine sample with ethylacetate and derivatization with N,N bis(trimethylsilyl)-trifluoracetamide containing 1% trimethylchlorosilane. The concentration of 3–MGA was quantified by comparing the signals obtained with calibration curves of the pure compound, using a CP-Sil 8 CB column (Varian, Middelburg, The Netherlands) on a HP 6890 Gas Chromatograph (Agilent, Amstelveen, The Netherlands). An 8000 Top Gas Chromatograph and Trace Mass Spectrometer Plus (InterSciences, Breda, The Netherlands) was used to verify the identity of both 3–methylglutaconic isoforms. Body fluid NMR spectroscopy and quantification of the *cis* and *trans* forms of 3–MGA were performed essentially as described elsewhere[92].

Biochemical and histological analysis in muscle and fibroblast samples
A surgical muscle biopsy was performed as well as a skin biopsy in all cases using standard methods. The samples were used for histological, histochemical and detailed biochemical investigations. Measurement of the 3–methylglutaconyl–CoA hydratase activity and Cardiolipin analysis were performed in blood or fibroblasts by standard methods[42]. Oxidative phosphorylation was evaluated in muscle and fibroblasts, including ATP production measurement from pyruvate oxidation in muscle, and complex I–V activity in both tissues[93].

Complex V assembly and activity/ ANT1 evaluation

BN-PAGE, blotting and complex V in-gel activity was performed as described[94], loading 60 mg of protein of OXPHOS complexes isolated from a mitoplast fraction of the patient and control cybrids and muscle homogenates. For Western blotting, monoclonal antibodies against mitochondrial ATP synthase subunit alpha and CoII-70 kDa (complex II) (Invitrogen, Breda, The Netherlands) were used. For the complex V in-gel activity assay the gel was incubated overnight at room temperature with the following solution: 35mM Tris, 270mM glycine, 14mM $MgSO_4$, 0.2% $Pb(NO_3)2$ and 8mM ATP, pH 7.8[94]. ANT1 evaluation was performed by Western blot analysis[62].

Genetic analysis

PCR amplification of both exons and their flanking intronic DNA sequences of the *OPA1* and *OPA3* genes were performed as described[46] in all patients. Mitochondrial depletion studies were performed in patients 1, 3, 7–9, 11, 12 and 19 as described[95]. Mitochondrial DNA mutations were evaluated using a standard mitochip analysis (GeneChip© Human Mitochondrial Resequencing Array 2.0, Affymetrix, Inc.). Deletions were analysed by long template PCR. Sequencing of the nuclear coded structural complex I genes and *RYR1* mutation analysis was performed on an ABI 3730 DNA analyser using BigDye terminator chemistry (Applied biosystems, Lekkerkerk a/d IJssel, The Netherlands).

Molecular investigations included sequence analysis of the structural genes of the oxidative phosphorylation complex I (*NDUFS1, NDUFS2, NDUFS4, NDUFS7, NDUFS8, NDUFV1*), and of the *POLG1, DGUOK* and *SUCLA2* genes depending on the biochemical results from the muscle biopsy and fibroblasts[91]. In the three patients with complex V deficiency, highly overlapping clinical phenotype and consanguinity we performed genome-wide homozygosity mapping using the 10K and 250K Affymetrix Single Nucleotide Polymorphisms arrays[96]. Homozygous areas were found on the chromosomes 2, 4, 8, 10 and 14. Upon the overlapping clinical and biochemical features with the patients described by [97] we checked the T*MEM70* gene for disease causing mutations.

Results

Clinical patient characteristics

Based on the clinical phenotype we divided the patients into the following four distinctive sub-groups: encephalomyopathic form (CNS and muscle involvement without liver involvement), hepatocerebral form (encephalomyopathy and liver dysfunction), cardiomyopathic form (motor developmental delay with CM, no or mild encephalopathy) and myopathic form (skeletal muscle involvement, no central nervous system involvement). We describe eight new patients, the other ten patients (1–6, 8, 15, 16, 18) have already been published as case reports, we therefore refer to the original papers. The essential clinical findings are summarized in Table 1.

Patients	1	2	3	4	5	6	7	8	9	10	11	12	13	14	15	16	17	18
Presentation	EM	EM	EM	EM	EM	HC	HC	HC	HC	HC	HC	CM	CM	CM	CM	CM	CM	M
Gender	M	M	F	F	F	M	F	M	F	M	F	F	F	F	M	F	M	M
Ethnicity	F	F	T	D	T	G	D	D	D	D	G	R	R	R	D	D	G	D
Consanguinity	+	+	+	+	+	-	-	-	-	NA	-	S	S	S	-	-	-	-
Age at onset (years)	0	0	0	0	0	0.8	16	0.3	0.3	9	0.3	0.5	0.8	0.8	0.4	0.6	0.5	0
Present age (years)	13	9	3[a]	16[a]	12	1.5[a]	16[a]	1[a]	3[a]	11	3[a]	3	9	5	11	7	4	10
PMR	+++	+++	++	++	++	+++	-	+	++	+	+++	+/-	+/-	-	-	+/-	+	-
Regression	+	++	+	+	+	-	+	+	+	+	-	-	-	-	-	-	-	-
Liver-involvement	-	-	-	-	-	+	+	++	+	+	+	-	-	+/-	-	-	-	-
HCM	-	-	-	-	-	-	-	-	-	-	-	+	+	+	+	+	+	-
Dystonia	+	+	+	+	+	-	-	-	-	+	+	-	-	-	-	-	-	-
Encephalopathy	-	-	-	+	+	+	+	+	+	+	+	-	-	+/-	-	-	-	-
Epilepsy	-	-	+	-	-	+	+	+	+	+	+	-	-	-	-	-	-	-
Hearing loss	+	+	+	+	+	-	-	-	-	-	NA	-	-	-	-	-	-	-
Cataract	-	-	-	-	-	-	-	-	-	-	-	-	-	-	+	+	-	
Brain atrophy	+	+	+	+	+	+	-	-	+, DM	+	+, DM	NA	NA	NA	+, DM	-	NA	NA
Leigh-like syndrome	+	-	+	+	+	-	+	-	-	-	-	NA	NA	NA	-	-	NA	NA
MDC	8		8	8	9	8	4	4	7	7	6	5	5	5	8	8	5	3
3-MGA excretion[b]	20-22	24-25	31-76	16-68	37-141	28	26	25	38	4-23	16-33	80	121	44-64	29-60	13-38	18-200	9-38
Other metabolites in urine	MMA	MMA	-	-	-	-	-	-	-	EMA	-	-	-	-	-	-	-	EMA
Complex I deficiency[c]	+	+	+	+	+	+	-	+	+	+	+	+	+	+	+	+	+	+
Complex V deficiency[c]	-	-	-	-	-	-	-	-	-	--	-	++	++	++	NA	NA	-	+
Mt DNA depletion	+	+	NA	NA	NA	+	+	+	NA	-	+	NA	NA	NA	NA	NA	NA	-
Mutation	*SUCLA2*						*POLG1*					*TMEM70*						*RYR1*

Table 1. *Clinical and biochemical features in 18 patients with 3-MGA-uria type IV. [a]Age deceased (years); [b]Normal<20 mmol/mmol creat.; [c]in muscle or fibroblasts; CCH = corpus callosum hypoplasia; DM = delayed myelinization; EM = encephalomyopathic type; EMA = ethylmalonic acid; HC = hepatocerebral type; M = myopathic type; MDC = mitochondrial disease criteria; MMA = methylmalonic acid; NA = not available; S = suspected; 3-MGA = 3-methylglutaconic acid; +, mild; ++, moderate; +++, severe. F = Faroese, T= Turkish, G= German, R = Roma.*

Encephalomyopathic form

Patients 1 and 2 (patients 11 and 12)[95]: Both patients initially presented with muscular hypotonia, poor suck and failure to thrive (FTT). In patient 1 later hearing loss, kyphoscoliosis and developmental delay as well as severe regression occurred. Patient 2 developed extrapyramidal symptoms and myoclonic seizures in the first year of life. Hearing evaluation revealed a sensorineural deafness followed by chochlear implant.

Patients 3–5: These patients were recently reported as MEGDEL association by our group (patients 1, 2 and 4)[68]. The three children presented with severe infections in the neonatal period, hypoglycemia and lactic acidemia were seen. Feeding problems and FTT made tube feeding necessary in two cases. All but one child had a delayed motor development and muscle hypotonia. One patient did not develop at all, the other patient showed psychomotor regression, one had epilepsy and all were mentally retarded. The patients developed severe spasticity, combined with extrapyramidal symptoms. One patient showed behavioural problems with constant laughing. Two patients died at the age of three and 16 years, respectively. No cardiologic alteration was noted. The MRI of the brain revealed characteristic bilateral hyper-dense lesions of the basal ganglia and diffuse cerebellar and/or cerebral atrophy in all patients. Visual evoked potential analysis was bilaterally delayed in two patients, however, no optic atrophy was noted. The BAEP studies showed severe sensori-neural hearing loss in all patients, making hearing devices necessary.

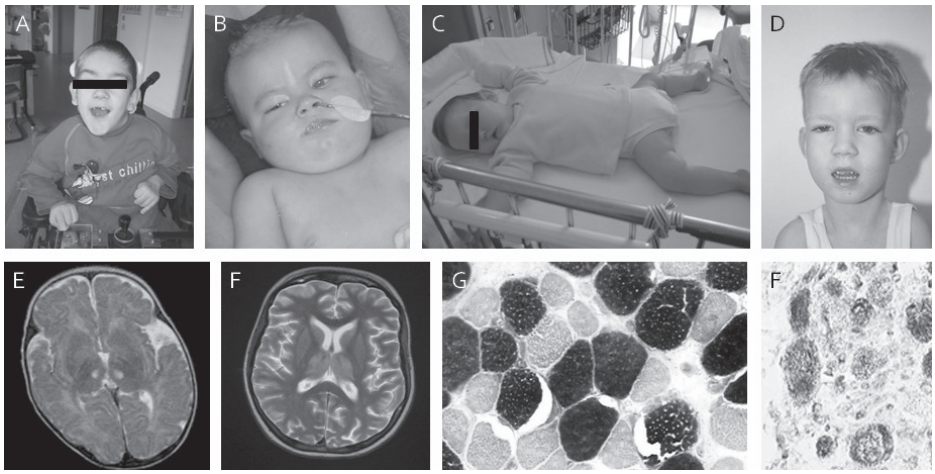

Figure 2. *A) One of the patients with SUCLA2 mutation with myopathic face by rigid dystonia. B) Patient 8 with a POLG1 mutation demonstrating the mask-like face due to facial dystonia, note the tube feeding. C) Patient 16 at the age of 8 months with extreme hypotonia. (D) Patient 18, note the myopathic face. E) Cerebral MRI of a patient with SUCLA2 mutation: Leigh disease and hyperintensities on T2-weighed images in both thalami. F) Cerebral MRI of Patient 7 with a POLG1 mutation: hyperintensities in all basal ganglia with sparing of the putamina in T2-weighed images. G) Transverse light microscopic serial sections of quadriceps muscle of Patient 15, note the myosin ATP-ase staining (bar 50 mm) and fibre type*

dysproportion. H) Transverse light microscopic serial sections of quadriceps muscle of Patient 18, Areas devoid of oxidative activity (cores), as well as predominance of type I fibers with the presence of centrally located nuclei or of rods comparable to central core disease (NADH TR staining).

Hepatocerebral form

Patient 6 (patient 3)[69]: The male patient had an older brother with a similar clinical phenotype. At the age of eight months FTT, hypotonia, mental retardation and myoclonic seizures became obvious. He died at the age of 17 months following intractable seizures and a progressive synthetic and cytotoxic liver failure.

Patient 7: The female patient presented at the age of 16 years with a progressive neurological dysfunction of the left hemisphere (headache, hemi-anopsia, latent left-sided paresis and aphasia). Up to then, the medical history was negative, as was the family history. She was diagnosed with, and treated for acute disseminated encephalomyelitis. She suffered from an organic psychosyndrome and epilepsy, treated with valproic acid. After a brief period of clinical improvement she presented with a relapse in combination with gastrointestinal symptoms, and showed a neurological regression with apathy, agitation, anorexia and liver failure (synthetic/ cytotoxic) and deceased in a multi-organ failure due to a gram-negative sepsis. Autopsy revealed spongiosis in thalamus and nucleus caudatus, suggestive of Morbus Alpers-Huttenlocher.

Patient 8 (patient 5)[69]: From the age of four months the male patient was followed for FTT, muscular hypotonia and delayed psychomotor development, later also regression. The EEG showed a burst suppression pattern and he had severe epilepsy. Hepatomegaly and elevated liver-function tests were noted as well. At the age of 13 months he died due to cardiorespiratory insufficiency after multi-drug treatment (without Valproic acid) during status epilepticus.

Patient 9: The female patient was born prematurely by 31 weeks gestation after a pregnancy complicated by severe hyperemesis. Two other pregnancies, in which solely intrauterine growth retardation (IUGR) was noted, ended with a stillbirth. The neonatal period was uncomplicated, the cerebral ultrasound showed a right sided subepidermal hemorrhage and bilateral mild periventricular leucomalacia. At the age of 3.5 months she was diagnosed with epilepsy, muscle hypertonia and psychomotor development delay. From the age of two years on she suffered from unexplained encephalopathic periods with atonia, apneas and stupor. These episodes of deep coma (Glasgow coma scale 3), lasted for about 72 h and then she became conscious again spontaneously and quickly. Continuous EEG-registration then showed a bizarre pattern of burst suppression changing with hours nearly without any cortical activity. MRI showed mild periventricular leucomalacia, irregularly widened ventricles, gracile corpus callosum and a partial pachygyria. Repetitive drug-screening in blood and urine was negative. She received a gastrostomy due to severe FTT and gastro-esophageal reflux after malrotation correction. Transient elevations of transaminases were noted. At age three years she died due to cardio-respiratory failure in an encephalopathic state.

Patient 10: The male patient was born at 26 weeks of gestation, with intrauterine growth retardation. No family history is available. He had an infantile encephalopathy with epilepsy and a delayed psychomotor development. He was noted to have episodes with hypo- and hyperthermia, extraordinary resistance to pain and severe FTT. At the age of 9 years he was admitted with a stroke-like episode with hemiplegia after valproic acid use for seizures. The MRI suggested a hemi-encephalitis. After a multiorgan failure with liver dysfunction and synthesis-failure, pancreatitis and a long-time depressed consciousness, his residual hemiparesis and speech problems are improving over time.
Patient 11: The pregnancy with this female patient was complicated by an early growth retardation and microcephaly, and she was born at term by caesarean section. Genetic and metabolic analysis was initiated at the age of three months due to severe microcephaly, dysmorphic features comparable to Brachmann-de Lange syndrome, psychomotor retardation, no development (could not sit or roll over, and made no contact), muscle hypotonia, epilepsy, severe FTT, feeding difficulties and tracheomalacia. She received tube feeding. She suffered from recurrent episodes of hyperthermia, liver dysfunction and intractable seizures and died at the ageof 2.5 years.

Cardiomyopathic form
Patient 12–14: These three female patients from a large Roma family descent from a possible inbred community. There are several additional siblings known with an overlapping phenotype. Patient 12, the index patient presented with severe FTT, arterial hypertension, CM and Wolf-Parkinson-White syndrome at the age of three years. Patient 13, a maternal cousin of patient 12 had HCM in combination with an aorta stenosis, pulmonary valve stenosis and occasional extrasystoles. Patient 14 presented with feeding problems leading to FTT and was evaluated from the age of 8 months onwards four times for periods of encephalopathy with extremely elevated lactate (11 mmol/l, N<52.1 mmol/l), alanine and glutamine/glutamate levels by normal liver enzyme and intermittently high ammonia concentrations. She had a normal motor development, only slight mental retardation and suffered from myoclonic episodes. Besides a HCM, an aortic valve stenosis was detected with rhythm disturbances (occasional extrasystoles). None of the patients had hypotonia. At the age of three, five and nine years, respectively, they have a nearly normal psychomotor development, short stature, FTT, but no neurological or other organ involvement. They all shared dysmorphic facial features including high forehead, curved eyebrows, flat midface, long philtrum, low implanted ears and thin lips.
Patient 15 and 16 (Cases 1, 2)[62]: patient 15 was evaluated for severe muscle hypotonia with hyporeflexia, delayed motor development and a severe, stable HCM with mild left ventricular outflow obstruction. His sister, patient 16, had a lactic acidosis at birth, no hypotonia. An echocardiogram detected HCM without an obstructive component. Both children developed early bilateral cataracts. Cranial MRI showed delayed myelinization for patient 15, in patient 16 it was normal. At the age of 11 and seven years, respectively, they

have a normal psychomotor development and severe exercise intolerance, both receive speech therapy.
Patient 17: The male patient was noted to have a severe muscle hypotonia from the age of five months, swallowing problems, recurrent infections and loss of motor skills. By ten months of age a non-obstructive CM was detected with mitral valve insufficiency, a tricuspidal aortic valve and pericardial effusion. Due to severe FTT and swallowing problems he got a gastrostomy. He received a lipid enriched diet. Physical examination revealed mild hepatomegaly, with transient elevation of the liver function tests. At the age of 4 years he is developing impressively, walks independently and communicates on an approximate age appropriate level.

Myopathic form
Patient 18 (patient 5)[98]: In this male patient generalized hypotonia, multiple contractures, swallowing problems and a lack of facial expression were apparent at birth. In spite of several severe infections he never needed artificial ventilation. He had FTT and his multiple episodes of hypoglycaemia were successfully treated with raw cornstarch. Besides a severe generalized muscle disease, he is unable to crawl or walk and therefore wheelchair dependant, he has no other organ involvement. By the age of ten years the patient attends a regular school.

Biochemical patient characteristics
As shown in Table 1, urine organic acid analysis with GC–MS and in vitro NMR spectroscopy showed an increased urinary excretion of 3–MGA in all patients in at least one sample. The excretion of 3–MGA in the children ranged between 4 and 200 mmol/mmol creat (control <20), with a strict 1 : 1 ratio of the *cis* and *trans* isoforms of 3–MGA (Figure 1). The excretion of 3–hydroxyisovaleric acid (3–HIVA) in the samples was within the normal range (data not shown). Hence, we conclude that our patients show 3–MGA–uria.
3–MGA–uria types I, II (Barth syndrome) and III (Costeff syndrome) were excluded in all patients as the activity of 3–methylglutaconyl–CoA hydratase, the cardiolipin levels and molecular analysis of the *OPA3* gene, respectively, showed no abnormalities (data not shown). Smith-Lemli-Opitz-syndrome and glycogen storage disorder were ruled out as well.
As all our patients scored above three points on the clinical diagnostic scoring system for mitochondrial disorders (MDC, see Table 1)[91] the possibility of a respiratory chain defect was further explored. Indeed, as shown in Table 2, the biochemical analysis of mitochondrial function in the fresh muscle biopsy and/or fibroblast cell lines showed disturbed oxidative phosphorylation in all 18 patients with an ATP production from pyruvate oxidation ranging between 0.9 and 37 nmol ATP/ h/mU CS (control range 42–81 nmol/h/mU/CS).

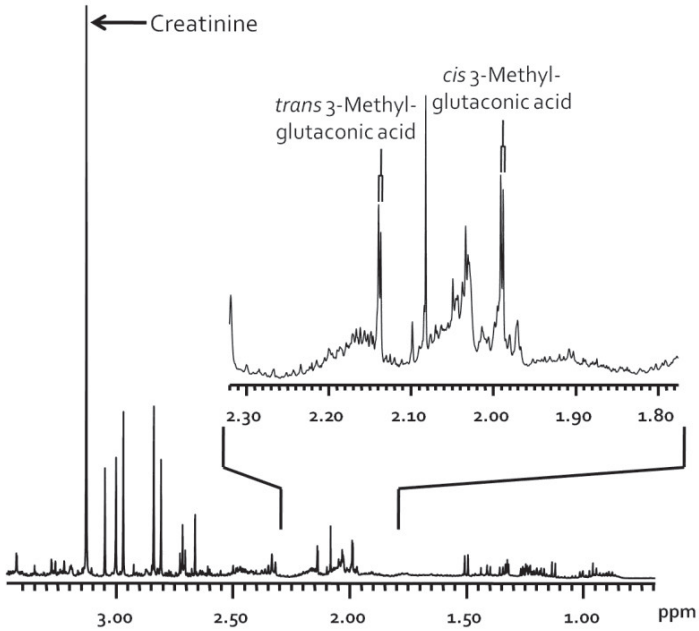

Figure 1. *NMR spectroscopy demonstrating two resonances of the cis and trans forms of 3–methylglutaconic acid (urine sample of Patient 5).*

In the subgroup of children with the encephalomyopathic form (patients 1–5), including the patients 3–5 with the MEGDEL association, all children had (when measured) a decreased ATP production from pyruvate oxidation (24–37 nmol ATP/h/mU CS) in fresh muscle biopsy. Four patients demonstrated complex I deficiency (either in muscle or fibroblasts), and one patient with *SUCLA2* defect had additional complex IV deficiency. The activities in fibroblasts were normal, with exception of a complex I deficiency in patient 5. The 3–MGA excretion levels were mildly to moderately and intermittently increased in the MEGDEL patients (16–141 mmol/mmol creat) and mildly elevated (20– 25 mmol/mmol/creat) in the other patients.

Patients	1	2	3	4	5	6	7	8	9	10	11	12	13	14	15	16	17	18
Presentation	EM	EM	EM	EM	EM	HC	HC	HC	HC	HC	HC	CM	CM	CM	CM	CM	CM	M
ATP production[b]	NA	NA	37	24	26	30	34	11	NA[a]	31	13	0.9	NA	NA	4.7	1.9	5.5	4
C I activity[c]	85	69	93	N	N	54	N	77	54	87	67	63	NA	82	21	26	13	83
C II activity[c]	NA	NA	NA	NA	NA	N	N	86	N	N	N	N	NA	N	NA	N	N	93
C III activity[c]	NA	N	N	NA	N	90	N	82	N	NA	N	N	NA	N	27	26	80	24
C IV activity[c]	N	43	N	NA	N	N	N	99	N	N	N	N	NA	N	35	20	N	N
C V activity[c]	NA	NA	NA	N	N	N	N	NA	NA	N	N	4.9	NA	0.4	NA	NA	N	N
Enzyme complex deficiencies in fibroblasts	-	-	-	NA	CI 84%	-	-	-	-	-	-	CI 80%, CV 20%	CI 63%, CV 5%	CI 97%, CV 37%	-	-	-	-
Abnormal muscle histology/histo-chemistry	-	-	+	-	-	+	+	-	NA	-	+	-	NA	NA	+	+	+	+
Abnormal Electron microscopy	-	+	NA	NA	NA	-	-	+	NA	NA	NA	NA	NA	NA	+	+	NA	+

Table 2. *Biochemical analysis of the mitochondrial function in the muscle biopsy and fibroblast lines of 18 patients with 3-MGA-uria type IV. Abnormal findings in bold.* [a] *Frozen muscle biopsy;* [b] *ATP production from pyruvate oxidation (control range 42–81 nmol/h/mU/CS);* [c] *Enzyme activities as percentage of lowest controls; C = complex of respiratory chain, HC = hepatocerebral type; M = myopathic type; LM = lipid myopathy; N = normal; NA = not available.*

In the subgroup of children with the hepatocerebral form (patients 6–11) all children had moderately to severe decreased ATP-production (13–34 nmol ATP/h/mU CS). All but patient 7 had a decreased activity of complex I, two had additional complex III deficiency, patient 8 demonstrated multiple enzyme deficiencies. The enzyme measurements in fibroblasts were normal in all children. Patient 11 additionally underwent a liver biopsy which revealed a complex I and IV deficiency. The 3–MGA–uria was intermittent in most of the children with normal results alternating with mildly elevated excretion (23–38 mmol/mmol creat).

The patients 12–17 with the cardiomyopathic form show very low ATP production from pyruvate oxidation; 0.9–5.5 nmol ATP/h/mU CS. Patients 12–14 have similar biochemical features as described by Sperl et al.[61] with severe complex V deficiency (0.4–4.9% of lowest controls). In patient 13, due to a positive family history, only a skin biopsy was performed, showing mild complex I (63%) and severe complex V deficiency (5%). In patients 12 and 14 mild complex I (80–97%) and severe complex V deficiency (20–37%) were found in fibroblasts. The two patients with Sengers-like syndrome (patients 15 and 16) had severe combined multi-complex deficiency (complexes I, III and IV). The 3–MGA–uria was moderate in patients 12, 13 and 14 (44–121 mmol/mmol creat), intermittently very high in patient 17 (up to 200 mmol/mmol creat) and mildly to moderately elevated (13–60 mmol/mmol creat) in the other patients.

Patient 18 with the myopathic form had a multiple complex deficiency (complex I activity 83%, complex II 93%, complex III 33% and complex IV activity 24% of lowest controls, respectively) and a very low ATP production from pyruvate oxidation of 4.0 mmol ATP h/mU CS. No abnormalities were detected in fibroblasts. 3–MGA-excretion in urine was mild (9–38 mmol/mmol creat).

Histology/electron microscopy

Alterations were found on histology by light microscopy in the majority of patients, ranging from fibre type disproportion in patients 3, 6, 11, 15 and 16, critical illness myopathy in patient 7 to increased percentage of lipid vacuoles, suggesting lipid myopathy in patient 17 (Table 2). In patient 15 necrotizing regions were detected and severely decreased COX-activity, SDH-staining was diffusely increased in several type I fibres (Figure 2). The histology and histochemistry of patient 16, with the identical clinical phenotype, was normal. Significant histological alterations were also found in patient 18 (Figure 2) with the myopathic subtype. Areas devoid of oxidative activity (cores) were observed in the skeletal muscle biopsies, as well as predominance of type I fibres with the presence of centrally located nuclei or of rods comparable to central core disease.

Electron microscopy showed abnormal structure of mitochondria in patient 2, absent cristae in patient 8 and zones with absent mitochondria in patient 18. In patient 15 many mitochondrial aggregations and an increased number of lipid droplets were found in many fibres. The mitochondria were abnormal with a severe loss of christae, also ring-shaped

mitochondrial were seen. These alterations were also seen in patient 16, but less impressive.

Genetic studies

Molecular analysis of the mitochondrial DNA detected no mutation in any of the patients. Additional sequencing of the nuclear coded structural genes of the oxidative phosphorylation complex I (*NDUFS1, NDUFS2, NDUFS4, NDUFS7, NDUFS8, NDUFV1*) showed no disease causing mutations.

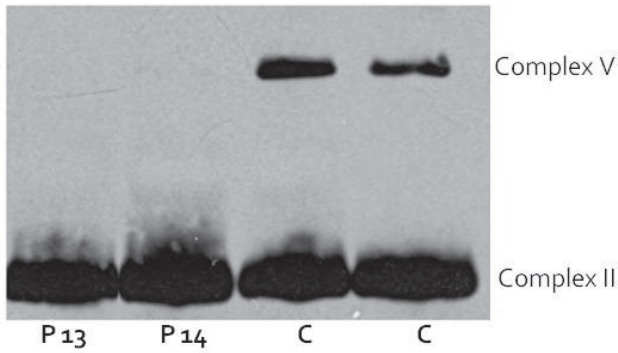

Figure 3. *One-dimensional Blue Native-PAGE showing severely reduced expression of holo-complex V in fibroblasts of two patients from the cardiomyopathic subgroup. Complex V was detected by an antibody against ATP-synthase subunit alpha. As a loading control complex II levels were visualized using an antibody against the 70 kDa FP subunit. P = patient, C = control.*

Mitochondrial depletion analysis was performed in eight children, and mitochondrial depletion was confirmed in patients 1, 2, 6, 7, 8, 11, but not in patients 10 and 18[69, 95]. No associated mitochondrial DNA deletions were found. Mutations in the *DGUOK* and *POLG1* genes were evaluated in all patients, *TK2, SUCLA2, P53R2, MPV17* were analysed appropriate to the phenotype. Patients 1 and 2 (patients 13 and 11, respectively)[95] harboured homozygous *SUCLA2* mutations (c.534 + 1G4A). *POLG1* mutations were detected in the patients 6 (G2869C/G1399A; Patients 3 in[69]), 7 (G1399A/G1399A) and 8 (G680C/G1399A, patient 5 in[69]). In the three Patients 12–14 with complex V deficiency we performed genome-wide homozygosity mapping revealing several homozygous regions that were shared by all three patients tested. No homozygosity was found in any of the previously described nuclear encoded structural assembly genes. Upon the finding of a homozygous region on chromosome eight and the overlapping clinical and biochemical phenotype with [97], we performed mutation analysis of the *TMEM70* gene. This revealed a homozygous substitution c.317-2A4G in Patients 12–14 identical with those recently described[97]. Western blotting with monoclonal antibodies against mitochondrial ATP synthase subunit alpha and CoII-70 kDa (complex II) showed a severely reduced amount of

holo-complex V in the fibroblasts of these patients (Figure 3). In Patient 18 *RYR1* mutations (c14804-1G4T/c.10616G4A; Patient 5 in[98]) were detected.

Discussion

Until now, several distinct metabolic disorders have been described demonstrating 3–MGA–uria, affecting the leucine degradation pathway or mitochondrial function in variable degree and severity. Besides these clinically and biochemically well-defined forms, the highly heterogeneous diagnostic category of 3–MGA–uria type IV encompasses patients with progressive neurologic impairment, variable organ involvement and OXPHOS dysfunction[99]. During our study within a 5-year period in the group of patients undergoing muscle biopsy based on standard clinical criteria, we detected a high number of children (18 out of 262) with 3–MGA–uria and oxidative phosphorylation complex deficiencies; almost 7% of the patients were diagnosed with 3–MGA–uria type IV. In nine children we confirmed a nuclear coded mutation underlying the disease, in one patient only mitochondrial depletion was found. One child, who is not included in the current study was additionally diagnosed with Barth syndrome. No *OPA1* mutations were elucidated in any of the patients. In spite of the presence of mitochondrial depletion in a high percentage of the mutation positive patients none of the children were diagnosed with mitochondrial mutations and no mitochondrial DNA deletion was confirmed in muscle tissue. Based on our findings we confirm the previous observation that 3–MGA–uria is an important diagnostic marker and could be used for screening in the diagnostic workup of a suspected dysfunction in the oxidative phosphorylation.

3–MGA–uria has been described as an associated finding in various mitochondrial DNA depletion syndromes [70, 71], however the finding of this organic aciduria is highly variable and frequently intermittent. In our patient group diagnosed with *POLG1* mutations, 3–MGA–uria was present in only three out of ten patients and in a large cohort of children with *SUCLA2* defect only 5 out of 16 showed 3–MGA–uria during their disease course (U. Steuerwald 2008, personal communications). The majority of these patients have normal concentration of 3–MGA in the urine[95]. This suggests that the metabolic marker could be indicative for mitochondrial depletion, but not directly related to the disease, even in the presence of the same mutation. One should interpret the presence of mild 3–MGA–uria very cautiously, the same level of excretion can be detected in children with primary and secondary liver disease, including glycogen storage disorder type I[79] and type IX (E. Morava: personal communication) or cholesterol synthesis defects[12] as a marker of lipid mobilization and upregulated cholesterol synthesis. These patients might present with elevated lactate levels and hypoglycaemia, still the clinical picture is distinct enough to be able to find the correct diagnosis.

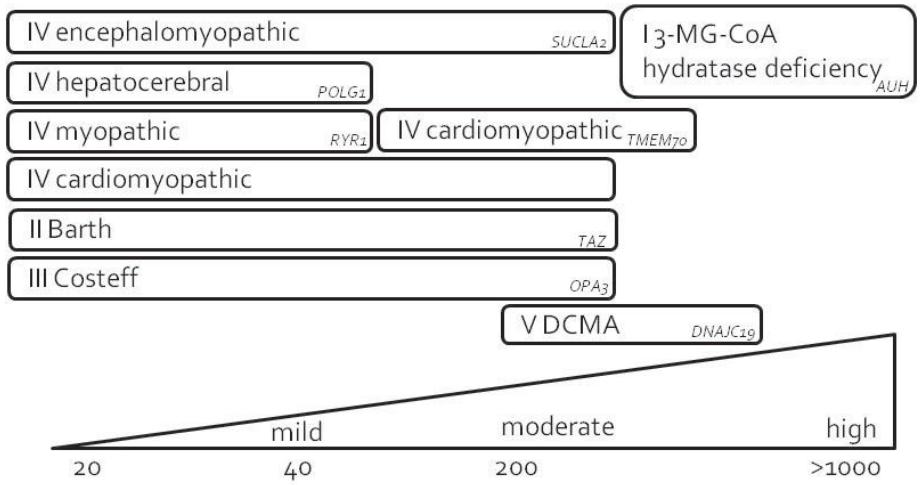

Figure 4. *Excretion levels of 3-MGA in urine in the different subtypes of 3-MGA-uria.*

In nearly all of our patients the finding of 3-MGA-uria was intermittent. Even the children carrying *POLG1* mutations had periods during the course of their disease without 3-MGA-uria. No correlation was found with either possible episodes of infection or the nutritional state in our patients. Since the underlying mechanism leading to 3-MGA-uria is still undiscovered, we have no appropriate explanation for this phenomenon. Interestingly variable excretion, even within 24 h [3], of 3-MGA was reported in several patients with Barth and Costeff syndrome (own experience;[1, 8]) seemingly unrelated to the clinical course or the severity of metabolic derangement (Figure 4).

By far the most patients described so far with 3-MGA-uria type IV dysfunction present with HCM[57, 58, 59, 61, 63]. The most striking biochemical feature in the patients described by Sperl et al., is a severe complex V deficiency, measured in muscle in fibroblasts and associated with a mild complex I deficiency[61]. This characteristic pattern has been described so far only in children with gypsy ethnicity originating from highly consanguineous families, in combination with normal mental development and characteristic facial features. These patients were recently diagnosed with a novel nuclear genetic defect leading to abnormal biogenesis of the respiratory chain complex V [97]. We have identified three patients (Patients 12–14) with the same *TMEM70* mutation, sharing the same ethnic background.

Interestingly all of our patients (Patients 12–17) with HCM had no regression and an only somewhat delayed or normal psychomotor development. Only in Patient 17 there is a moderate psychomotor retardation, but the patient is improving impressingly over time. Besides the slowly progressive HCM some of the children suffered from rhythm disturbances or congenital valve anomalies. Still one should emphasize the absence of associated neurological symptoms in this patient group. In both children diagnosed with Sengers like syndrome (Patients 15 and 16) infantile cataract was diagnosed at an early

stage of the disease. Cataract seldomly occurs at such a young age in children with a respiratory chain disease, and mostly presents in association with mtDNA deletions[100], mtDNA depletion[101] or in the classical Sengers syndrome (MIM 212350)[102]. Cataract has been observed several times in combination with 3–MGA–uria type IV in combination with HCM[63]. This unique symptom therefore might lead the clinician early on to the correct diagnosis. Based on the strong correlation of CM, 3–MGA–uria, complex V deficiency and cataract we strongly advice detailed cardiological and ophthalmological evaluation in all patients with 3–MGA–uria and a suspected OXPHOS disorder.

Patients with a diagnosis of 3–MGA–uria type IV present with an extremely variable clinical phenotype. NMR-spectroscopy of the urine in 3–MGA–uria type I[19] showed a 2 : 1 ratio for *cis* and *trans* isoforms of 3–MGA in all patients. Interestingly in the CSF only the *cis* stereoisomer was found. Additional to other biochemical features, these findings helped to differentiate patients with type I from the other 3–MGA types. In our study we expected to be able to delineate further patient groups upon the *cis* and *trans* ratios of 3–MGA in urine. Unfortunately the ratio was 1 : 1 in all patients and therefore NMR spectroscopy revealed no additional information compared to standard organic acid analysis.

Assigning clinical subgroups within the large patients group of 3–MGA–uria could however effectively facilitate the molecular diagnostic workup. There is a long ongoing discussion between clinical geneticists and molecular/biochemical geneticists regarding 'splitting or lumping' phenotypic groups in clinical syndromes; either based on biochemical and phenotypic patterns, to define relatively homogeneous groups for further genetic analysis or to be able to form larger groups for follow up and counselling. In the current study we tried to approach our patient group with 'splitting', leading to the discovery of the genetic aetiology in many children. Although forming smaller, but characteristic groups might lead to even more complex descriptions of an individual patient, it might also help in better prognosis assessment and optimal follow up in this unique patient group. By delineating patient groups we elucidated the genetic defect in ten out of 18 children. Depending on the phenotype, the presence of complex V deficiency and the finding of additional biochemical markers we recommend *POLG1, SUCLA2, TMEM70* and *RYR1* sequence analysis and mtDNA-depletion studies in children with 3–MGA–uria type IV.

In the patient group with encephalopathic presentation we found *SUCLA2* mutations in patients demonstrating an associated methylmalonic aciduria. Both patients came from the Faroer islands due to a founder effect. In the other children with progressive dystonia, Leigh like syndrome and deafness, a 'classical mitochondrial' presentation, no mitochondrial DNA deletion or mutation, no alteration in the *OPA1, POLG1* or *DGUOK* genes were discovered. Homozygosity mapping might reveal the underlying suspected nuclear gene defect in these consanguinous cases.

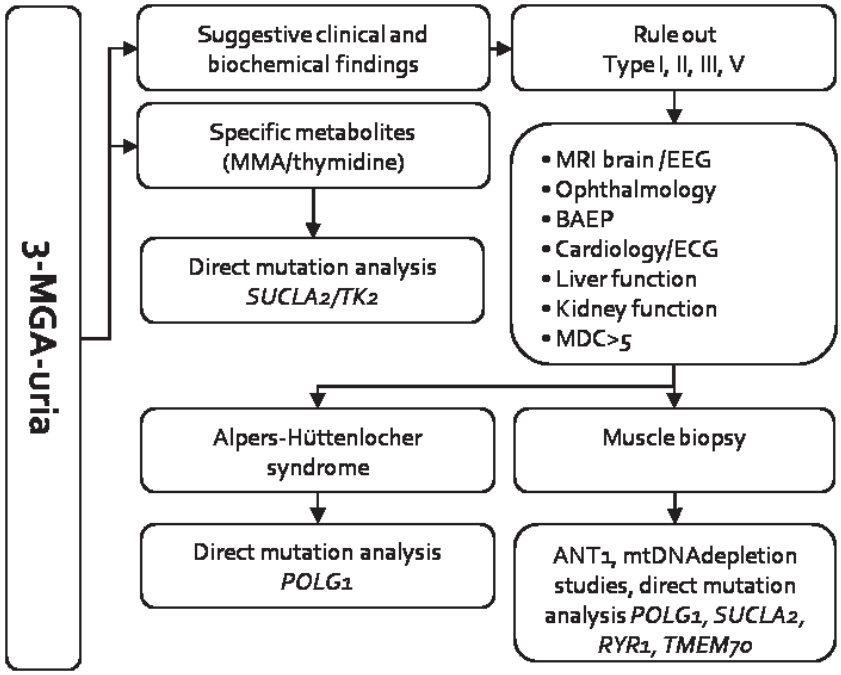

Figure 5. *Diagnostic flowchart. MDC= Mitochondrial disease criteria*[91].

Most patients with 3–MGA–uria type IV present with either neurodegenerative symptoms, or encephalopathy in combination with other organ involvement. In our patient cohort, but also in most of the so far published cases only a minority of children diagnosed with type IV have an isolated muscle disorder. Due to the distinct, syndromic presentation and the characteristic association of biochemical and clinical markers we suggest a practical evaluation protocol to facilitate an effective diagnostic route and optimalize counselling (Figure 5). Solving the genetic defect and assigning a syndrome diagnosis to a child with 'the unclassified' type IV 3–MGA–uria, finally 'excludes' the patient from this unclassified group.

Obviously in case of a classic syndromic presentation in a child with 3–MGA–uria and a suspected mitochondrial dysfunction, invasive diagnostics, such as muscle biopsy or skin biopsy should be avoided, if possible. By using the diagnostic flowchart we elucidated the underlying genetic defect in two additional patients with 3–MGA–uria. One male patient from the Faroer islands with MMA-uria, hypotonia and deafness, in whom a *SUCLA2* mutation could be confirmed, and a gipsy female with typical facial features and HCM, where we confirmed a *TMEM70* mutation. Both mutations were confirmed in blood, hence we spared the children undergoing muscle biopsy.

Chapter 4

3–methylglutaconic aciduria type IV: a syndrome with an evolving phenotype

S. Wortmann and E. Morava

Department of Pediatrics and the Institute of Genetic and Metabolic Disease (IGMD), Nijmegen Center for Mitochondrial Disorders (NCMD), Radboud University Nijmegen Medical Center, Nijmegen, The Netherlands

Clin Dysmorph. 2011, 20:168–169.

We read with interest the article 'Dysmorpholgy on Barth syndrome'[39] in this journal. Barth syndrome, also called 3–methylglutaconic aciduria (3–MGA–uria) type II, is an X-linked disorder of cardiomyopathy, neutropenia, mild cognitive impairment, and myopathy (MIM 302060). Hastings et al.[39] added a distinct facial appearance to the diagnostic features of the classic phenotype (Figure 1a).

Barth syndrome is one of the subtypes of the rapidly expanding group of genetic disorders associated with an elevated urinary excretion of 3–methylglutaconic acid (as reviewed in [103]for summary see Table 1). Four additional subtypes have been described so far. Of these four subtypes, three syndromes are well-defined multisystem disorders with clear-cut diagnostic features.

3–MGA–uria type	Involved gene (mode of inheritance)	Main features beside 3–MGA–uria
I	*AUH* (ar)	Slowly progressive leukoencephalopathy, adult onset of symptoms, ataxia, spasticity, dementia, no facial features
II (Barth syndrome)	*TAZ* (X-linked)	X-linked, cardiomyopathy, congenital neutropenia, mild cognitive impairment, myopathy, distinct facial features
III (Costeff syndrome)	*OPA3* (ar)	Infantile bilateral optic atrophy, extrapyramidal symptoms
IV 'unclassified'	Heterogeneous, examples below	Progressive neurological course of disease, clinical, biochemical, and radiological signs of mitochondrial encephalomyopathy, secondary facial dysmorphism
	SUCLA2 (ar)	Mild methylmalonic aciduria, dystonia, deafness, secondary facial dysmorphism
	TMEM 70 (ar)	ATP synthase deficiency, cardiomyopathy, myopathy, cognitive impairment, distinct facial features
	POLG (ar)	PMR, intractable epilepsy and early fulminant liver failure (Alpers syndrome)
	MEGDEL syndrome[a]	Leigh-like MRI, dystonia, deafness, secondary facial dysmorphism
V (DCMA syndrome)	*DNAJC19* (ar)	Canadese Dariusleut-Hutterite, dilative cardiomyopathy, nonprogressive cerebellar ataxia, dysmorphic features not reported

Table 1. *Overview of the different types of 3–methylglutaconic aciduria. ar = autosomal recessive; DCMA = dilated cardiomyopathy with ataxia; 3–MGA–uria = 3–methylglutaconic aciduria. [a]Genetic defect unknown.*

3–MGA–uria type I (MIM 250950) is a rare disorder of leucine catabolism, which we have currently redefined as a syndrome with slowly progressive leukoencephalopathy presenting in adulthood[26]. The other known subtypes are biochemically and genetically diverse, but all have an effect on mitochondrial function through different pathomechanisms. In type III or Costeff syndrome (MIM 258501), patients show infantile bilateral optic atrophy and extrapyramidal symptoms. Facial dysmorphism has not been reported so far. Recently, a Canadese Dariusleut–Hutterite family with dilative cardiomyopathy and nonprogressive cerebellar ataxia has been reported as dilated cardiomyopathy with ataxia (DCMA) syndrome or 3–MGA–uria type V (MIM 610198). No dysmorphic features were noted.

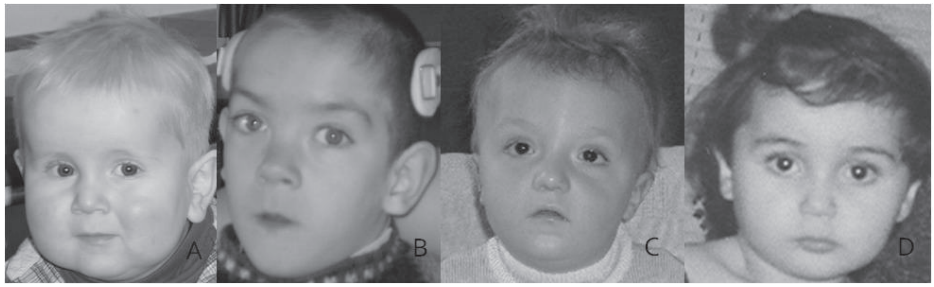

Figure 1: *Facial appearance in patients with 3-methylglutaconic aciduria (3-MGA-uria) types II and IV. A) A three-year-old boy with Barth syndrome (3-MGA-uria type II). Note the tall and broad forehead, the round face with the curved eyebrows, the prominent chin, and full cheeks. The ears are large and deep set. B-D) Patients with 3-MGA-uria type IV. Note the large and deep-set ears and the long philtrum in these patients, as well as the curved eyebrows in patients (B, C), and the full and broad forehead in patients (C, D). Patient (B) is a five-year-old patient with SUCLA2 mutation; note the mask-like appearance and the small mouth. Patient (C) is a one-year-old boy with POLG mutation. Patient (D) is a patient with MEGDEL association, aged four years.*

3-MGA-uria type IV (MIM 250951) has been defined by [9], based on the exclusion of the other well-defined 3-MGA-uria subtypes. He described one offspring of consanguineous Italian origin with severe psychomotor retardation and cerebellar dysgenesis. Since then the spectrum of patients not fitting into the known genetic subtypes, 3-MGA-uria type I, II, III, or V, has expanded rapidly. More than 100 patients have been described so far, classified as having 3-MGA-uria type IV, based on ruling out the other four syndromes.

But is 3-MGA-uria type IV a distinct genetic syndrome? Are there diagnostic criteria regarding organ involvementand dysmorphology? The clinical and genetic spectrum is certainly heterogenous, but within the spectrum there are several distinctive disorders. For example, one group of patients with mutations in *SUCLA2* (Figure 1b, MIM 603921[104]) leading to a distinct phenotype with mild 3-MGA-uria, mild methylmalonic aciduria, and severe mitochondrial encephalomyopathy with sensorineural deafness and dystonia. In addition, patients with the typicial trias of psychomotor retardation, intractable epilepsy, and early fulminant liver failure due to *POLG* mutations (Alpers syndrome, MIM 203700[11]) are described with 3-MGA-uria (Figure 1c).

Another rapidly growing group of children, mostly of gipsy origin, harbor mutations in *TMEM70*[64]. Their phenotype encompasses 3-MGA-uria, severe deficiency of the mitochondrial ATP synthase (complex V of the respiratory chain), cardiomyopathy, distinct facial appearance, and mild cognitive impairment. In a third group of patients with the unique syndromic presentation of 3-MGA-uria, sensorineural deafness and dystonia combined with a deficiency of the complex I of the respiratory chain (Figure 1d; MEGDEL association[68]); the genetic defect has not yet been elucidated.

Dysmorphic features are commonly present in 3-MGA-uria type IV (Figure 1b–d). Most of these appear during the course of disease, secondary to basal ganglia involvement (mask-like facial features), muscle wasting of the facial musculature, and hypotonia,

leading to an elongation of the face and long prominent ears. Some of these facial features are comparable with that described in patients with Barth syndrome (broad and tall forehead, curved eyebrows; Figure 1).

In addition to the well-recognized Barth syndrome, we want to draw attention for the rapidly growing group of 3-MGA-uria type IV. We define 3-MGA-uria type IVas a group of inborn errors with primary mitochondrial dysfunction, leading to a multisystem disease often with a distinctive syndromic appearance. 3-MGA-uria can easily be detected upon routine urinary organic acid analysis. This acid, in combination with other Biochemical, neuroradiological, and especially clinical signs and symptoms can guide the physician to the right diagnosis[11].

Chapter 5

Association of 3–methylglutaconic aciduria with sensori-neural deafness, encephalopathy, and Leigh-like syndrome (MEGDEL association) in four patients with a disorder of the oxidative phosphorylation

S. Wortmann[1], R. Rodenburg[1,2], M. Huizing[3], F. Loupatty[4], T. de Koning[5], L. Kluijtmans[2], U. Engelke[2], R. Wevers[2], J. Smeitink[1], E. Morava[1¤]

[1]Radboud University Nijmegen Medical Centre, Nijmegen Centre for Mitochondrial Disorders, Department of Pediatrics, [2]Laboratory of Pediatrics and Neurology, Nijmegen, The Netherlands; [3]National Human Genome Research Institute, National Institutes of Health, Bethesda, USA; [4]Academic Medical Centre Amsterdam, Laboratory Genetic Metabolic Diseases, Amsterdam, The Netherlands, [5]Academic Medical Centre Utrecht, Department of Pediatrics, Utrecht, The Netherlands.

Mol Genet Metab. 2006;88(1):47-52.

Abstract

In this paper, we describe a distinct clinical subtype of 3–methylglutaconic aciduria. 3-Methyl-glutaconic aciduria is a group of different metabolic disorders biochemically characterized by increased urinary excretion of 3–methylglutaconic acid. We performed biochemical and genetic investigations, including urine organic acid analysis, NMR spectroscopy, measurement of 3-methyl-glutaconyl-CoA hydratase activity, cardiolipin levels, *OPA3* gene analysis and measurement of the oxidative phosphorylation in four female patients with 3–methylglutaconic aciduria. 3–methylglutaconic aciduria type I, Barth syndrome, and Costeff syndrome were excluded as the activity of 3-methylglutaconyl-CoA hydratase, the cardiolipin levels, and molecular analysis of the *OPA3* gene, respectively, showed no abnormalities. The children presented with characteristic association of hearing loss and the neuro-radiological evidence of Leigh disease. They also had neonatal hypotonia, recurrent lactic acidemia, episodes with hypoglycemia and severe recurrent infections, feeding difficulties, failure to thrive, developmental delay, and progressive spasticity with extrapyramidal symptoms. Our patients were further biochemically characterized by a mitochondrial dysfunction and persistent urinary excretion of 3–methylglutaconic acid.

Introduction

3–methylglutaconic aciduria is a group of metabolic disorders biochemically characterized by increased urinary excretion of 3–methylglutaconic acid (3–MGA) and 3–methylglutaric acid. At the present time, four distinct forms have been recognized. 3–methylglutaconic aciduria type I (OMIM 250950) is an inborn error of leucine catabolism and is caused by the isolated defciency of 3–methylglutaconyl–CoA hydratase (3MGH; EC 4.2.1.18)[21, 22, 90]. These pediatric patients display a range of clinical manifestations varying from progressive neurologic deterioration to mild speech delay. Three additional forms of 3–MGA–uria have been documented—type II (Barth syndrome, OMIM 302060); type III (Costeff syndrome, OMIM 258501); type IV ("unspecified," OMIM 250951)—all characterized by normal hydratase activities and mildly elevated urinary levels of 3–MGA. The precise etiology of the increased 3–MGA excretion in these latter subtypes has not been elucidated yet. Among the four types, patients with 3–MGA–uria type 1 excrete the highest levels of 3–MGA.

Barth syndrome is a X-linked disorder presenting in males with cardiomyopathy, cyclic neutropenia, muscle hypotonia, and a normal cognitive function[32, 37]. The disorder is caused by mutations of the Tafazzin gene (*TAZ*)[44]. Patients with Barth syndrome demonstrate decreased levels of total cardiolipins and cardiolipin subclasses, especially tetralineoyl-cardiolipin[42, 105]. A skewed X-inactivation has been reported in obligate carriers, and no female patients have been reported yet[44, 106].

Costeff syndrome is a progressive, late onset disease with bilateral optic atrophy, extrapyramidal symptoms with choreiform movements, ataxia, and spasticity[45, 47]. Patients carry an autosomal dominant mutation in the *OPA3* gene underlying the neuro-ophthalmic presentation[46]. No mitochondrial dysfunction has been reported in Costeff syndrome patients so far.

The diagnosis of 3–MGA–uria type IV is based on the exclusion of the other, well-defined clinical subtypes[9, 23, 44, 46, 55, 107]. This type of mild, non-syndromic 3–MGA–uria is frequently associated with progressive neurological impairment and variable organ dysfunction[107]. Symptoms often present during the first year of life. In some patients clinical and biochemical features of a dysfunctional oxidative phosphorylation have been observed[73, 108]. It is very likely, that this heterogeneous group of patients can be further subdivided into different genetic disorders[55].

We performed biochemical and genetic investigations, including urine organic acid analysis, NMR spectroscopy, measurement of 3–methylglutaconyl–CoA hydratase activity, cardiolipin levels, *OPA3* gene analysis, and measurement of the oxidative phosphorylation, in four children with 3–MGA–uria, presenting with neuroradiological evidence of Leigh disease, hearing loss, recurrent lactic acidemia and hypoglycemia, and other clinical features comparable with a mitochondrial disorder.

As part of the regular work-up for a suspected disorder in the oxidative phosphorylation we applied the diagnostic criteria for mitochondrial disease[85] based on clinical symptoms,

metabolic alterations, and abnormal neuroimaging findings. Serum lactic acid (multiple measurements), pyruvic acid levels, blood gas, serum acylcarnitine, amino acid, and urine organic acid profiles were analyzed in all children.

Patients and methods

Patients

Patients	Patient 1 ♀	Patient 2 ♀	Patient 3[a] ♀	Patient4[b] ♀
Consanguinity	+	-	+	+
Bilateral sensory hearing loss	+	+	-	+
MRI: bilateral hyperdensity of basal ganglia	+	+	+	+
MRI: bilateral atrophy of the cerebrum	+	+	+	+
MRI: bilateral atrophy of the cerebellum	+	-	+	+
Neonatal features of "sepsis"	+	+	+	+
Recurrent infections	+	+	+	+
Failure to thrive	+	+	+	+
Feeding problems	+	+	+	+
Delayed motor development	+	+	+	-
Loss of motor skills	+	+	+	+
Mental retardation	+	+	+	+
Muscle hypotonia, progressive spasticity	+	+	+	+
Extrapyramidal symptoms	+	+	+	+
Epilepsy	-	+	-	-
Abnormal behaviour	-	-	+	+
3-MGA-uria mean level (Excretion range)*	53,5 (31–76)	47,2 (16–68)	132,5 (102-196)	125,0 (97-141)
Lactic aciduria	+	+	+	+
Hypoglycemia	+	+	+	+
Lactic acidemia (controls <2,1 mmol/L)	2,9–3,8	1,8–26	2,0–8,2	0,95–2,3
Clinical diagnostic score[c] [85]	8	8	9	8

Table 1. *Clinical and biochemical features in our patients. [a]Constant laughing; [b]Constant laughing, auto-mutilation; [c]Score 8–12: definite mitochondrial disorder;* (µmol/mmol creatinine, control <20).*

Cerebral spinal fluid investigations have been successfully performed in three patients (patients 1, 2, and 4). The children also underwent a diagnostic protocol of multiple investigations including ECG, chest X-ray, EEG, visual evoked potentials (VEP), acoustic evoked potentials (BAEP), sensory evoked potentials (SEP), and a cranial MRI. Based on the diagnostic score[85], an open muscle biopsy was performed under general anaesthesia in all four children. Molecular genetic analysis for Rett syndrome was requested in patients 3 and 4. The clinical features of the patients are described in Table 1.

All patients were born from an uneventful pregnancy by spontaneous delivery. In two cases decreased child movements were reported. Three couples of the parents were consanguineous and of Turkish origin (Table 1). One child had non-consanguineous Dutch parents. All children presented with severe infections in the neonatal period: two with CMV-infection, one with GBS-sepsis and one without a known causative agent. Except for patient 3 the children had neonatal hypoglycemia, patients 2 and 3 had later recurrent episodes of hypoglycemia, and all four patients had recurrent lactic acidemia from the first weeks of life. No lactic acid elevations were detected in patient 2 and 4 in blood after puberty, however, lactate levels remained repeatedly, significantly increased in the CSF. Feeding problems were present from the neonatal period, making tube feeding necessary in two cases, leading to failure to thrive. The children suffered from recurrent upper respiratory infections without proven alterations of the humoral or cellular immune system. All children (except for patient 4) had a delayed motor development and muscle hypotonia. In patient 1 there was no development at all, patient 4 had a developmental regression from the age of six years and in two of the cases further motor skills were lost during the early childhood (patients 2 and 3). The patients developed severe spasticity, combined with extrapyramidal symptoms. Mental retardation was present in all children. Two of the patients showed behavioural problems with constant laughing, and/or auto-mutilation (Table 1). Patient 1 died at the age of three and patient 2 at the age of 16 years.
The EEG showed no signs of epilepsy in any of the patients, except for a multifocal epilepsy in patient 2. No cardiologic alteration was noted. The MRI of the brain revealed characteristic bilateral hyper-dense lesions of the basal ganglia in all children.Diffuse cerebellar and cerebral atrophy was also observed in three out of the four patients. Visual evoked potential analysis was bilaterally delayed in two patients (patients 1 and 4), however, no optic atrophy was noted. The BAEP studies showed severe sensori-neural hearing loss in three patients, making hearing devices necessary. A severity assessment (Table 1) was applied based on the clinical, metabolic, and neurological (neuro-imaging) alterations. Using the mitochondrial diagnostic score[85] all children scored above 8 points (mitochondrial score 8–12; definite mitochondrial disorder) comparable with the clinical diagnosis of a respiratory chain disorder.

Mutation analysis

PCR amplification of both exons and their flanking intronic DNA sequences of the *OPA3* gene (GenBank Accession No. BC047316) was performed by using the oligonucleotide primers for exon 1-F1(5′-CGTACATACGTACTGACGCA-3′), R1(5′-TAAGCAACCACCT-GACAGG-3′), and for exon 2-F2 (5′-TCCCAGAGCGCAGCCTGAC-3′), R2 (5′-GCCAAGTTGCATCAAGATCCT-3′)[46]. The PCR products were electrophoresed on a 1 % agarose gel, extracted from the gel (Qiaquick Gel Extraction, Qiagen, Valencia, CA) and directly sequenced. Automated sequencing was performed on a Beckman CEQ 2000, by the CEQ Dye Terminator Cycle Sequencing kit, according to the manufacturer's protocol (Beckman Coulter).

Screening for the common mitochondrial point mutations was carried out using Pyro-sequencing™ according to the protocol of the manufacturer. Deletions were analyzed by long template PCR. Additional sequence analysis of the mitochondrial ND genes and sequencing of the nuclear coded structural complex I genes was performed (in patients 1 and 3) on an ABI 3730 DNA analyzer using BigDye terminator chemistry (Applied biosystems, Lekkerkerk a/d IJssel, The Netherlands).

In vitro NMR spectroscopy

Body fluid NMR spectroscopy and quantification of the cis and trans forms of 3–MGA were performed essentially as described elsewhere[19, 92].

Sample preparation

The urine samples were centrifuged before analysis. An aliquot (70 µL for urine) of 20.2 mM trimethylsilyl-2,2,3,3-tetradeuteropropionic acid (TSP, sodium salt; Aldrich) in D_2O was added to 700 µL of the urine, providing a chemical shift reference (δ = 0.00), a concentration reference and a deuterium lock signal. The pH of the urine was adjusted to 2.50 ± 0.05 with concentrated HCl. Finally, 650 µL of the sample was placed in a 5 mm NMR tube (Wilmad Royal Imperial).

One-dimensional ^{1}H NMR spectroscopy

Urine samples were measured at 500 MHz on a Bruker DRX 500 spectrometer equipped with a triple-resonance inverse (TXI) $^1H\{^{15}N, ^{13}C\}$ probehead and equipped with x, y, z gradient coils. ^{1}H spectra were acquired as 128 transients in 32K data points with a spectral width of 6002 Hz. Sample temperature was 298 K and the H_2O resonance was presaturated by single-frequency irradiation during a relaxation delay of 10 s, and a 90° excitation pulse was used. Shimming of the sample was performed automatically on the deuterium signal. To improve the spectral resolution, the samples were spun (7 Hz) during the measurements. The resonance linewidths for TSP and metabolites were <1 Hz. A π/2-shifted sine-bell window function was applied to the FID. Fourier transformation was performed after zero-filling to 64K data points. The phase and the baseline were corrected manually. The *cis* 3–MGA and *trans* 3–MGA resonances and the TSP singlet were fitted semi-automatically with Lorentzian line shapes. The concentration of *cis* 3–MGA and *trans* 3–MGA were calculated from the relative integrals of the fitted line-shapes using the known concentration of TSP[92].

Cardiolipin analysis

Cardiolipin concentrations were measured in blood samples or in cultured skin fibroblasts. High–performance liquid chromatography–electrospray mass spectrometry was applied to quantify total cardiolipin and subclasses of cardiolipin molecular species, foremost tetralineoyl-cardiolipin[42].

Biochemical analysis in muscle and fibroblast samples

Parallel with routine immune-histological analysis and electronmicroscopy, the ATP production from pyruvate oxidation and the activity of the mitochondrial complexes I–V in our patients were measured in a fresh muscle biopsy sample and in cultured fibroblasts as described elsewhere[93, 109].

Results

As shown in Table 1, urine organic acid analysis and in vitro NMR spectroscopy showed an increased urinary excretion of 3–MGA, with a strict 1:1 ratio of the *cis* and *trans* isoforms of 3–MGA. The excretion of 3–MGA in the children was consecutively the following: patient 1 (62, 45, 76, and 31 ;mean 53.5); patient 2 (31, 68, 54, and 16; mean 47.2); patient 3 (107, 196, 115, and 102; mean 132.5); patient 4 (141, 97, 106, and 116; 125.0) µmol/mmol creatinine, respectively (controls: <20 µmol/mmol creatinine). The excretion of 3–hydroxyisovaleric acid in the most recent samples were 46, 10, 16, and 33 µmol/mmol creatinine, respectively; controls: <42 µmol/mmol creatinine. Hence, we conclude that our patients suffer from 3–MGA–uria.

3–MGA–uria type I, Barth syndrome, and Costeff syndrome were excluded as the activity of 3methylglutaconyl-CoA hydratase, the cardiolipin levels, and molecular analysis of the *OPA3* gene, respectively, showed no abnormalities.

Biochemical measurements in muscle	P 1	P 2	P 3	P 4
ATP production from pyruvate oxidation (nmol ATP/h/mU CS) Control range 42–81 nmol/h/mU/CS, N: 22	37	24	43	26
Complex I activity (mU/mU/CS) Control range (70–251 mU/mU/CS), N: 24	65	180	63	112
Complex III activity (mU/mU/CS) Control range (2200–6610mU/mU/CS), N: 22	2422	ND	2994	3040
Complex IV activity (mU/mU/CS) Control range (650–2810mU/mU/CS)	971	1092	1079	1590
Enzyme measurements in fibroblasts				
Complex I activity (mU/mU/CS) Control range (100–310mU/mU/CS)	160	ND	16	ND
Complex III activity (mU/mU/CS) Control range (1320–2610mU/mU/CS)	1810	ND	1487	ND
Complex IV activity (mU/mU/CS) Control range (680–1190mU/mU/CS)	709	ND	571	ND

Table 2. *Biochemical analysis of the mitochondrial function in the muscle biopsy sample and fibroblast lines of the patients. Decreased results in bold. ND = not determined, P= patient.*

The clinical symptoms of our patients are demonstrated in Table 1. As all our patients scored above 8 points on the clinical diagnostic scoring system for mitochondrial disorders a respiratory chain defect was suspected. Indeed, the biochemical analysis of mitochondrial function in the fresh muscle biopsy and/of that of fibroblasts showed reduced oxidative phosphorylation in all four patients. Patient 1 had a slight decrease in the

ATP production from pyruvate oxidation with a decreased activity of the mitochondrial enzyme complex I, but no alterations in fibroblasts. Patients 2 and 4 had a more pronounced decrease in the ATP production, but no alteration in the enzyme complex activities. Patient 3 had normal ATP production, however the activity of complex I in muscle and that of complex I and III in fibroblasts were decreased (Table 2).
Mutation analysis of the MELAS 3243A>G, MERRF 8344A>G and Leigh/NARP 8993T>C point mutations and long template PCR analysis for mitochondrial deletions were normal in all children. Sequence analysis of the mtDNA for mutations in the genes *ND1, ND2, ND3, ND4,* tRNA Leu (uur), tRNA Lys and sequencing the mRNA of the nuclear coded *NDUFS1, NDUFS2, NDUFS4, NDUFS7,* and *NDUFS8* genes detected no mutations in patients 1 and 3.

Discussion

Until now, four types of 3–MGA–uria have been described, three of which have a distinct genetic background. Patients diagnosed with unclassified 3–MGA–uria, or type IV, present with mild increased urinary levels of 3–MGA. Although this type of non-syndromic 3–MGA–uria is frequently associated with progressive neurological impairment and variable organ dysfunction[55], some patients have been reported with variable features of mitochondrial dysfunction, or the biochemical finding of disturbed oxidative phosphorylation [61, 107, 108, 110]. Therefore it is very likely that this heterogenous group of patients could be further subdivided into different genetic disorders[55].
Indeed, here we describe a distinct clinical subtype of 3–MGA–uria. All of our patients are biochemically characterized by a mitochondrial dysfunction and a recurrent mild urinary elevation of 3–MGA. The level of 3–MGA excretion, confirmed by the in vitro NMR analysis, was comparable to that previously described in type IV 3MGA-uria (Table 1). It is also important to note the equal presence of *cis* and *trans* isoforms ("no stereospecifcity") of 3–MGA in the urine of the children.
Engelke et al.[19] described recently a 2:1 *cis/trans* 3–MGA isoform ratio in 3–MG CoA hydratase deficiency (3–MGA–uria type I), and in a second disorder of leucine metabolism; 3-OH-3-methylglutaryl-CoA lyase deficiency, as well. Stereo-specificity has been already observed for 3-methylcrotonyl CoA carboxylase, another enzyme in leucine metabolism. Non-enzymatic isomerization of *cis* and *trans* 3-methylglutaconyl CoA has been also described under alkaline conditions. Further investigations are required to find the background of the different *cis/trans* ratios in the different types of 3–MGA–urias. The lack of stereospecificity in these four patients with mitochondrial dysfunction and 3–MGA–uria further supports the biochemical homogeneity of our clinical group.
3-Methylglutaconyl CoA hydratase deficiency and Barth syndrome were excluded in our patients. Although the children have many features in common with that of Costeff syndrome, except for the optic atrophy, recent studies reported the presence of *OPA3* mutations in patients without the development of optic atrophy[48]. However, sequence

analysis of the *OPA3* gene revealed no mutations in our cases. Moreover, no mitochondrial dysfunction has been reported in patients with Costeff syndrome.

The finding of the neuro-radiological evidence of Leigh(-like) disease is rather specific for oxidative phosphorylation disorders. The combination of Leigh syndrome and hearing loss has been previously described in association with both mitochondrial and nuclear coded mutations. Hypotonia, lactic acidemia, hypoglycemia, feeding difficulties, failure to thrive, developmental delay, progressive spasticity, and extrapyramidal symptoms are less specific, but common features of mitochondrial dysfunction. 3–MGA–uria, however is not a common finding in respiratory chain defects.

Biochemical evaluation confirmed a deficient oxidative phosphorylation in the muscle biopsy and/or in fibroblasts of the four children. Previous reports on mitochondrial dysfunction in association with 3–MGA–uria, however showed a very different clinical presentation in patients[61, 73, 108, 110], suggesting genetic heterogeneity. There are only a few reports on clinically comparable patients with 3–MGA–uria. One patient described by Broide et al.[111] showed clinical signs of sepsis at the age of three days, without a proven underlying infective agent. Hepato-splenomegaly and hepatic dysfunction, later on severe feeding difficulties and failure to thrive occurred. Hypotonia of the trunk and hypertonia of the extremities, neurosensory hearing loss and the neuro-radiological picture of Leigh syndrome with bilateral symmetric changes in basal nuclei region have been noted. The mitochondrial respiratory chain enzyme activity in muscle biopsy was reduced by 50 %[111].

In addition al Aqeel et al.[112] described patients with 3–MGA–uria with neonatal acidosis and hypoglycemia. In one case the clinical features were very similar to that of our patients, including a possible sepsis, myoclonus epilepsy, and deafness. Brain imaging showed global cerebral/cerebellar atrophy, loss of the cerebral white matter, and bilateral putaminal necrosis, suggestive for Leigh-like syndrome. One of the patients died at three years of age. Unfortunately, no data concerning oxidative phosphorylation were given.

So far, no underlying mutation has been discovered in our patients. The presence of consanguinity in three out of four cases could be comparable with an autosomal recessive inheritance. We have not found the etiology of the mitochondrial dysfunction associated increased 3–MGA excretion either. In the lack of a proven inborn error in the leucine metabolism one might hypothesize that the metabolic abnormalities occur due to an interaction between different epigenetic factors and the primary disease causing gene defect.

Based on the association of the clinical features and biochemical abnormalities we suggest that our patients form a distinct clinical subgroup of deficient oxidative phosphorylation and 3–MGA–uria; with deafness, encephalopathy, and neuro-radiological evidence of Leigh-like disease (MEGDEL association). Further genetic mapping studies might be helpful for the elucidation of the etiology within the heterogeneous group of 3–MGA–uria type IV.

Chapter 6

Mutations in the phospholipid remodeling gene *SERAC1* impair mitochondrial function and intracellular cholesterol trafficking and cause dystonia and deafness

S. Wortmann[1,2], F. Vaz[3], T. Gardeitchik[1,2,4], L. Vissers[2,5,6], G. Renkema[1,2,7], J. Schuurs-Hoeijmakers[5], W. Kulik[3], M. Lammens[8], C. Christin[9], L. Kluijtmans[4], R. Rodenburg[1,2,4], L. Nijtmans[1,2], A. Grünewald[10], C. Klein[10], J. Gerhold[1,2], T. Kozicz[11,12], P. van Hasselt[13], M. Harakalova[14], W. Kloosterman[14], I. Barić[15], E. Pronicka[16], S. Kalkan Ucar[17], K. Naess[18], K. Singhal[19], Z. Krumina[20], C. Gilissen[5], H. van Bokhoven[5,6,11], J. Veltman[5], J. Smeitink[1,2], D. Lefeber[2,4,21], J. Spelbrink[1,2,22], R. Wevers[2,4*], E. Morava[1,2*], A. de Brouwer[5*]

[1]Department of Pediatrics, [2]Institute of Genetic and Metabolic Disease (IGMD), [4]Laboratory of Genetic, Endocrine and Metabolic Diseases (LGEM), Department of Laboratory Medicine, [5]Department of Human Genetics, [6]Nijmegen Centre for Molecular Life Sciences, [7]Centre for Systems Biology and Bioenergetics, [8]Department of Pathology, [21]Department of Neurology, Radboud University Nijmegen Medical Centre, [11]Donders Institute for Brain, Cognition and Behaviour, [12]Department of Animal Physiology, Radboud University Nijmegen, Nijmegen, [3]Department of Clinical Chemistry and Pediatrics, Laboratory Genetic Metabolic Disease, Academic Medical Center, [9]Department of Clinical Epidemiology, Biostatistics and Bioinformatics, Bioinformatics Laboratory, Academic Medical Center, University of Amsterdam, Amsterdam, The Netherlands.[10]Section of Clinical and Molecular Neurogenetics, Department of Neurology, University of Lübeck, Lübeck, Germany. [13]Department of Metabolic Diseases, Wilhelmina Children's Hospital Utrecht, [14]Department of Medical Genetics, University Medical Center Utrecht, Utrecht, The Netherlands. [15]Department of Pediatrics, University Hospital Centre Zagreb and School of Medicine, Zagreb, Croatia. [16]Department of Metabolic Diseases, Children's Memorial Health Institute, Warsaw, Poland. [17]Department of Pediatrics, Ege University Faculty of Medicine, Izmir, Turkey. [18]Department of Pediatric Neurology, Karolinska University Hospital, Stockholm, Sweden. [19]Department of Neurology, All India Institute of Medical Science, Delhi, India. [20]Medical Genetics Clinic, Children's University Hospital, Riga, Latvia. [22]Institute of Biomedical Technology and Tampere University Hospital, Pirkanmaa Hospital District, University of Tampere, Tampere, Finland. *Equal contribution.

After Nat Genet. 2012;44(7):797-802.

Abstract

Using exome sequencing, we identify *SERAC1* mutations as the cause of MEGDEL syndrome, a recessive disorder of dystonia and deafness with Leigh-like syndrome, impaired oxidative phosphorylation and 3–methylglutaconic aciduria. We localized SERAC1 at the interface between the mitochondria and the endoplasmic reticulum in the mitochondria-associated membrane fraction that is essential for phospholipid exchange. A phospholipid analysis in patient fibroblasts showed elevated concentrations of phosphatidylglycerol-34:1 (where the species nomenclature denotes the number of carbon atoms in the two acyl chains:number of double bonds in the two acyl groups) and decreased concentrations of phosphatidylglycerol-36:1 species, resulting in an altered cardiolipin subspecies composition. We also detected low concentrations of bis(monoacylglycerol)-phosphate, leading to the accumulation of free cholesterol, as shown by abnormal filipin staining. Complementation of patient fibroblasts with wild-type human SERAC1 by lentiviral infection led to a decrease and partial normalization of the mean ratio of phosphatidylglycerol-34:1 to phosphatidylglycerol-36:1. Our data identify SERAC1 as a key player in the phosphatidylglycerol remodeling that is essential for both mitochondrial function and intracellular cholesterol trafficking.

The lipid bilayer surrounding cells and organelles consists mainly of phospholipids, such as the common phospholipids phosphatidylcholine and phosphatidylethanolamine and also the less abundant specialized phospholipids cardiolipin and bis(monoacylglycerol)phosphate (Figure 1).

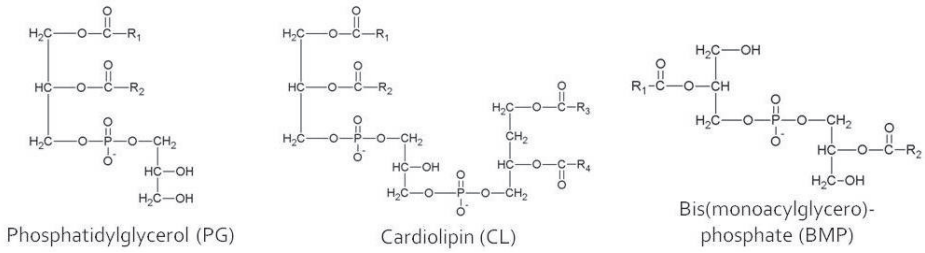

Figure 1. *Structural formula of key phospholipids.*

Bis(monoacylglycerol)phosphate and cardiolipin are both synthesized from phosphatidylglycerol, which is made *de novo* in mitochondria[113, 114]. Bis(monoacylglycerol)-phosphate is an anionic phospholipid that is necessary for intracellular cholesterol trafficking[115]. Cardiolipin is essential for the stability and catalytic activity of mitochondrial membrane proteins and is key for apoptosis[116, 117]. Abnormal cardiolipin acyl chain composition and accumulation of monolysocardiolipins results in Barth syndrome (MIM# 302060)[41], a 3–methylglutaconic aciduria (3–MGA–uria) with (cardio)myopathy, neutropenia and oxidative phosphorylation (OXPHOS) dysfunction [32, 103]. Barth syndrome is caused by mutations in *TAZ*, which encodes tafazzin, a transacylase that is required for cardiolipin remodelling[44]. Here we identify the causative genetic defect in 15 individuals with MEGDEL syndrome (Supplementary Note), which we have previously defined as 3–MGA–uria with impaired OXPHOS, deafness, encephalopathy, Leigh-like magnetic resonance imaging (MRI), progressive spasticity and dystonia[11, 68].

MEGDEL syndrome was predicted to be an autosomal recessive disorder based on its occurrence in one large pedigree with two affected siblings (patients 6 and 7) and an affected first cousin (patient 3) and in several individuals from consanguineous families (Supplementary Table 1). To find the underlying genetic cause of the syndrome, we sequenced the exomes (~21,000 genes) of two affected individuals using the SureSelect 50 Mb human exome kit and a multiplexed sequence analysis on a SOLiD 4 system. For this analysis, we selected the affected cousin (patient 3) and an unrelated subject (patient 5), who is the affected child of a consanguineous marriage. We applied several filtering steps in which we excluded all nongenic, intronic and synonymous variants, other than those occurring at canonical splice sites, and focused on variants not reported in dbSNP or found in in-house–sequenced exomes under the assumption of an autosomal recessive inheritance pattern[118]. Only a single gene, *SERAC1* (NM_032861.3), contained homozygous variants in both affected individuals (Supplementary Table 2). For patient 3, 73 of 74 (99%)

reads showed a C>T transition at chromosome 6 (hg19):g.158,567,859 indicating a homozygous r.442C>U transition at the mRNA level that is predicted to result in a premature stop codon (p.Arg148X; Supplementary Figure 1). Similarly, for patient 5, 50 of 52 (96%) reads showed a G>C substitution at chromosome 6 (hg19):g.158,538,758 in the canonical donor splice site of exon 13. Of note, both mutations were located in homozygous regions of size 5.8 Mb and 9.7 Mb, respectively, as shown by homozygosity mapping using 250K arrays (Supplementary Table 3). Conventional Sanger sequencing confirmed the presence of these mutations as well as their homozygous state in patients 3 and 5 and in the two cousins of patient 3. We identified neither of these two mutations in 369 healthy ethnically matched controls.

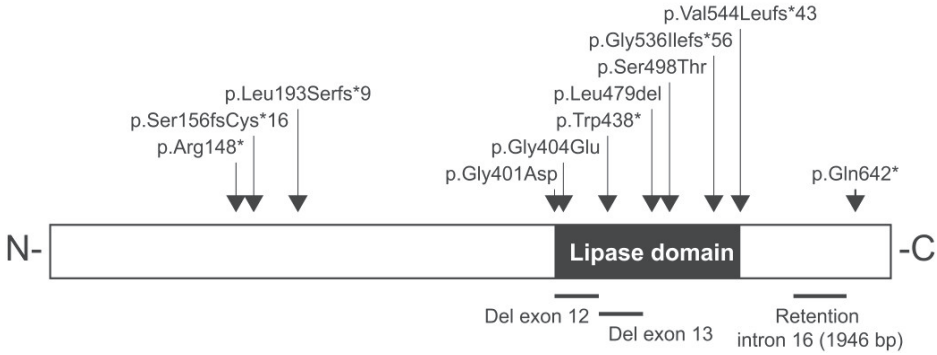

Figure 2. *Schemetic representation of human SERAC1 showing the positions of all mutations identified. The black box represents the lipase/ esterase domain. Del = deletion.*

An analysis of the protein coding sequence of *SERAC1* in 11 additional unrelated individuals clinically diagnosed with MEGDEL syndrome identified 12 additional homozygous and compound heterozygous mutations that were absent in 369 healthy ethnically matched controls. In total, we identified 14 different mutations in 15 affected individuals from 13 families, including three nonsense, three canonical splice site, four frameshift and three missense mutations and one in-frame deletion of a single amino acid (Table 1, Figure 2, Supplementary Table 4 and Supplementary Note). We found the two canonical splice site mutations in exons 13 and 16 and the missense mutation in exon 14 (c.1493G>C) in two, three and two unrelated subjects, respectively, indicating common ancestry, which was confirmed by their matching haplotypes (Supplementary Figure 2 and Supplementary Note). In addition, an mRNA transcript analysis showed that the exon 13 splice site mutations resulted in skipping of this exon (Supplementary Figure 3). Eight mutations resulted in a premature termination codon more than 55 nt before the last exon-exon boundary and, hence, should give rise to nonsense-mediated decay of the *SERAC1* mRNA. Indeed, a quantitative PCR analysis of *SERAC1* mRNA levels in fibroblasts from patients 3

and 5 showed 12% ($P < 0.0001$) and 40% ($P < 0.029$) of the *SERAC1* levels in control fibroblasts, respectively (Supplementary Figure 4 and Supplementary Note).

Patient	Mutation (nt)	Mutation (aa)	Mutation type	(Predicted) effect
3,6,7	c.442C>T	p.Arg148*	Nonsense	NMD
15	c.466_467insGCGGGAAATGT	p.Ser156fsCys*16	Frameshift	NMD
14	c.576delT	p.Leu193Serfs*9	Frameshift	NMD
1	c.1167_1170delTCAG	exon 12 skipping	Canonical splice site	NMD
13	c.1202G>A	p.Gly401Asp	Missense	Impaired Lipase function
8	c.1211G>A	p.Gly404Glu	Missense	Impaired Lipase function
10	c.1309_1313dupACATG	p.Trp438*	Nonsense	NMD
5,12	c.1403+1G>C	exon 13 skipping	Canonical splice site	NMD
4	c.1435_1437delCTT	p.Leu479del	In frame deletion of single aa	Impaired Lipase function
14,15	c.1493G>C	p.Ser498Thr	Missense	Impaired Lipase function
9	c.1598_1599dupATAGTGTCCCTCATCAT	p.Gly536Ilefs*56	Frameshift	NMD
2	c.1627_1628dupTC	p.Val544Leufs*43	Frameshift	NMD
10,11,13	c.1822_1828+10delTCAGCAGGTATTCACTCinsACCAACAGG	intron 16 retention	Canonical splice site	Truncation of last 45 amino acid residues
11	c.1924C>T	p.Gln642*	Nonsense	Truncation of last 13 amino acid residues

Table 1. *Mutations in SERAC1 in individuals with MEGDEL syndrome. Overview of all mutations found in SERAC1 in the different patients. Both the mutations and their (predicted) effects are given. bp=basepairs (counting only the protein coding sequence), nt=nucleotide, aa=amino acid, NMD=Nonsense-mediated mRNA decay.*

SERAC1 (serine active site containing 1) encodes a protein with a serine-lipase domain that is a member of the PGAP-like protein domain family (PFAM PF07819). Nothing is known about the function of this protein, although the presence of a conserved lipase domain containing the consensus lipase motif GXSXG[119] strongly suggests a function in lipid metabolism. SERAC1 is present in all eukaryotes and is highly conserved, especially its lipase domain (Supplementary Table 5 and Supplementary Figure 5). The three amino acids (Gly401, Gly404 and Ser498) affected by the missense mutations and Leu479, which was deleted in one affected individual, are all located within this lipase domain and are fully conserved down to the fruit fly (Figure 2 and Supplementary Figure 5). Both the SIFT and PolyPhen-2 programs[120, 121] predict these changes to be detrimental to protein function. Moreover, Ser498 is the serine of the consensus lipase motif GXSXG (Supplementary Figure 5)[119, 120].

Barth and MEGDEL syndromes share 3–MGA–uria and mitochondrial dysfunction. This, in combination with the presence of a lipase domain in SERAC1, formed the rationale for our phospholipid analysis in MEGDEL fibroblasts (Figure 3). The concentrations and acyl chain compositions of the major phospholipid classes (phosphatedylcholine, phosphatidylethanolamine, phosphatidylserine and phosphatidyl-inositol; data not shown) were normal. However, we found higher concentrations of phosphatidylglycerol-34:1 and lower concentrations of phosphatidylglycerol-36:1 species in all five affected individuals analyzed as compared to ten control fibroblast cell lines (Figure 3 a,b). A more detailed analysis of the mass spectrometry fragmentation spectra of phosphatidylglycerol-34:1 and phosphatidylglycerol-36:1 showed that the most abundant species of these phosphatidylglycerol molecules corresponded to 1-palmitoyl(16:0)-2-oleoyl(18:1) phosphatidylglycerol and 1-stearoyl(18:0)-2-oleoyl(18:1) phosphatidylglycerol (Supplementary Figure 6a). The median phosphatidylglycerol-34:1 concentration in patient fibroblasts was 220% of that in control fibroblasts, whereas the median phosphatidylglycerol-36:1 concentration in patient cells was 20% of that in control fibroblasts, resulting in a mean ratio of phosphatidylglycerol-34:1 to phosphatidylglycerol-36:1 of 8.4 in patient fibroblasts as compared to 0.7 in control fibroblasts, justifying this ratio as a clinically relevant diagnostic marker (Figure 3b).

In contrast to individuals with Barth syndrome, the total concentrations of cardiolipin were unaltered in fibroblasts from patients with MEGDEL syndrome (Figure 3b). However, there were differences in cardiolipin species composition in the patient fibroblasts compared to the control fibroblasts. Patients with MEGDEL syndrome had significantly higher concentrations of cardiolipin-66:3, cardiolipin-66:4, cardiolipin-68:3, cardiolipin-68:4 and cardiolipin-68:5 (Figure 3), which are derived from phosphatidylglycerol-34:1, than control individuals, whereas other cardiolipin species were the same between the two groups (Supplementary Figure 7). The inability to convert phosphatidylglycerol-34:1 to phosphatidylglycerol-36:1 leads to the accumulation of phosphatidylglycerol-34:1 and subsequent incorporation into cardiolipin.

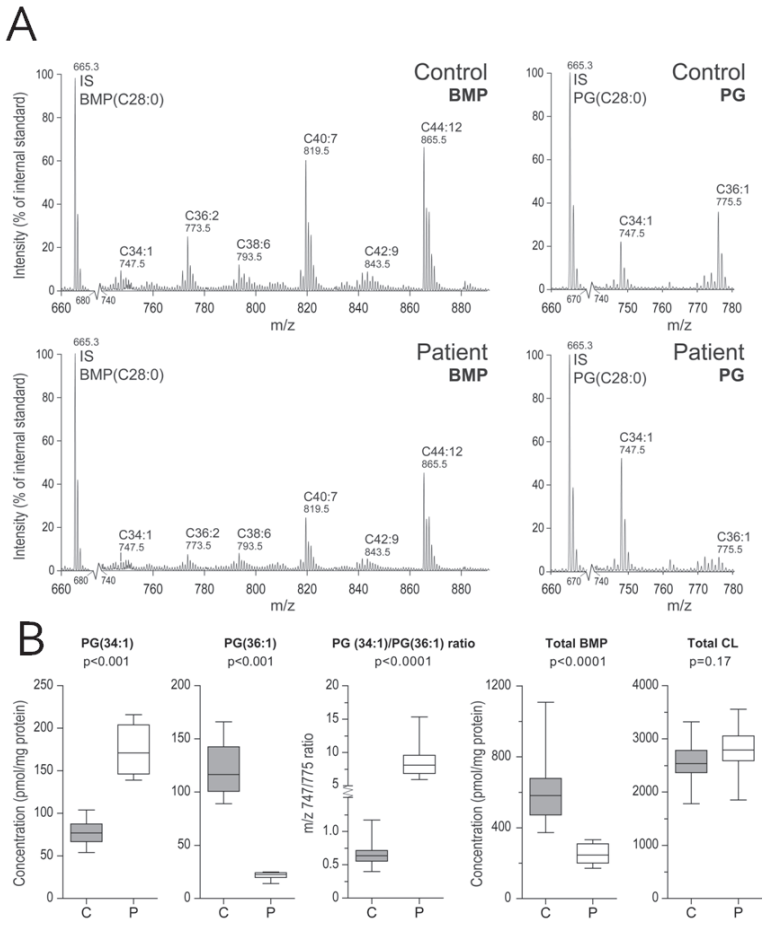

Figure 3 A, B. *SERAC1 and its role in phosphatidylglycerol remodeling. A) Representative high-performance liquid chromatography (HPLC) tandem mass spectrometry spectra of bis(monoacylglycerol)phosphate (BMP) and phosphatidylglycerol (PG) in fibroblasts. In patients with MEGDEL syndrome, phosphatidylglycerol-34:1 accumulates, phosphatidylglycerol-36:1 is deficient and bis(monoacylglycerol)phosphate concentrations are low. B) Box and whisker plots (minimum and maximum) of phosphatidylglycerol-34:1 and phosphatidylglycerol-36:1 concentrations, the ratio of phosphatidylglycerol-34:1 to phosphatidylglycerol-36:1, total concentrations of bis(monoacylglycerol)phosphate and total concentrations of cardiolipin (CL) in controls (C, n = 10) and patients (P, n = 5).*

In Barth syndrome, it is firmly established that cardiolipin alterations lead to OXPHOS dysfunction through different mechanisms, for example, by affecting the stability and assembly of inner mitochondrial membrane respiratory chain complexes[41]. Therefore, the alteration in the concentrations of cardiolipin species is probably directly related to the

OXPHOS dysfunction present in different tissues of patients with MEGDEL syndrome (Supplementary Tables 1 and 6). It is of note that the OXPHOS abnormalities in MEGDEL syndrome seem less pronounced than those in Barth syndrome, which may relate to the substantial differences in total cardiolipin content between the two diseases and the fact that monolysocardiolipins accumulate in Barth syndrome but are normal in patients with MEGDEL syndrome. Morphologically, however, we found an aggregation of degrading mitochondria in the muscle of patients with MEGDEL syndrome using electron microscopy (Supplementary Figure 8). We evaluated autophagy and mitophagy under basal conditions and under induced cellular stress in fibroblasts by analyzing the concentrations of mitochondrial marker proteins (GRP75 and $MTCO_2$) and autophagy and mitophagy marker proteins (LC_3, Mfn2, P62 and Parkin) and found no differences between patients and controls (Supplementary Figure 9 and Supplementary Note). Mitochondrial fusion and fission were also normal in patients with MEGDEL syndrome, as evidenced by semiquantitative immunohistochemistry and a quantitative PCR analysis of the fusion and fission protein markers Fis1, Drp1, Opa1 and Mfn1 (Supplementary Figure 10 and Supplementary Note).

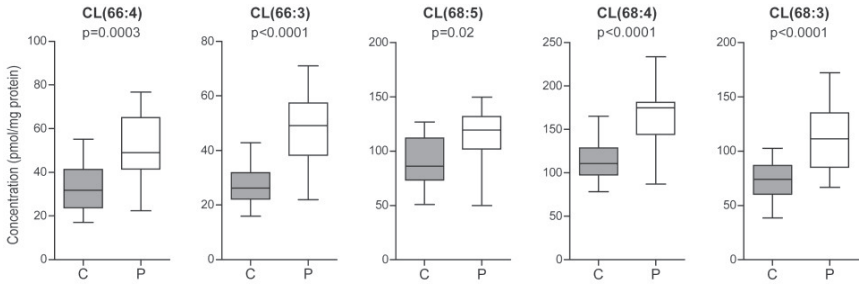

Figure 4. *Cardiolipin species composition in patients and controls. Box and whisker plots (minimum and maximum) showing the concentrations of the cardiolipin (CL) species cardiolipin-66:3, cardiolipin-66:4, cardiolipin-68:3, cardiolipin-68:4 and cardiolipin-68:5 in control (C, n = 10) and patient (P, n = 5) fibroblasts. These specific cardiolipin species are significantly more abundant in patients than in controls. No significant differences were found in the other cardiolipin species: cardiolipin-70:7 through cardiolipin-70:5, cardiolipin-72:8 through cardiolipin-72:5 and cardiolipin-74:8 through cardiolipin-74:6.*

Besides changes in phosphatidylglycerol and cardiolipin species composition, the median bis(monoacylglycerol)phosphate concentration in patients was 40% of that in controls (Figure 3 B). The four most abundant bis(monoacylglycerol)phosphate species (34:1, 36:2, 40:7 and 44:12) had identical acyl chain composition in patients and controls (Supplementary Figure 6 B). Low bis(monoacylglycerol)phosphate concentrations are known to lead to free cholesterol accumulation in late endosomes[122]. We assessed the accumulation of unesterified cholesterol in patient and control fibroblasts. For comparison, we used Niemann-Pick type C (NPC) fibroblasts, which are known to accumulate

unesterified cholesterol[123]. All three patients with MEGDEL syndrome tested clearly had more filipin staining than the control (Figure 5).

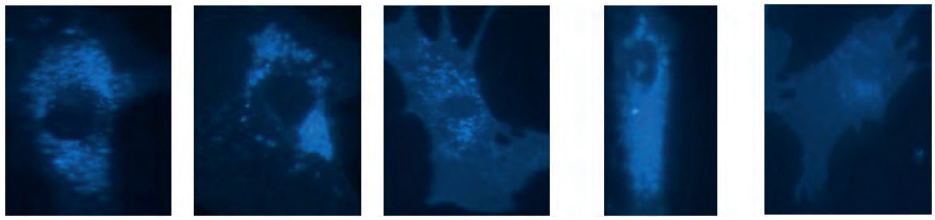

NPC MEGDEL P_3 MEGDEL P_4 MEGDEL P_5 Healthy control

Figure 5. *Filipin staining of fibroblasts from patients with MEGDEL syndrome, a patient with Niemann-Pick disease type C (NPC) as positive control and a healthy control showing background fluorescence. Scale bar, 5 μm.*

Figure 6 A,B,C. *Subcellular localization of SERAC1. A,B) Immunodetection of SERAC1 in total cell lysate (TC), cytoplasmic fraction (CF), crude mitochondrial fraction (CMF) and ER of HeLa (A) or HEK293 (B) cells showing SERAC1 enrichment in the CMF and ER. Calnexin (MAM-ER marker), NDUFS3 and COXII (inner mitochondrial membrane markers) and creatine kinase-B (CK-B; cytoplasmic marker) were used for comparison. C) Immunodetection of SERAC1 in CMFs subjected to no or mild digitonin treatment and incubated with or without proteinase K (Prot K) in the absence or presence of Triton X-100 showing SERAC1 association with the mitochondria, ER and MAMs of HEK293 cells. Calnexin, TOM20 (mitochondrial outer membrane marker) and NDUFS3 were used for comparison.*

In general, the localization of the fluorescent signal seemed more prominent in the perinuclear region of the MEGDEL fibroblasts as compared to the NPC fibroblasts, which showed an abundance of small aggregates with positive fluorescence throughout the cell. These results suggest an accumulation of unesterified cholesterol in patients with MEGDEL syndrome. This conclusion is supported by the lipid storage found in the muscle of patients with MEGDEL syndrome (Supplementary Figure 8). Because intracellular accumulation of cholesterol may lead to lower blood cholesterol concentrations, we reinvestigated all subjects with mutations in *SERAC1*. Notably, 4 of 11 patients with MEGDEL syndrome in whom cholesterol was measured had a cholesterol concentration below the lower reference range limit, but for the total group of 11 patients in this study, the serum cholesterol concentrations were not statistically different from controls (Supplementary

Table 1). *SERAC1* is ubiquitously expressed, with markedly high expression in fetal muscle and in adult brain (Supplementary Figure 11 and Supplementary Note). Prediction of the subcellular localization of SERAC1 by PSORT II suggested a mitochondrial localization (a 43.5% chance of mitochondrial localization compared to a 30.4% chance of cholesterol may lead to lower blood cholesterol concentrations, we reinvestigated all subjects with mutations in *SERAC1*. Notably, four of 11 patients with MEGDEL syndrome in whom cholesterol was measured had a cholesterol concentration below the lower reference range limit, but for the total group of 11 patients in this study, the serum cholesterol concentrations were not statistically different from controls (Supplementary Table 1).

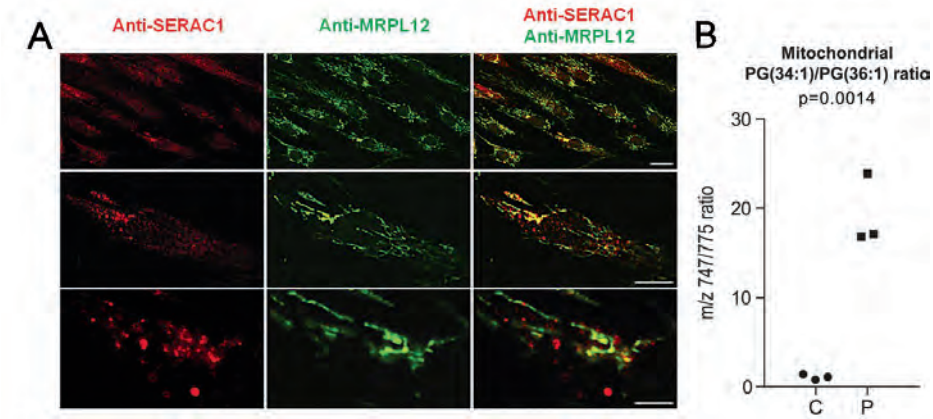

Figure 7 A, B. *Subcellular localization of SERAC1. A) Partial colocalization of SERAC1 with the mitochondrial matrix marker MRPL12 in control fibroblasts showing SERAC1 in close proximity to mitochondria. Scale bar, upper two rows, 5 µm; bottom row, 2.5 µm. The bottom row shows the images at the highest magnification. B) Ratio of phosphatidylglycerol (PG)-34:1 to phosphatidylglycerol-36:1 in the CMF of patient (P, n = 3) and control fibroblasts (C, n = 3).*

We postulate that phosphatidyl-glycerol-34:1 is the primary precursor of bis(monoacylglycerol)phosphate species and that the inability to produce phosphatidylglycerol-36:1 from phosphatidylglycerol-34:1 causes bis(monoacylglycerol)phosphate deficiency (Figure 8).

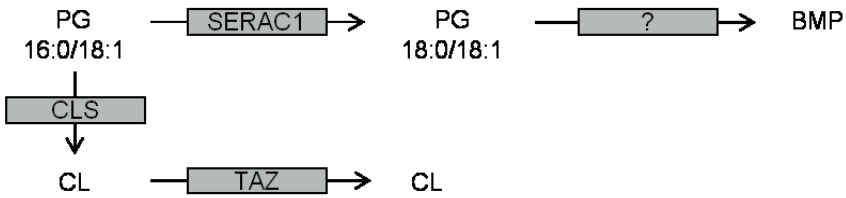

Figure 8. *The role of SERAC1 in phosphatidylglycerol remodeling. CLS = cardiolipin synthase; IS = internal standard; TAZ = tafazzin.*

SERAC1 is ubiquitously expressed, with markedly high expression in fetal muscle and in adult brain (Supplementary Figure 11 and Supplementary Note). Prediction of the subcellular localization of SERAC1 by PSORT II suggested a mitochondrial localization (a 43.5% chance of mitochondrial localization compared to a 30.4% chance of cytosolic localization and an 8.7% chance of nuclear localization). Accordingly, a western blot analysis showed that SERAC1 was absent from the cytosol (Figure 6 A) but was enriched in the crude mitochondrial and endoplasmic reticulum (ER) fractions compared to total cell lysates (Figure 6 A, B and Supplementary Note). Subsequent treatment of crude mitochondrial fractions with proteinase K showed that the amount of SERAC1 decreased, whereas the outer mitochondrial membrane protein marker TOM20 was fully degraded (Figure 6 C). However, calnexin, an ER marker protein that is enriched in the mitochondria-associated membranes (MAMs)[124] that co-purify with the crude mitochondrial fraction[125], showed a similarly confined protection pattern as SERAC1 after proteinase K treatment.

This finding, together with the SERAC1 enrichment in the ER (Figure 6 B), suggests that SERAC1 localizes at the ER and at the ER-mitochondria interface. This is supported by immunohistological studies in which SERAC1 was found in close proximity to the mitochondria but only partially colocalized with the mitochondrial matrix protein MRPL12 (Figure 7 A). In addition, the difference in the mean ratio of phosphatidylglycerol-34:1 to phosphatidylglycerol-36:1 between patients and controls was more evident in the crude mitochondrial fraction compared to in the total fibroblasts (19.3 compared to 8.4, respectively; Figure 7 B). This indicates that phosphatidylglycerol remodeling probably occurs in this fraction, which is in line with the proposed intracellular localization of SERAC1 at the interface of the two compartments and the fact that the exchange of phospholipids has been shown to be a key function of the MAM[126].

The localization of SERAC1 at the contact sites between the ER and mitochondria, the low concentrations of phosphatidylglycerol-36:1 and the accumulation of phosphatidylglycerol-34:1 in MEGDEL fibroblasts indicate that SERAC1 catalyzes the remodeling of phosphatidylglycerol and is involved in the transacylation-acylation reaction to produce phosphatidylglycerol-36:1. The altered acyl chain composition of the affected phosphatidylglycerol molecules suggests that SERAC1 catalyzes the transfer of stearic acid (18:0) from an as yet unknown donor to 1-palmitoyl(16:0)-2-oleoyl(18:1) phosphatidylglycerol to produce 1-stearoyl(18:0)-2-oleoyl(18:1) phosphatidylglycerol and, thus, effectively exchanges palmitic acid (16:0) on the sn-1 position of phosphatidylglycerol-34:1 for stearic acid (18:0).

To support this role of SERAC1 in phosphatidylglycerol remodeling, we successfully complemented two patient fibroblast lines with wild-type human SERAC1 by lentiviral infection, which led to a decrease and partial normalization of the mean ratio of phosphatidylglycerol-34:1 to phosphatidylglycerol-36:1 from 8.6 to 4.0 (Figure 9), directly linking mutations in *SERAC1* to compromised phosphatidylglycerol remodeling. We found no differences in the concentrations and subspecies distribution of other phospholipids

(phosphatidylcholine, phosphatidylethanolamine and phosphatidylserine; Supplementary Figure 12).

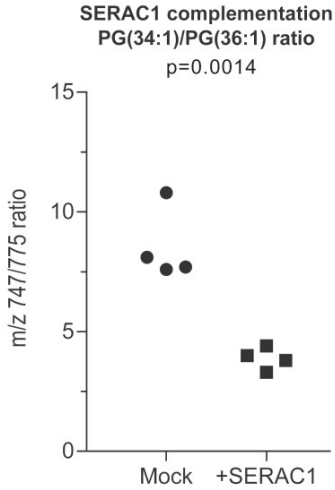

Figure 9. *The ratio of phosphatidylglycerol (PG)-34:1 to phosphatidylglycerol-36:1 in patient fibroblasts complemented with wild-type SERAC1. Fibroblasts from patients were infected with a mock vector (n = 4) or an expression vector containing wild-type SERAC1 (+SERAC1, n = 4). Complementation of SERAC1 (for western blot see Supplementary Figure 13) restores the ratio of phosphatidylglycerol-34:1) to phosphatidylglycerol-36:1.*

In conclusion, mutations in *SERAC1* cause a clinically recognizable progressive neurological deafness dystonia syndrome (MEGDEL). MEGDEL syndrome is a phospholipid remodeling disorder, but it also classifies as a defect in intracellular cholesterol trafficking. Our data identify SERAC1, a protein located at the contact sites between mitochondria and the ER, as a key player in the remodeling of phosphatidylglycerol, particularly of those species needed for the synthesis of bis(monoacylglycerol)phosphate. SERAC1 is crucial for both mitochondrial function and intracellular cholesterol trafficking. This study identifies SERAC1 as catalyzing the first enzymatic reaction in the as yet unknown bis(monoacylglycerol)phosphate biosynthetic pathway.

Methods

Library generation

Exome enrichment required 3 µg of genomic DNA, and an AB SOLiD optimized SureSelect 50 Mb human exome kit (Agilent) was used for enrichment, representing exonic sequences for ~21,000 genes (including >99% genes from the September 2009 version of CCDS and >95% of the RefSeq genes and transcripts from the June 2010 version of RefSeq, as specified by the company). The manufacturer's instructions (version 1.5) for enrichment

were followed, with a minor modification being a reduction of the number of post-hybridization ligation-mediated PCR cycles from 12 to 9. To allow for multiplexing libraries before sequencing, we used post-hybridization sample barcodes (Agilent) that were compliant with SOLiD sequencing technology.

SOLiD sequencing

Enriched exome libraries were equimolarly pooled in sets of four based on a combined library concentration of 0.7 pM. Subsequently, the obtained pool was used for emulsion PCR and bead preparation using the EZ Bead system according to the manufacturer's instructions (version 05/2010; Life Technologies). For each pool of four exome libraries, a full sequencing slide was used on a SOLiD 4 System (Life Technologies), thereby anticipating that all four samples would be represented by 25% of the total beads sequenced on the slide.

Mapping of variants

Color space reads were mapped to the hg19 reference genome with the SOLiD bioscope software v1.3, which uses an iterative mapping approach. Single nucleotide variants were subsequently called by the diBayes algorithm 1 using high stringency settings and requiring calls on each strand. Small insertions and deletions (indels) were detected using the SOLiD Small InDel Tool. Variants and indels were selected using strict quality settings, which included the presence of at least five unique variant reads (different start sites), as well as the variant being present in at least 20% of all reads. All called variants and indels were combined and annotated using a custom analysis pipeline, resulting in HCDiff files for each patient.

Custom bioinformatic analysis pipeline

For the filtering steps, we excluded all nongenic, intronic (other than canonical splice sites) and synonymous variants, reducing the number of variants to an average of 5,363 per patient. Then, all known variants were excluded by comparison with data from dbSNPv132 (>30 million variants) as well as with data from our in-house variant database.

At the time of this study, this in-house database contained variants from 177 in-house–performed exomes, contributing a further 332,849 unique variants. Of note, if the variant observed in a patient occurred at a genomic position that was known in dbSNPv132 but the change was different from that in dbSNP (for example, A>C in dbSNP but A>T in the patient), the variant was not excluded from analysis. The filtering step using these data further reduced the average number of variants to 227 per patient. Next, as a recessive disease model was expected and given the assumption of a common ancestral allele (based on parental consanguinity), we prioritized the variants according to the percentage of variant reads. To do this, we used the threshold of >70% variant reads as an indicator for homozygous variants. This prioritization resulted in an average of 19 variants per patient.

Homozygosity mapping

Genomic DNA was extracted from peripheral blood lymphocytes using standard salting-out procedures[127]. Genotyping was performed using the Affymetrix NspI 250K SNP array. All SNP array experiments were performed and analyzed according to the manufacturer's protocols (Affymetrix). Homozygosity mapping was performed using PLINK v1.06 using a homozygous window of 50 SNPs and tolerating two heterozygous SNPs and ten missing SNPs per window.[128]

Lipid analysis

Fibroblast cell lines were harvested by centrifugation at 200g for 5 min at room temperature, washed once with PBS, pelleted by centri-fugation at 200g for 5 min at room temperature and snap frozen in liquid nitrogen. The concentrations of the following phospholipids were analyzed: phosphatidylglycerols, bis(monoacylglycerol)phosphate, phosphatidic acids, phosphatidylcholines, phosphatidylethanolamines, phosphatidyl-serines, phosphatidylinositols, cardiolipins, sphingomyelines and their lyso-analog species. The relative abundances of the species in the sample extracts were determined by HPLC tandem mass spectrometry using a Surveyor HPLC system hyphenated to a TSQ Quantum AM tandem mass spectrometer (Thermo Finnigan Corporation). The mass spectrometer was operated alternating in the negative and positive ion electrospray ionization mode in consecutive runs, as described in detail previously[129]. The method was adjusted by adding two extra internal standards (C14:0-phosphatidylglycerols and C14:0-bis(monoacylglycerol)phosphate, m/z 665.3) for more accurate quantification of the phosphatidylglycerols and bis(monoacylglycerol)phosphate. Acyl-chain compositions were determined by the product-ion scans of the respective quasi-molecular ions.

Filipin staining of fibroblasts

Fibroblasts were grown on coverslips and washed three times with PBS. The cells were fixed in 3% paraformaldehyde and 2% glutaraldehyde in PBS for 1 h in the dark. After three washes with PBS, the cells were incubated with filipin solution (5% in dimethylformamide and PBS, 1:50 (v/v)) for 1 h in the dark[130]. After washing three times in 0.5% bovine serum albumin in PBS, cells on the coverslips were washed once with ultrapure water and inserted into a drop of glycerin on a microscope glass slide. Digital images were captured with a Carl Zeiss Axioskop-20 (Carl Zeiss).

Colocalization studies

Fibroblasts on coverslips were washed 4× for 15 min in PBS, followed by incubation in 0.5% Triton X-100 (Sigma-Aldrich) in PBS for 30 min. After a short rinse in PBS, cells were incubated in 2% normal donkey serum (NDS) in PBS for 30 min, followed by an incubation in a mixture of primary antisera in 2% NDS in PBS for 16 h at room temperature. The following sera were used: polyclonal (rabbit) anti-SERAC1 (1:100; HPA025716; Sigma-Aldrich) and monoclonal (mouse) anti-MRPL12 (1:750; #ab58334; Abcam). After several washes in

PBS, a secondary antiserum cocktail consisting of Cy2-conjugated anti-mouse IgG (1:100) and Cy3-conjugated anti-rabbit IgG (1:100) (Jackson Immunoresearch Laboratories) were applied in blocking agent tyramide signal amplification (B/TSA) in PBS for 2.5 h at room temperature. After several rinses in PBS, cells were coverslipped with Fluorsave (Calbiochem) and studied with a Leica confocal laser scanning microscope (Leica Microsystems).

Fluorescence semiquantitative immunohistochemistry

For fluorescent immunohistochemistry, fibroblasts on culture glass were washed six times for 10 min at room temperature and incubated in 0.5% Triton X-100 in blocking buffer consisting of PBS and 2% NDS (Jackson Immunoresearch Laboratories) for 30 min. Then, sections were incubated for 16 h in affinity-purified primary anti-Drp1 (1:100; mouse; 611112; BD Biosciences), anti-Fis1 (1:100; rabbit; IMG-5113A; Imgenex), anti-Mfn1 (1:75; chicken; NB110-58853; Novus Biologicals) and anti-OPA1 (1:25; mouse; 612607; BD Biosciences) in blocking buffer. After three 15-min washes in PBS, they were incubated in Cy3-conjugated donkey anti-rabbit IgG (for Fis1), Cy3-conjugated donkey anti-mouse IgG (for Drp1 and OPA1) and Cy3-conjugated donkey anti-chicken IgG (for Mfn1) in blocking buffer for 2 h, rinsed and coverslipped with antifade mounting medium (Vectashield Vector Laboratories). Digital images were taken at a resolution of 1,200 × 1,600 dpi using the Leica DMRBE system with a Leica digital camera (Leica Microsystems) connected to an IBM computer running Scion Image software (version 3.0b; NIH).

The specific signal density in an individual fibroblast, corrected for background density, was measured for 20 random cells using Image J software version 1.37 (NIH) and expressed in arbitrary units.

Lentiviral infections

The pLenti6.2-SERAC1 construct ('+SERAC') or the control construct pLenti6.2V5-AcGFP ('mock') were transfected into 10-cm dishes containing 293FT cells together with a packaging mix consisting of the plasmids pLP1, pLP2 and pLP/VSVG using Lipofectamine 2000 (Invitrogen). At 24 h after transfection, the medium was refreshed, and the supernatants containing the viral particles were harvested at 72 h after transfection. Subsequently, supernatants were cleared by centrifugation at 300g for 5 min, and the viral particles were stored at –80 °C before use. Infections were performed on fibroblasts in 75 cm^2 flasks with 2 ml of virus containing the supernatant in the presence of 6 µg/ml polybrene (Sigma-Aldrich). At 24 h after infection, the medium was refreshed, and after 48 h, the selection medium was added (M199, 20% FCS (100U/ml) and penicillin and streptomycin (100 µg/ml)) and 2 µg/ml blasticidin (InvivoGen). Cells were selected for 14 d, in which time the mock-infected cells (without virus) died. Blasticidin-resistant cells were used for biochemical analysis within six passages after transduction.

Supplementary information

Patients

Patients were under treatment of one of the contributing clinicians (SW, PvH, IB, EP, SKU, KN, KS, ZK, JS, EM). Written informed consent was obtained from all patients and our *research project was approved by the local ethics committee (Commissie Mensgebonden Onderzoek Regio Arnhem-Nijmegen) according to the World Medical Association* Declaration of Helsinki.

Haplotype analysis by using short tandem repeat (STR) markers

Primers to amplify polymorphic short tandem repeat markers on 9q34.11 were designed by using the Primer3 program (http://frodo.wi.mit.edu/cgi-bin/primer3/primer3_www.cgi)[131]. An M13 tail was added to the 5′ and 3′-ends of the primers. Markers were amplified by using an M13 forward primer labeled with one of the fluorophores, FAM, VIC, NED and ROX, at the 5′-end and a M13 reverse primer with a 5′-gtttctt-3′ added to its 5′-end to reduce tailing[132, 133]. Primer sequences are shown in Supplementary Table 4 and PCR conditions are available upon request. Final PCR products were mixed with eight volumes of formamide and half a volume of Genescan™ 500(-250) LIZ size standard (Applied Biosystems, Foster City, USA), and analysed with the ABI PRISM 3730 DNA analyzer (Applied Biosystems, Foster City, USA). The results were evaluated by Genemapper (Applied Biosystems, Foster City, USA).

Mutation analysis

Primer sequences for amplification of all protein coding exons of *SERAC1* (GenBank ID NM_032861.3) are shown in Supplementary Table 4. PCR conditions are available upon request. PCR products were sequenced using the ABI PRISM BigDye Terminator Cycle Sequencing V2.0 Ready Reaction Kit and analysed with the ABI PRISM 3730 DNA analyzer (Applied Biosystems, Foster City, USA).

Cell culturing

Different cell types were cultured under specific conditions for each experiment. Fibroblast cell lines for NMD inhibition and lipid analysis were cultured in RPMI 1640 medium (Gibco, Breda, The Netherlands) containing 10% (v/v) fetal calf serum (FCS; Sigma, Zwijndrecht, The Netherlands), 1% 10 U/µl Penicillin-10 µg/µl Streptomycin (Gibco, Breda, The Netherlands), and 1% GlutaMAX (Gibco, Breda, The Netherlands)[134].

Fibroblast that were used for the preparation of cell lysates, filipin staining, co-localization, and lentiviral infections were grown in E199 medium (Gibco, Breda, The Netherlands) supplemented with 10% FCS (Lonza, Breda, The Netherlands) and 1% 10 U/µl Penicillin-10 µg/µl Streptomycin (Gibco, Breda, The Netherlands).

Fibroblasts that were used for assessment of mitophagy and autophagy, and fusion and fission, were kept in high glucose Dulbecco's Modified Eagle's Medium supplemented with 10% FCS (Lonza, Breda, The Netherlands) and 1% 10 U/µl Penicillin-10 µg/µl Streptomycin

(Gibco, Breda, The Netherlands). All fibroblasts were grown at 5% CO_2 and a temperature of 37°C. HEK293 and HeLa cells were cultured in DMEM (Gibco, Breda, The Netherlands) supplemented with 10% FCS (Lonza, Breda, The Netherlands) and 1% 10 U/µl Penicillin-10 µg/µl Streptomycin (Gibco, Breda, The Netherlands). All cells were grown at 5% CO_2 and a temperature of 37°C.

Nonsense-mediated decay (NMD) inhibition by cycloheximide
Fibroblasts were cultured to a density of $0.5*10^6$ cells/ml. Subsequently, 20 µl cycloheximide (concentration: 100 mg/ml DMSO) was added to the medium. After incubation for 4 hrs at 37°C, cells were harvested by centrifugation at 200x*g* for 5 min at room temperature, washed once with phosphate-buffered saline (PBS), pelleted by centrifugation at 200x*g* for 5 min at room temperature, and snap frozen in liquid nitrogen.

First strand synthesis
RNA was isolated from EBV-LCLs of patients and control individuals by using the NucleoSpin RNA II kit (Macherey-Nagel, Düren, Germany) according to the manufacturer's protocols. The integrity of the RNA was assessed on 1.2% agarose gel, and the concentration and purity determined by optical densitometry. The OD_{260}/OD_{230} and OD_{260}/OD_{280} ratios were in between 1.8 and 2.0. Half a µg of total RNA was transcribed into cDNA by using the iScript cDNA synthesis kit (Bio-Rad Laboratories, Hercules, CA, USA) according to the manufacturer's protocol. cDNA was purified by using the NucleoSpin extract II kit (Macherey-Nagel, Düren, Germany) according to the manufacturer's protocol. In case of expression profiling, total RNA from different human adult and fetal tissues was ordered from Stratagene Europe (Amsterdam, The Netherlands). All fetal tissues are from 20 or 21 weeks-old embryos after gestation, except for cochlear RNA that was isolated from an 8 weeks-old embryo by using the NucleoSpin RNA II kit (Macherey-Nagel, Düren, Germany) according to the manufacturer's protocols. To remove residual traces of genomic DNA, the cochlear RNA was treated with DNase I (Invitrogen, Leek, The Netherlands) while bound to the RNA binding column. The integrity, concentration, and purity of the RNA were assessed as described above.
Of all tissues, 5 µg of total RNA was transcribed into cDNA by using the iScript cDNA synthesis kit (Bio-Rad Laboratories, Hercules, CA, USA) according to the manufacturer's protocol. cDNA was purified by using the NucleoSpin extract II kit (Macherey-Nagel, Düren, Germany) according to the manufacturer's protocol.

Quantitative PCR (QPCR) analysis
SYBR Green-based real-time quantitative PCR (QPCR) expression analysis was performed on a 7500 *Fast* Real-Time PCR System (Applied Biosystems, Foster City, CA, USA) by using *Power SYBR Green* PCR Master Mix (Applied Biosystems, Foster City, CA, USA) according to the manufacturer´s instructions. Primers were designed by the primer3 program (http://frodo.wi.mit.edu/cgi-bin/primer3/primer3_www.cgi)[131]. Primer sequences are given

in Supplementary Table 4. PCR products encompassed at least one boundary between two exons. *GUSB* was used as reference gene[134]. RNA was isolated from fibroblasts of patients and control individuals by using the NucleoSpin RNA II kit (Macherey-Nagel, Düren, Germany) according to the manufacturer's protocols. QPCR quantifications were performed in duplicate on the equivalent of 7.8 ng of total RNA from the first strand synthesis, and included a water control. Experimental threshold cycles (Ct) values were within the range of cDNA dilutions used to validate the primers. The melt curves of all PCR products showed a single PCR product. All water controls were negative. Differences in expression of a gene of interest between the individual samples of the patients and five controls were calculated by the comparative Ct or $2^{\Delta\Delta Ct}$ method[135, 136]. The *p*-value was derived from the standard score (Z-value) calculated for each individual as compared to the normal distribution of the five controls. Since we assume a lower expression level as a result of nonsense-mediated mRNA decay (NMD), a one-sided test was enough to reject the null hypothesis, i.e., no statistically significant difference between the expression of *SERAC1* in fibroblasts of a patient and that in fibroblasts of controls. We used an alpha level of 0.05, because only one gene was assessed.

Tissue expression analysis

QPCR quantifications were performed in duplicate on the equivalent of 12.5 ng total RNA input. Experimental threshold cycles (Ct) values were within the range of cDNA dilutions used to validate the primers. The melt curves of all PCR products showed a single PCR product. All water controls were negative. *GUSB* and *PPIB* were used as reference genes. Differences in expression of a gene of interest between two samples were calculated as described above.

Preparation of cell lysates and cellular fractionation

Fibroblasts, HEK293 cells, or HeLa cells were harvested by centrifugation at 200x*g* for 5 min at room temperature and washed twice in PBS. Total cell lysates were obtained by resuspension of fresh cells in 50 µL PBS containing 2% (v/v) B-Laurylmaltoside. After ten minutes of incubation on ice, unbroken cells and nuclei were spun down. Protein concentrations in the supernatant were determined using a MicroBCA protein assay kit (Thermo Scientific, Etten-Leur, The Netherlands). To the supernatant an equal volume of Tricine sample buffer (Biorad laboratories, Ede, The Netherlands) containing 2% (v/v) 2-mercaptoethanol was added and the mixture was kept at room temperature for 60 minutes before further processing.

To obtain cytoplasmic fraction, crude mitochondria and endoplasmic reticulum (ER), fresh cell pellets were resuspended in isotonic buffer (0.25 M sucrose, 5 mM Tris/HCl, pH 7.5, and 0.1 mM phenylmethylsulfonylfluoride(PMSF)) and pottered eight times at 2500 rpm to homogenize the cells. Unbroken cells and nuclei were removed by centrifugation at 600x*g* for 15 min. Supernatants were centrifuged at 10,000x*g* for 25 min to obtain crude mitochondria. The supernatant of this centrifugation step was either used as cytoplasmic

fraction or subjected to centrifugation at 100,000x*g* for 60 min to obtain ER. The crude mitochondrial pellet was washed twice with the isotonic buffer containing 1 mM EDTA.

Proteinase K protection assay

A Proteinase K protection assay was used to determine the SERAC1 localisation more precisely. Fresh crude mitochondrial fractions were prepared from HEK293 cells and resuspended in PBS. Half of the sample was used to generate a mitoplast by permeabilizing the outer membrane with digitonin (8µg/µl PBS; ~50% (TLC), Sigma–Aldrich, Zwijndrecht, The Netherlands). Mitochondrial and mitoplast pellets were resuspended in PBS and the protein concentration was determined using a MicroBCA protein assay kit (Thermo Scientific, Etten-Leur, The Netherlands). The total volume was adjusted to a final protein concentration of 2 µg/ml. Mitochondria and mitoplasts were treated with proteinase K in different concentrations (1 or 10 µg/ml) in the absence or presence of 1% Triton X-100 for 15 min at 4°C. The reaction was terminated by the addition of 200 µM PMSF and an equal volume of Tricine sample buffer (Biorad laboratories, Ede, The Netherlands) containing 2% (v/v) 2-mercaptoethanol immediately followed by incubation of 5 minutes at 95°C.

SDS PAGE and Immunodetection

Equal amounts of protein of the obtained total cell lysates, crude mitochondria, ER, and cytosol were loaded and separated on a 10% polyacrylamide gel. Gels were blotted to nitrocellulose transfer membranes (Whatman, s'Hertogenbosch, the Netherlands).

We used the following specific antibodies: rabbit anti-SERAC1 (1:500; HPA 025716; Sigma–Aldrich, Zwijndrecht, The Netherlands); mouse anti-NDUFS3, (1:1,000; MS112; Mitosciences, Eugene, Oregon, USA); mouse anti-TOM20 (1:1,000; 612278; BD transduction laboratories, Breda, The Netherlands); rabbit anti-Calnexin (1:1,000; 2433S; Cell signaling technologies, Leiden, The Netherlands); Rabbit anti-Actin (1:500; NB600-533; novus biological, Cambridge, UK), mouse anti-COX II (1:10,000; A6404; Invitrogen, Leek, The Netherlands), and mouse anti-CK-B antibody (1:1,2000; 21E10)[137]. Secondary antibodies used for detection were goat anti-(rabbit Ig) Ig peroxidase (1:10,000; GARPO; Invitrogen, Leek, the Netherlands) and goat anti-(mouse Ig) Ig peroxidase (1:10,000; (GAMPO; Invitrogen, Leek, the Netherlands), and donkey anti-goat (1:10,000; sc-2020; Santa Cruz Biotechnology, Heidelberg, Germany). Signal was generated using the ECL Prime Western Blotting reagent (Amersham Biosciences, Roosendaal, the Netherlands).

OXPHOS measurements

OXPHOS measurements in different tissues were performed as reported earlier[93, 138, 139]. The measurement of the oxygen consumption rate in the presence of pyruvate and malate as mitochondrial respiration substrates was performed as described previously[140].

Assessment of autophagy and mitophagy

In all assays, fibroblast passage numbers (<10) were matched. To challenge cellular processes of mitophagy by increasing the amount of dysfunctional mitochondria, fibroblasts were treated with the potassium ionophore valinomycin (1µM for 1h, Sigma-Aldrich, St. Louis, CA, USA)[141]. Proteins were extracted using RIPA buffer (50mM Tris-HCl pH7.6, 150mM NaCl, 1% DOC, 1% NP-40) containing 0.1% SDS. Cells were dissolved in the appropriate amount of buffer and incubated on ice for 30 min. Next, lysates were centrifuged at 16,000xg for 20min at 4°C. The supernatant was transferred into a new tube and used for Western blotting. Western blot analysis was performed as previously published[142] using antibodies raised against β-actin (1:1000000, #A2228, Sigma-Aldrich, St. Louis, CA, USA), GRP75 (1:1000000, #ab2799, Abcam, Cambridge, UK), LC3 (1:1000, #4108, Cell Signaling Technology, Boston, MA, USA), Mfn2 (1:1000, #ab56889, Abcam, Cambridge, UK), MTCO2 (1:1000, #ab91317, Abcam, Cambridge, UK), P62 (1:1000000, #5114, Cell Signaling Technology, Boston, MA, USA) and Parkin (1:1000, #4211, Cell Signaling Technology, Boston, MA, USA).

Assessment of fusion and fission

QPCR was performed in a total volume of 25 µl buffer solution containing 5 µl of template cDNA, 12.5 µl 2× SYBR Green Master mix (Applied Biosystems, Foster City, CA, USA), 1.5 µl DEPC-treated MQ water and 15 µM of each primer. Primers (see Supplementary Table 4) were designed in Vector PrimerExpress software (Applied Biosystems). The cycling protocol was 95°C for 10 min followed by 40 reaction cycles at 95°C for 15 sec and at 60°C for 1 min, using a 7500 GeneAmp PCR system (Applied Biosystems). For each reaction, the cycle threshold (Ct) was determined, i.e., the number of cycles needed to detect fluorescence above the arbitrary threshold (0.8). At this threshold, Ct values are within the exponential phase of the amplification. Standard curves were included in duplicate with cDNA concentrations ranging from 6.25 to 100 ng cDNA per sample. Using these curves, in which every Ct value corresponds to a certain amount of cDNA, the quantity of cDNA was calculated for each sample with Applied Bioscience 7500 System Software. All data were normalized to *GAPDH* expression.

Cloning of human SERAC1

The full length open reading frame of *SERAC1* was amplified from full length cDNA clone HsCD00323657 (PlasmID, DF/HCC DNA Resource Core, Boston, MA, USA) using specific primers with Gateway AttB flanking sites with an inframe stop codon (Supplementary Table 4). PCR amplification was performed with Phusion® High-Fidelity DNA Polymerase (New England Biolabs, Ipswich, MA, USA) according to the manufacturer's protocol using HF buffer and an annealing and extension temperature of 72°C. Next, the product was cloned into the pDONR201 vector using the Gateway BP Clonase II Enzyme Mix (Invitrogen, Leek, The Netherlands) according to the manufacturer's instructions. The resulting entry clone was verified by sequence analysis and subsequently recombined with

the pLenti6.2V5-DEST destination vector (Invitrogen, Leek, The Netherlands) using the Gateway LR Clonase II Enzyme Mix (Invitrogen, Leek, The Netherlands) according to the manufacturer's protocol.

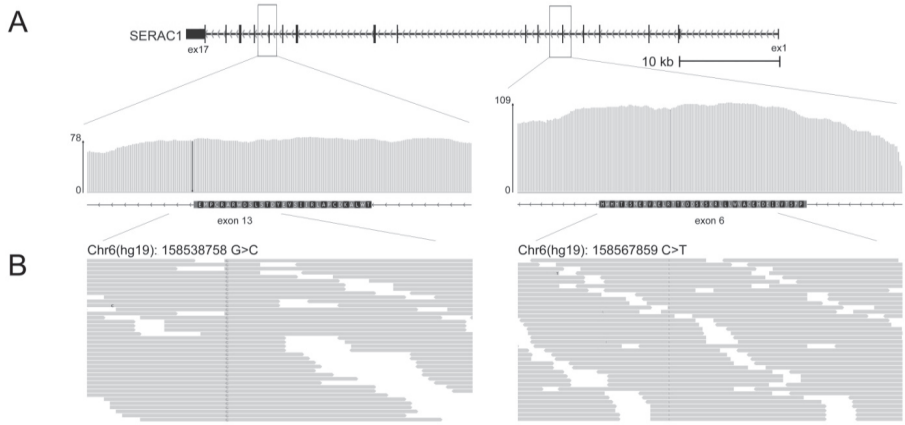

Supplementary Figure 1. *SERAC1 exome sequencing. For patient 3 (right side), 73 of 74 (99%) reads showed a C to T transition at chr6(hg19):g.158567859, indicating a homozygous r.442C>U transition at mRNA level which is predicted to result in a premature stop codon, (p.Arg148X). For patient 5 (left side), 50 of 52 (96%) reads showed a G to C splice site substitution at chr6(hg19):g.158538758 in the canonical donor splice site of exon 13.*

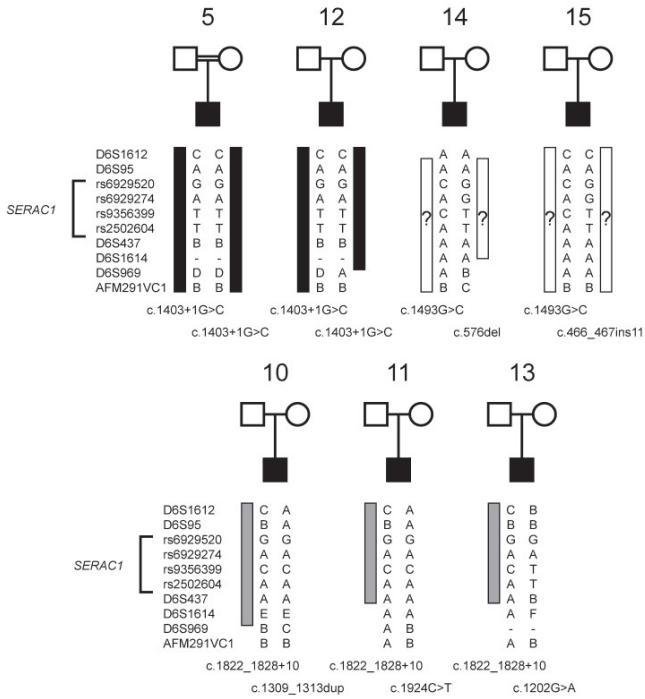

Supplementary Figure 2. *Haplotype analysis. Haplotypes of patients with identical mutations on one or both alleles. Black bars represent the haplotype segregating with the mutation resulting in skipping of exon 13 (c.1403+1G>C). White bars indicate the haplotype carrying the p.Ser498Thr change (c.1493G>C). The question mark indicates that it is uncertain which haplotype actually segregates with the mutation. Phase could not be determined because parents were not available for analysis. Grey bars represent the haplotype carrying with the exon 16 retention change (c.1822_1828+10delinsACCAACAGG). SNPs, rs6929520, rs6929274, rs9356399, and rs2502604 are respectively within exon 4, exon 4, exon 5, and exon 15 of SERAC1. Mutations are given underneath the respective haplotypes.*

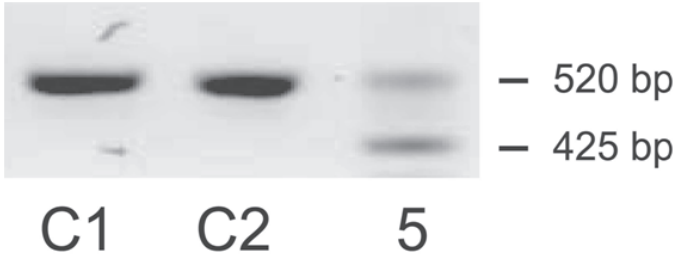

Supplementary Figure 3*. Effect of the c.1403+1G>C mutation on SERAC1 mRNA transcript. Shown is the normal transcript length of SERAC1 in fibroblasts of controls (C1, C2: 520 bp) and the transcript without exon 13 in fibroblasts of patient 5 (425 bp). Fibroblasts of the patient have been treated by cycloheximide before harvesting to inhibit nonsense mediated decay (NMD). PCR primers are given in Supplementary Table 4 and PCR conditions are available upon request.*

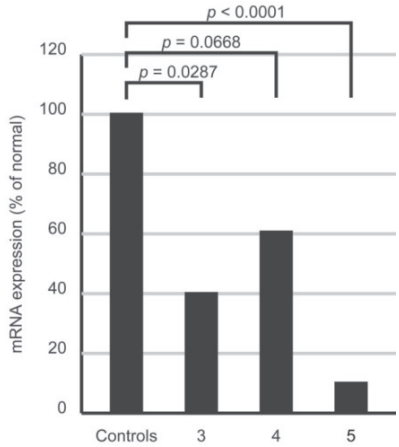

Supplementary Figure 4. *Effect of different mutations on SERAC1 expression. Effect of the c.442C>T (p.Arg148X; 3), c.1435_1437del (p.Leu479del; 4), and c.1403+1G>C (exon 13 skipping; 5) mutations on SERAC1 expression. Shown are mRNA expression levels in fibroblasts of the respective patients 3, 4, and 5 as compared to the average expression level of SERAC1 in five controls.*

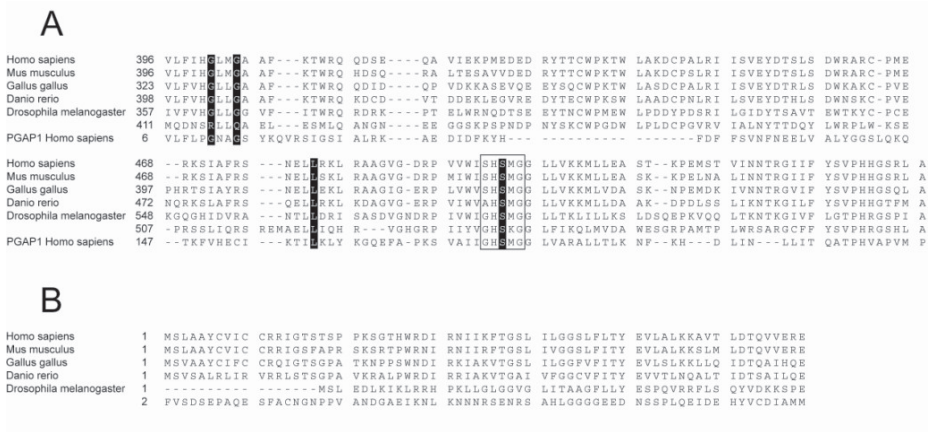

Supplementary Figure 5. *Cross-species alignment of the functional domains of SERAC1. A) Alignment of lipase/esterase domain from human (Homo sapiens; Q96JX3), mouse (Mus musculus; Q3U213), chicken (Gallus gallus; ENSGALT00000022317), zebrafish (Danio rerio; Q5SNQ7), and fruit fly (Drosophila melanogaster; CG5455/CG10383). The box indicates the region containing the consensus lipase motif GxSxG[119, 143]. The deleted amino acid residue, Leu479, and the amino acid residues that are affected by the missense mutations, Gly401, Gly404, and Ser498 are highlighted by black boxes and conserved in all five species. In case of the fruit fly orthologues CG10383 and CG5455, respectively amino acid residues 382-495 and 436-458, are not given, since these have no resemblance to an amino acid sequence in the other animal species. B) Alignment of the first 60 amino acid residues on the N-terminus containing the predicted N-terminal signal sequence and/or transmembrane domain (see also Supplementary Table 5).*

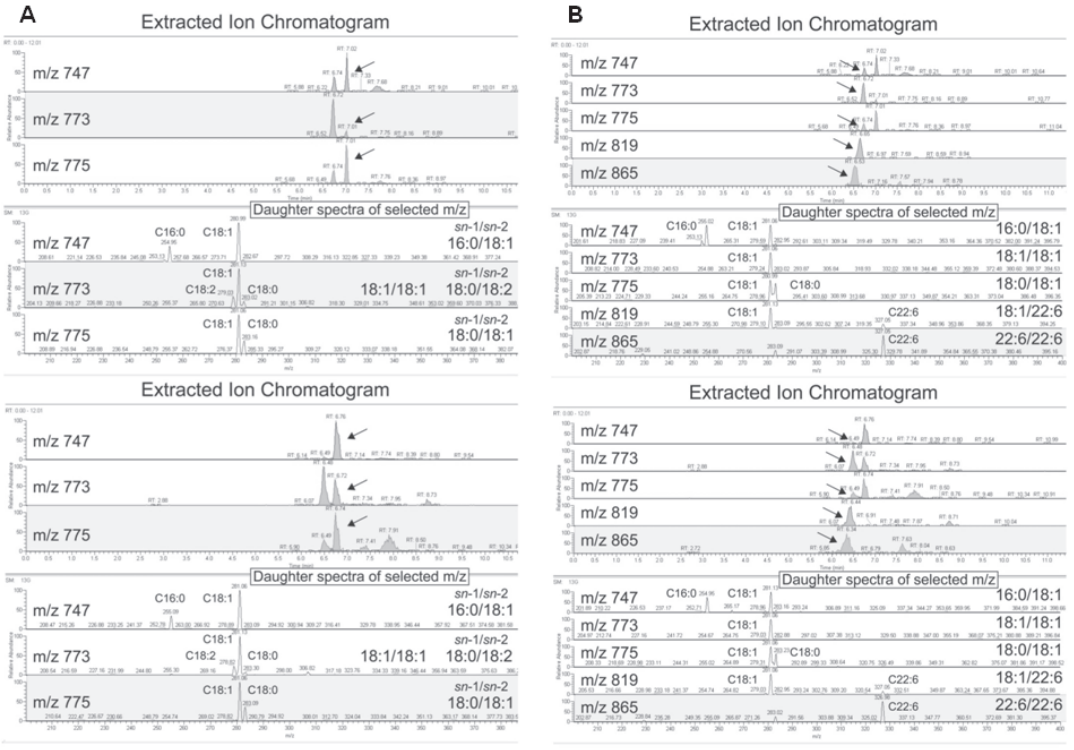

Supplementary Figure 6 A/B. *Representative daughter analysis of most abundant bis(monoacylglycerol)phosphate species Representative daughter analysis of A) most abundant phosphatidylglycerol and B) bis(monoacylglycerol)phosphate species, showing that acyl chain composition of these specific species are similar between control (upper panel) and patient fibroblasts (lower panel). Arrows indicate which chromatographic peaks were selected and represented in the corresponding daughter spectra below.*

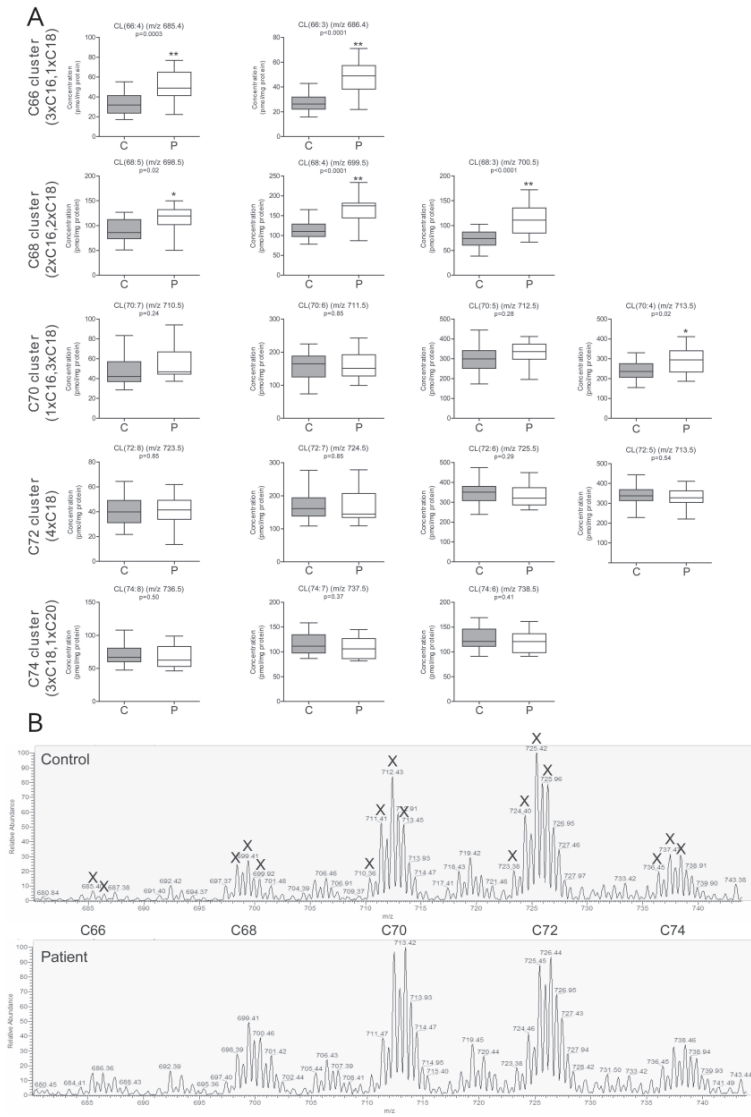

Supplementary Figure 7. *Cardiolipin species in patients and controls. A) Box and whisker plots (minimum/maximum) of individual cardiolipin (CL) species levels in controls (n=10) and patients (n=5). Significantly higher levels of cardiolipin (66:3), cardiolipin(66:4), cardiolipin(68:3), cardiolipin(68:4), and cardiolipin(68:5) were found in patients (see also Figure 3) which are the cardiolipin species that can be synthesized from phosphatidylglycerol (34:1). B) Representative cardiolipin spectra from a patient and a control. Crosses indicate the selected species presented in the box and whisker plots.*

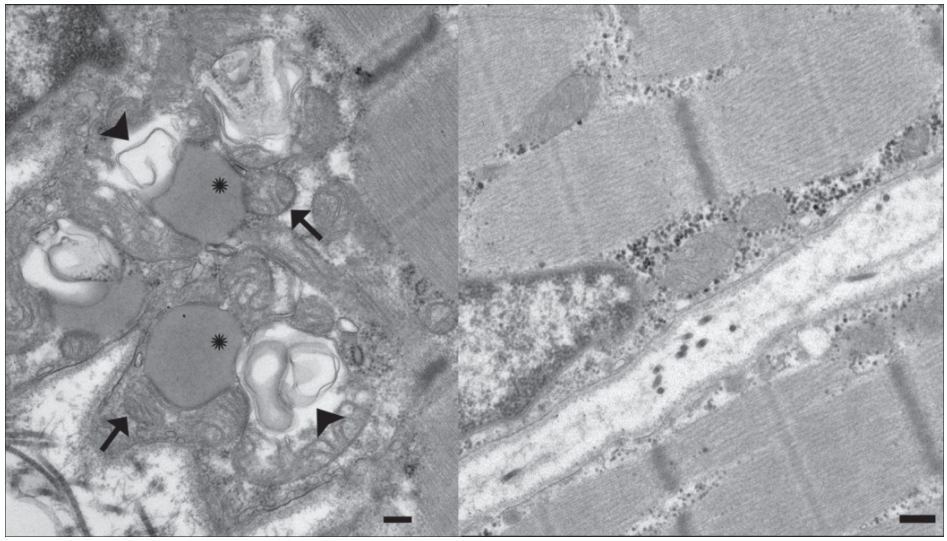

Supplementary Figure 8. *Electron microscopy of muscle tissue of MEGDEL patient and healthy control. Left panel: electron microscopy of m. quadriceps of patient 1 showing aggregates of degrading mitochondria in striated muscle cell: mitochondrial cristae (arrows), and lysosomes with neutral fat droplets (asterisks) and membranous remnants (arrowheads, bar = 0.2µm). Right panel: electron microscopy of same muscle of healthy control for comparison.*

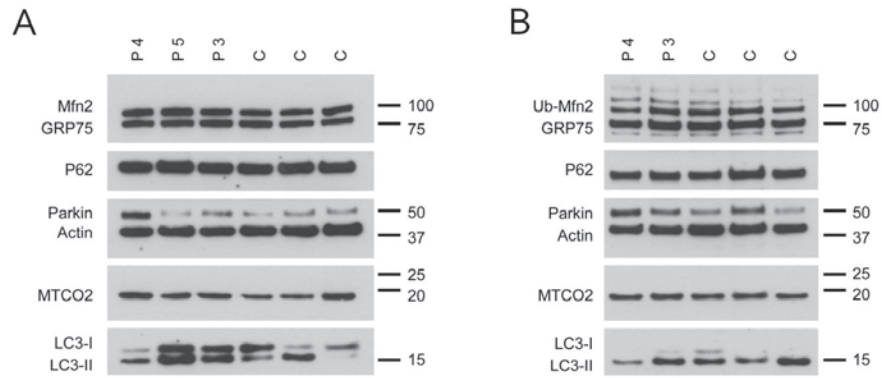

Supplementary Figure 9. *Expression of mitochondrial and mitophagy markers in patients and control fibroblasts. Fibroblasts from patients P_3, P_4 and P_5 and three controls were cultured under basal conditions or treated with 1µM valinomycin for 1h and Western blotting was performed with antibodies against GRP75, LC_3, Mfn2, $MTCO_2$, P62, and Parkin. A) Under basal conditions, protein levels of the investigated mitochondrial (GRP75 and $MTCO_2$) and auto-/mitophagy (LC_3, Mfn2, P62 and Parkin) markers were comparable in patients and controls. B) After valinomycin stress, ubiquitinated forms of Mfn2 were detected in all samples indicating comparable accumulation of dysfunctional mitochondria. Furthermore, a similar shift of the LC_3-II to LC_3-I ratio toward LC_3-II, in line with elevated numbers of autophagosomes in the cells, was observed in patient and control cells. Protein levels of*

GRP75, MTCO2, P62 and Parkin were comparable in both groups. β-actin expression served as loading control. GRP75 = glucose-regulated protein 75 (mortalin); LC3 = microtubule-associated protein 1A/1B-light chain 3; LC3-I = soluble form of LC3; LC3-II = membrane-bound form of LC3; Mfn2 = mitofusin 2; MTCO2 = mitochondrial cytochrome c oxidase subunit II; P62 = sequestosome-1; Ub-Mfn2 = ubiquitinated mitofusin 2.

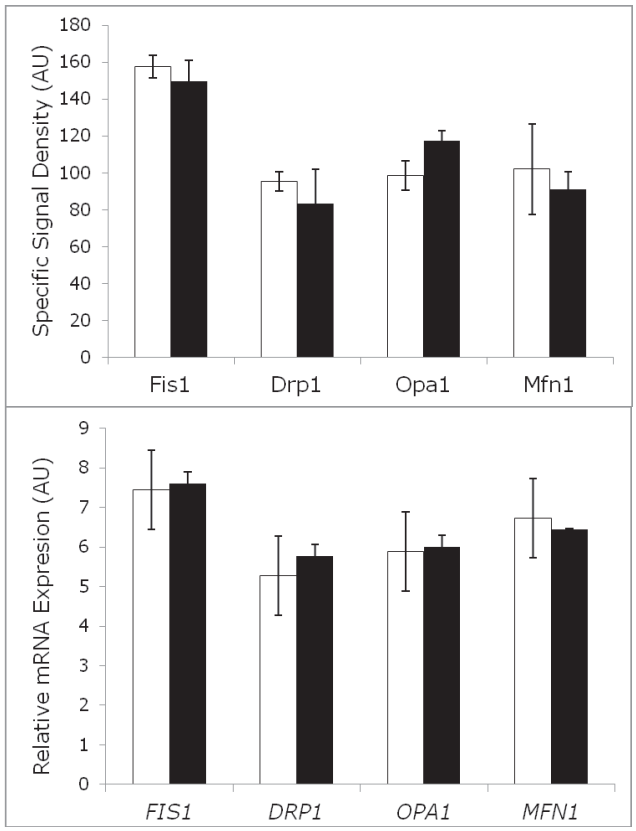

Supplementary Figure 10. *Assessment of fusion and fission in patient and control fibroblasts. Semi-quantitative immunohistochemistry (upper panel) and QPCR (lower panel) showed now difference in expression of fusion and fission markers between patients (black bars) and control fibroblasts (white bars).*

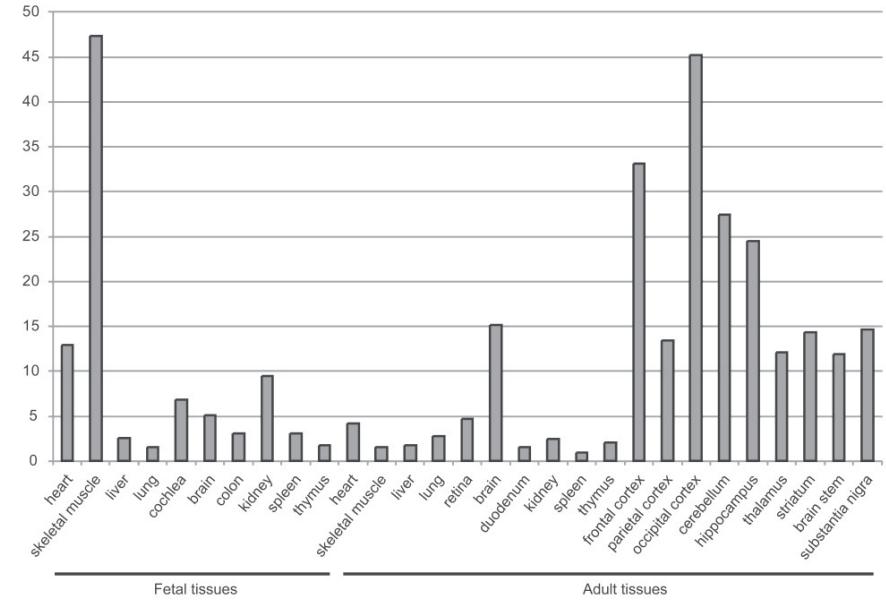

Supplementary Figure 11: *Expression of SERAC1 in different human tissues. Expression of SERAC1 by mRNA expression analysis in human fetal and adult tissues. Relative expression levels are given as the fold change in comparison to the tissue with the lowest expression level.*

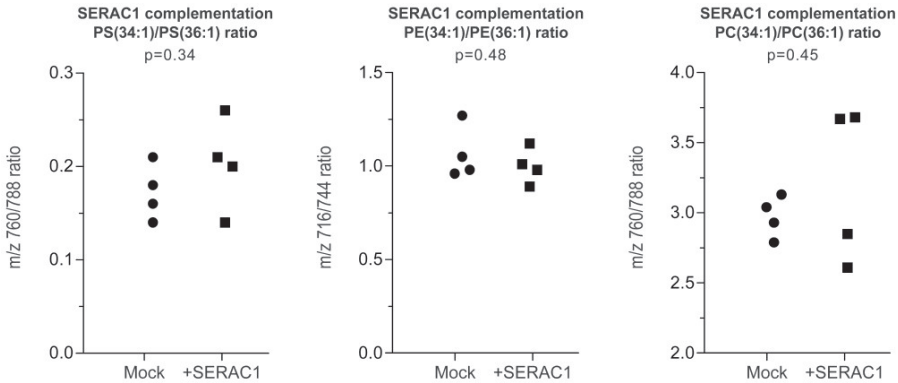

Supplementary Figure 12. *Phosphatidylserine, phosphatidylethanolamine, and phosphatidylcholine species ratios in patient fibroblasts complemented with wild type SERAC1. Fibroblasts from patients were infected with a mock vector (n=4) or an expression vector containing wild type SERAC1 (n=4). Complementation of SERAC1 (for Western blot see Supplementary Figure 13) does not affect the phosphatidylserine (PS) PS(34:1)/PS(36:1), phosphatidylethanolamine (PE) PE(34:1)/PE(36:1), and phosphatidylcholine (PC) PC(34:1)/PC(36:1) ratios. The phophatidylinositol (PI) PI(34:1)/PI(36:1) ratio could not be calculated since the amount of PI(34:1) is below the detection level in both mock and SERAC1-infected cells. Total levels of these four phospholipids were unaffected as well (data not shown).*

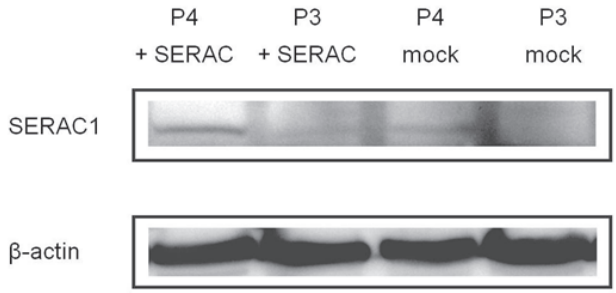

Supplementary Figure 13. *SERAC1 expression in stably infected patient fibroblasts. Western blot analysis of patient fibroblasts stably infected with pLenti6.2-SERAC1 or the control construct pLenti6.2V5-AcGFP. Shown is the expression of SERAC1 and the loading control β-actin. SERAC1 infected fibroblasts from patient 4 (lane 1,3) and 3 (lane 2,4) showed increased expression of SERAC1 (lane 1,2) as compared to the fibroblasts infected with GFP only (lane 3,4). No SERAC1 was visible in GFP-infected fibroblast from patient 4 (lane 4) since the protein is shortened due to the truncating mutation and the SERAC1 antibody is directed against the C-terminal part of the protein that is not present anymore in this patient.*

Patient, gender	1♀	2♀	3♀ ES	4♀	5♂ ES	6♀	7♂	8♂	9♂	10♀	11♀	12♀	13♂	14♂	15♂
Ethnicity (consanguinity)	T(+)	D(-)	T(+)	T(+)	Pa(+)	T(+)	T(+)	Af(+)	T(-)	Po(-)	Po(-)	I(-)	S(-)	S(-)	S(-)
PMR	+	+	+	+	+	+	NA	+	+	+	+	+	+	+	+
Spasticity/ dystonia	+/+	+/+	+/+	+/+	+/+	+/+	NA	+/+	+/+	-/+	+/+	+/+	+/+	+/+	+/+
Sensori-neural deafness	+	+	+	+	+	+	NA	+	+	+	+	-	+	+	+
MRI	LS, A	LS, A	LS, A	LS, A	LS	LS, A	NA	LS	LS, A	LS, A	NA	LS, A	LS, A	NA	LS
Age regression/ current age	3m/10y*	1y/16y*	6m/15y	3y/15y	4y/11y	NA/7y	0/1w*	1y/9y*	4m/4y	NA/5y	NA/8y	6y/10y	6m/9y*	8m/15y*	8m/3y*
Elevated lactate/alanine	+/-	+/+	+/+	+/+	-/-	+/+	+/NA	+/+	+/-	+/+	+/+	+/+	+/-	+/NA	+/-
Urinary 3–MGA**	42-76	16-68	102-196	50-141	>20	20-40	NA	85-100	40-97	81	58	116	51-141	50-158	>20
Cholesterol***	NA	4.9-5.2	2.2-3.0	3.6-4.5	3.5	2.7-3.4	NA	NA	3.5	3.6	3.1	4.0	2.1-4.7	2.5-3.7	NA
OXPHOS dysfunction	M+, F-	M+, F-	M+, F+	M+, F-	M-, F-	F+	NA	M+, F+	F-	M+	M+	NA	M+	M+	M-
Abnormal EM of mitochondria	M+	M+	M+	M+	NA	NA	NA	NA	NA	NA	NA	NA	M-	NA	M-
Abnormal phospholipid spectrum in fibroblasts	NA	+	+	+	+	NA	NA	+	NA	NA	NA	NA	NA	NA	NA
Abnormal filipin staining	NA	NA	+	+	+	NA	NA	NA	NA	NA	NA	NA	NA	NA	NA

Supplementary Table 1. *Major clinical and biochemical findings in 15 MEGDEL patients. Major clinical and biochemical findings in 15 individuals with MEGDEL syndrome due to mutations in SERAC1. ES=patients in whom exome sequencing was performed. A = Afghanistan, D = Dutch, I = Indian, Pa = Pakistani, Po = Polish, S = Swedish, T = Turkish. NA = not available. PMR = Psychomotor retardation. LS = Leigh(-like) syndrome, A = atrophy, m = months, w = weeks, y = years. M = muscle, F = fibroblasts, L = liver. *deceased, **3–MGA = 3–methylglutaconic aciduria in mmol/mol creatinine (N<20). ***only values of patients > 1 year, in mmol/l; Normal range: 2.6-5.6. OXPHOS= oxidative phosphorylation. Patients 1-4 are the original patients in the same order as in[68], patient 3 is the niece of patients 6 (sister) and 7 (brother), patient 10 is the patient in[144], patient 13 is patient 1 and patient 14 is patient 24 in[145].*

	Patient 5	Patient 3
Total number of sequenced reads ($\times 10^6$)	124.46	133.81
Total number of mapped reads ($\times 10^6$)	96.52	107.57
Total number of bases mapped (Gb)	4.54	5.12
Total bases mapping to targets (Gb)	3.89	4.33
% targets with 10x coverage	82	80
Mean target coverage (fold)	68	73
Median target coverage (fold)	53	56
QC filtering*	23,231	23,470
After exclusion of nongenic, intronic & synonymous variants	5,405	5,320
After exclusion of known variants	213	240
Of which fit a recessive model of disease**	21	17
Gene(s) with mutation in both patients	1 (*SERAC1*)	

Supplementary Table 2. *Raw sequencing statistics and prioritization of variants. * >5 unique variant reads and >20% of all reads, **>70% variant reads*

Start SNP	End SNP	Chr.	Start position	End position	Size (Mb)	% exons covered <10x	Median coverage per exon
Patient 3							
SNP_A-2200063	SNP_A-2151802	2	152,051,481	163,277,032	11.2	3.1	100
SNP_A-2050760	SNP_A-1898944	7	46,239	9,744,833	9.6	36.4	52
SNP_A-2186469	SNP_A-2109663	4	1,128,925	9,968,684	8.5	27.9	60
SNP_A-2204105	SNP_A-1883568	11	12,072,213	20,006,336	7.9	9.2	71
SNP_A-2077486	SNP_A-1937604	20	55,392,174	62,535,594	7.2	46.0	31
SNP_A-2186392	SNP_A-2158961	4	23,757,800	30,390,253	6.6	6.7	84
SNP_A-2058596	SNP_A-2241984	6	174,769	6,011,668	5.8	15.5	61
SNP_A-2150721	SNP_A-2012220	6	154,074,079	160,018,988	5.8	7.8	78
SNP_A-1835443	SNP_A-4237011	6	148,740,251	154,056,121	5.3	5.5	76
Patient 4							
SNP_A-2028616	SNP_A-2107608	2	153,527,691	199,457,084	45.9		
SNP_A-1849616	SNP_A-2249544	8	78,593,899	122,515,531	43.8		
SNP_A-1908661	SNP_A-2290879	1	205,608,153	232,419,619	26.6		
SNP_A-2110513	SNP_A-1880093	9	82,562,184	107,751,593	25.0		
SNP_A-1980980	SNP_A-4232001	5	23,630,961	46,383,335	22.8		
SNP_A-2284739	SNP_A-2223106	1	142,569,068	163,772,455	20.5		
SNP_A-4230532	SNP_A-2137016	8	126,885,591	146,292,734	19.3		
SNP_A-1981478	SNP_A-1863137	5	49,560,859	68,720,419	19.2		
SNP_A-2035113	SNP_A-1886785	5	70,701,990	87,566,731	16.9		
SNP_A-2183027	SNP_A-1862731	2	110,285,766	124,754,515	14.8		
SNP_A-2118367	SNP_A-4223408	1	238,548,667	249,143,646	10.5		
SNP_A-1820584	SNP_A-1919785	6	156,850,664	165,588,607	8.6		
SNP_A-4225410	SNP_A-2078652	1	113,101,799	121,251,791	8.1		
SNP_A-4214375	SNP_A-2162165	15	80,902,266	86,758,895	5.9		
SNP_A-2091399	SNP_A-4197277	11	45,665,915	51,563,636	5.8		
SNP_A-4237484	SNP_A-1996154	9	14,244,413	19,925,073	5.7		
Patient 5							
SNP_A-2074590	SNP_A-1988005	6	130,217,785	146,960,353	16.7	4.3	102
SNP_A-4239249	SNP_A-4240714	15	85,477,430	95,642,676	10.2	18.3	68
SNP_A-1933498	SNP_A-1805304	6	150,367,320	160,154,099	9.7	6.3	87
SNP_A-1793270	SNP_A-2262914	12	72,610,000	81,027,095	8.7	5.1	104
SNP_A-1917086	SNP_A-4199152	2	224,951,090	233,227,833	8.3	7.4	96
SNP_A-2280193	SNP_A-1806609	16	51,693,011	59,588,971	7.9	22.1	63
SNP_A-2017397	SNP_A-2018641	21	29,385,244	36,789,212	7.4	9.1	84
SNP_A-2234180	SNP_A-2298494	15	71,956,136	79,214,192	7.3	24.5	64
SNP_A-1866954	SNP_A-4232940	15	79,264,037	85,175,750	5.9	14.5	73

Supplementary Table 3. *Homozygous regions (<5 Mb) in patients 3, 4, and 5 as determined by homozygosity mapping. The region containing SERAC1 on chromosome 6 is printed in bold. Positions are according to UCSC Human Genome Browser, Hg19.*

	Forward primer (5'→3')	Reverse primer (5'→3')
	Sequencing	
Exon 2	tggaaagttttcttcgtagtcttg	gggcctataaatttggggtg
Exon 3	tgtgtgtttgtgtctaaggatagg	ccaagagaaagcactcctcag
Exon 4	cgatggctactcagtcactagg	caggaacttggttttcacgg
Exon 5	ttgaaacgttggagcatagtg	ggcctgattaattttccatagc
Exon 6	gagccacgattgtgtcactg	tgaccttgtgatccaaccag
Exon 7	ttgcacttgggaaattttgg	atagaaggaacagccccctcc
Exon 8	ctgggtgggtgactgttttc	ttcatttacctgcctccctg
Exon 9	cttgacgaggacacaggttg	gccacatttagatgataggctg
Exon 10	tccaaccaagagctaagcag	tgaacatatcatgaggggtagag
Exon 11	acttctccgccaaggacag	caacctccaattcttttgtgg
Exon 12	gttttcccagcaaacctgtg	ccctaagggaaagaagaactg
Exon 13	tggtaccacttcgagaccag	ccactgcttattgacagcaaac
Exon 14	ggggccaggagttcaataag	gagaaaggaacagcatggaac
Exon 15	ccctgtttgtaggcttgcac	agcccaacccaaaatttcc
Exon 16	cttagtggcttcttggcagg	gcagggagaggtaatacccg
Exon 17	tgcaatcaaacttcaggttcc	tctgcaacacactccagacc
	RT-PCR analysis	
RT-PCR	ctcaggctgggtttccatc	tccacaaaattcagcacctg
	QPCR analysis	
***GUSB* (NM_000181.1)**	agagtggtgctgaggattgg	ccctcatgctctagcgtgtc
***PPIB* (NM_000942.4)**	cggaaagactgttccaaaaac	gattacacgatggaatttgctg
***SERAC1* (NM_032861.3)**	tctcctaccacctcctttgc	ggtaaggaagccagcaactg
DRP1	cgccgacatcatccagct	tctccgggtgacaattccag
FIS1	gtctgtggaggacctgctgaa	ttgctccgcaccaggc
MFN1	ccatcattggtgaggtgctatc	acaacattgcattgataacagagct
OPA1	tgtgaggtctgccagtctttagtg	tgtccttaattggggtcgttg
	STR markers analysis	
D6S415	gaccagatgggtgactacctg	ggccaccagaagtaaagcag
D6S1612	ccagtgaattaaggcctcgtc	ccttggcgacagagtgaaac
D6S1655	caggacatggacattcagacc	agcagacctccaaaacaagc
D6S95	tcggattagtttgctgtaccc	gcttgggcaacaagagtaaaac
D6S437	aatgatcactgctaggcttcc	cattttccctgctgtggtg
D6S1614	tcagaatgtttgtgcgtgtg	ttctgcttggggcttattatg
D6S969	gcatccattgaagtttcttcc	aatccacaagtccatactgagg
AFM291VC1	aggtgagcttccttgaccac	tctgtcgacctggtcatttg
	Cloning	
Forward primer	ggggacaagtttgtacaaaaaagcaggcttcgaaggagatagaaccatgtccctggctgcttattgcgtcatc	
Reverse primer	ggggaccactttgtacaagaaagctgggtcctagttttcaaggtctttggctaaagcttcacg	

Supplementary Table 4: *Primer sequences . Primer sequences of primers used for direct DNA sequencing, RT-PCR, QPCR analysis and cloning of SERAC1 (NM_032861.3). Primers for STR marker analysis to determine the haplotypes in patients 5, and 10-15 are given without their M13 tails.*

Organism	Protein ID	Gene ID	Identity	Lipase domain	TM domain (HMMTOP)[20]	TM domain (TMHMM)[21]
Homo Sapiens	NP_116250	*SERAC1*	100%	396-540	-	-*
Mus Musculus	Q3U213	*SERAC1*	87%	396-540	-	32-54*
Gallus Gallus	ENSGALT0000 0022317	*SERAC1*	64%	323-469	-	-*
Danio Rerio	Q5SNQ7	*SERAC1*	61%	398-544	36-53	-*
Droso-phila Melano-gaster	NP_609896 NP_651481	*CG10383* *CG5455*	22% 18%	357-623 411-582	16-32 625-644	16-33* -

Supplementary Table 5: *Structure of SERAC1 in different vertebrates and the fruit fly. Structure of SERAC1 in different vertebrates and the fruit fly. Domains are given from first to last amino acid residue. The lipase domain is fully conserved from human to fruit fly. *TMHMM predicts a N-terminal signal sequence.*

Patient	1	2	3	4	5	6	7	8	9	10	11	12	13	14	15
Muscle															
ATP	Low (88%)	Low (57%)	Border-line (100%)	Low (62%)	NA	NA	NA	Low (80%)	NA	NA	NA	NA	normal	normal	normal
Complex-deficiency	I 93%	none	I 90%	none	none	NA	NA	I 94%, III 75%	NA	IV 20%, V 50%	IV50%	NA	II+III 51%	II+III 77%, IV 82%	none
Electron microscopy	Ab-normal	Ab-normal	Ab-normal	Ab-normal	NA	NA	NA	NA	NA	NA	NA	NA	normal	NA	normal
Fibroblasts															
Complex-deficiency	none	none	I 16%, IV 84%	none	none	II (96%)	NA	I 100%, III 96%	none	NA**	NA	NA	NA	NA	NA

Supplementary Table 6. *Measurements of oxidative phosphorylation in available tissues of MEGDEL patients. Table showing alteration in oxidative phosphorylation in different tissues of MEGDEL patients (Percentage of lowest control). Taken together data are available for 13 patients, of whom 10 show disturbed oxidative phosphorylation in one or more tissues. **low membrane potential, increased ROS production*[144].

Chapter 7

3–methylglutaconic aciduria - lessons from 50 genes and 970 patients

S. Wortmann[1+], L. Kluijtmans[2], R. Rodenburg[1,2], J. Sass[3], J. Nouws[1], E. van Kaauwen[2], T. Kleefstra[4], L. Tranebjaerg[5], M. de Vries[1], P. Isohanni[6], K. Walter[7], F. Alkuraya[8], I. Smuts[9], C. Reinecke[10], F. van der Westhuizen[10], D. Thorburn[11], J. Smeitink[1], E. Morava[1*], R. Wevers[2*]

[1]Nijmegen Center for Mitochondrial Disorders (NCMD) at the Department of Pediatrics and the Institute of Genetic and Metabolic Disease (IGMD), [2]Laboratory of Genetic, Endocrine and Metabolic Diseases (LGEM), Department of Laboratory Medicine and [4]Department of Human Genetics, Radboud University Medical Centre, Nijmegen, The Netherlands. [3]University Children's Hospital Zurich, Zurich, Switzerland and Laboratory of Clinical biochemistry and Metabolism, University Children's Hospital Feiburg, Freiburg Germany. [5]Wilhelm Johannsen Centre of Functional Genomics, ICMM, The Panum Institute, University of Copenhagen and Department of Audiology, Bispebjerg Hospital, Copenhagen, Denmark. [6]Research Program of Molecular Neurology, Biomedicum Helsinki, University of Helsinki and Clinic Group of Pediatric Neurology, Department of Gynecology and Pediatrics, Helsinki University Central Hospital, Helsinki, Finland. [7]Department of Pediatric Cardiology, University Hospital Aachen, Aachen, Germany. [8]College of Medicine, Alfaisal University and Developmental Genetics Unit, King Faisal Specialist Hospital and Research Center, Riyad, Saudi Arabia
[9]Department of Paediatrics and Child Health, Steve Biko Academic Hospital, University of Pretoria, Totiusdal, Pretoria and [10]Centre for Human Metabonomics, North-West University, Potchefstroom, South Africa. [11]Murdoch Childrens Research Institute and Victorian Clinical Genetics Services, Royal Children's Hospital, Melbourne, Victoria, Australia. *Equal contribution.

J Inherit Metab Dis. 2013, DOI 10.1007/s10545-012-9579-6.

Abstract

Elevated urinary excretion of 3–methylglutaconic acid is considered rare in patients suspected of a metabolic disorder. In 3–methylglutaconyl–CoA hydratase deficiency (mutations in AUH), it derives from leucine degradation. In all other disorders with 3–methylglutaconic aciduria the origin is unknown, yet mitochondrial dysfunction is thought to be the common denominator. We investigate the biochemical, clinical and genetic data of 388 patients referred to our centre under suspicion of a metabolic disorder showing 3–methylglutaconic aciduria in routine metabolic screening. Furthermore, we investigate 591 patients with 50 different, genetically proven, mitochondrial disorders for the presence of 3–methylglutaconic aciduria. Three percent of all urine samples of the patients referred showed 3- methylglutaconic aciduria, often in correlation with disorders not reported earlier in association with 3–methylglutaconic aciduria (e.g. organic acidurias, urea cycle disorders, haematological and neuromuscular disorders). In the patient cohort with genetically proven mitochondrial disorders 11 % presented 3–methylglutaconic aciduria. It was more frequently seen in ATPase related disorders, with mitochondrial DNA depletion or deletion, but not in patients with single respiratory chain complex deficiencies. Besides, it was a consistent feature of patients with mutations in *TAZ, SERAC1, OPA3, DNAJC19* and *TMEM70* accounting for mitochondrial membrane related pathology. 3–methylglutaconic aciduria is found quite frequently in patients suspected of a metabolic disorder, and mitochondrial dysfunction is indeed a common denominator. It is only a discriminative feature of patients with mutations in *AUH, TAZ, SERAC1, OPA3, DNAJC19* and *TMEM70*. These conditions should therefore be referred to as inborn errors of metabolism with 3–methylglutaconic aciduria as discriminative feature.

Introduction

In the urine of healthy individuals the branched-chain organic acid 3–methylglutaconic acid (3–MGA) is found only in traces. Elevated urinary excretion of 3–MGA (3–MGA–uria) was First described in patients with 3–methylglutaconyl–CoA hydratase deficiency (former type I, AUH, MIM ID: #250950), a defect of leucin catabolism leading to a late onset leukoencephalopathy[26].

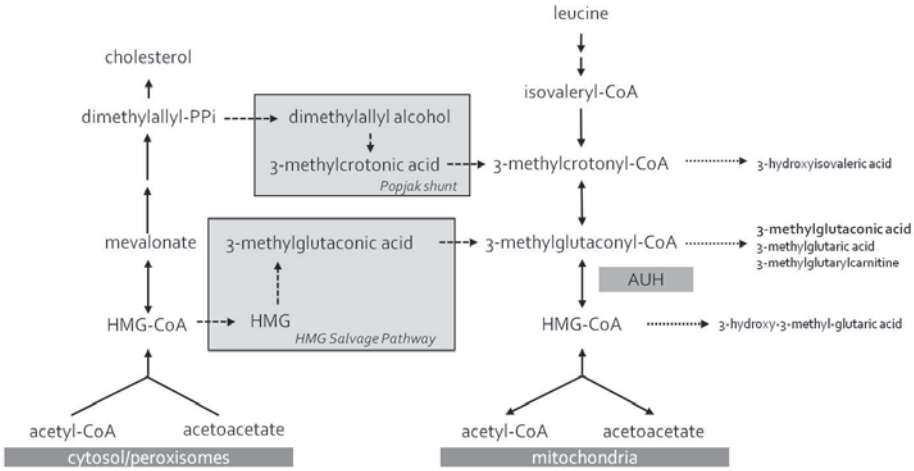

Figure 1 *Shunting between Cholesterol biosynthesis and Leucine catabolism. AUH = 3–methylglutaconyl–CoA hydratase (enzyme deficient in 3–MGA–uria type I). HMG–CoA = 3-hydroxy-3-methylglutaryl CoA (adapted from[103]).*

Only in 3–methylglutaconyl–CoA hydratase deficiency the origin of 3–MGA is known, therefore it can be considered a "primary 3–MGA–uria". This is in contrast to all other disorders in which 3–MGA–uria is seen, where the pathomechanismunderlying this biomarker is still not elucidated. However, 3–MGA–uria is the hallmark of several phenotypically heterogeneous but highly distinctive "3–MGA–urias" which were given Roman numbers randomly (Barth syndrome (former type II, *TAZ*, MIM ID: #302060), Costeff syndrome (former type III, *OPA3*, MIM ID: #258501) and DCMA syndrome (former type V, *DNAJC19*, MIM ID #610198)). Besides these well defined syndromes, there is a confusing and ever growing subgroup encompassing all "unclassified" patients, designated 3–MGA–uria type IV (MIM ID 25951).

Recently the underlying genetic defects of several of these disorders were elucidated allowing more insight into the underlying pathophysiology. Combined with the findings presented in this paper, we propose a proper pathomechanism based classification and new nomenclature of these "inborn errors of metabolism (IEM) with 3–MGA–uria as discriminative feature" which is presented in a separate article in this issue of JIMD (Wortmann et al JIMD 2013).To prevent confusion we will use the new nomenclature in this article as well. The old and new nomenclature are shown in parallel in Table 1.

	New nomenclature (affected gene)	Old nomenclature
Inborn errors with 3–MGA–uria as discriminative feature		3–MGA–uria
Primary 3–MGA–uria	3–methylglutaconyl–CoA hydratase deficiency *(AUH)*	3–MGA–uria type I
Secondary 3–MGA–uria	TAZ defect or Barth syndrome *(TAZ)*	3–MGA–uria type II
	OPA3 defect or Costeff syndrome *(OPA3)*	3–MGA–uria type III
	SERAC1 defect or MEGDEL syndrome *(SERAC1)*	3–MGA–uria type IV
	DNAJC19 defect or DCMA syndrome *(DNAJC19)*	3–MGA–uria type V
	TMEM70 defect *(TMEM70)*	3–MGA–uria type IV
	Not otherwise specified (NOS) 3–MGA–uria	3–MGA–uria type IV

Table 1 . *New and old nomenclature.*

After exclusion of the well-defined syndromes described above, each patient with elevated urinary 3–MGA has always been labelled as 3–MGA–uria type IV (MIM ID: 250951). This rapidly growing, clinically heterogeneous group challenges the physician in planning further diagnostic steps and does lead to serious confusion. Does 3–MGA–uria always indicate a mitochondrial disorder? Are there specific mitochondrial disorders one should search for in patients with 3–MGA–uria? Has every patient with an occasionally elevated urinary 3–MGA to be labelled 3–MGA–uria type IV?

In this study we address these questions above with a bidirectional approach by evaluating 977 patients. Group 1 patients (n=388) were referred to our hospital in the period 1992–2010 and had increased urinary 3–MGA. We report the clinical, biochemical and genetic data on these patients, which will reflect the diversity of underlying causes of 3- MGA excretion. Group 2 consisted of 589 patients with a vast array of 50 genetically proven mitochondrial disorders in whom organic acid analysis in urine had been performed. The group was included to evaluate the occurrence of 3- MGA-uria in mitochondrial disorders.

Material and methods

Urinary organic acid analysis

Urinary organic acid analysis was performed by gas chromatography/ mass spectrometry (GC–MS) on a HP 6890 Gas Chromatograph (Agilent, Amstelveen, The Netherlands). 3–MGA was quantified on the basis of an in house synthesized 3–MGA model compound. For quantification purposes flame ionisation detection with standard calibration curve was used. The reference range for urinary 3–MGA was 0–20 mmol/mol creatinine and has been established on ahealthy subject population in our laboratory. In selected cases additionally 1H-NMR spectroscopy on a Bruker DRX 500 spectrometer was performed[19].

Group 1: diagnoses and sampling circumstances in patients with 3–MGA–uria; inclusion and exclusion criteria

The Radboud University Nijmegen Medical Centre (RUMC) is a tertiary academic referral centre in the Netherlands with afocus on mitochondrial disorders. The database of the Laboratory of Genetic, Endocrine and Metabolic Diseases (LGEM) at the RUMC was searched for all patients with elevated urinary 3–MGA excretion of > 20 mmol/mol

creatinine in the period 1992–2010. The charts of these patients were reviewed for the clinical circumstances at the time of sampling and for the diagnoses. Inclusion criteria: i) referral of the patient to RUMC under suspicion of a metabolic disorder (patients from whom only urine was received for analysis were not included), ii) routine metabolic screening completed (urinary organic acid analysis; serum lactate, amino acid and carnitine profile analysis, transferrin isoelectric focussing, and upon indication urine oligosaccharide analysis). Exclusion criteria: i) multi-organ-failure or ii) total parenteral nutrition at the moment of sampling.

Group 2: patients with genetically proven mitochondrial disorders

We aimed to investigate the excretion of 3–MGA in patients with genetically proven pathogenic mutations causing a mitochondrial disorder. As such we have considered patients with pathogenic mutations in nuclear or mitochondrial genes involved in the biogenesis and assembly of oxidative phosphorylation system (OXPHOS) complexes, mitochondrial nucleotide synthesis and transport, mitochondrial DNA replication and translation, mitochondrial protein processing and quality control, mitochondrial protein import, mitochondrial membrane biogenesis and maintenance, pyruvate metabolism and tricarboxylic acid (TCA) cycle. We have reviewed the clinical and aboratory files of patients under treatment in our hospital or under the care of one of our coauthors. Furthermore, we have searched the PubMed database for papers describing patients with genetically provenmitochondrial disorders of whom the results of urinary organic acid analysis were included in the paper.

Results

Group 1: diagnoses and sampling circumstances in 388 patients with 3–MGA–uria

Searching the database of the LGEM at the RUMC revealed 20991 urinary organic acid profiles measured between 1992 and 2010. In 647 (3 %) samples of 388 patients 3–MGA–uria was detected. Of these patients 69 did not fulfil the inclusion criteria, another 92 met the exclusion criteria (see 2.2), consequently 227 patients were eligible for further investigations.

The results are summarized in Table 2, and more details about the diagnosed disorders and the urinary organic acid results can be found in the supplementary data. Sixty onepatients were diagnosed with a classical metabolic disorder, 43 patients with other, non-metabolic disorders (see Table 2A, B). A subgroup of 23 patients were diagnosed with an inborn errors of metabolism with 3–MGA as discriminative feature (see Table 2C).

Diagnosis	n	frequency	Max. 3-MGA (mean)*	Other metabolites?
A Classical metabolic disorders	**61**			
Fatty acid oxidation disorder (FAOD)	22	P/D	42 (26)	Y
Methylmalonic aciduria (MMA)	4	P/D	55 (39)	Y
Propionic aciduria (PA)	6	P/D	94 (42)	Y
Glycogen storage disorder (GSD)	18	P/D	82 (44)	Y
Urea cycle disorder (UCD)	6	P/D	152 (52)	Y
Other metabolic disorder	5	SE	47 (34)	Y
B Other non-metabolic disorders	**43**			
Hematological disorder	4	R, SE	35 (27)	N,Y
Neuromuscular disorder (see also Table 3)	13	R, SE	50 (28)	N,Y
Genetic syndrome/ chromosomal abnormality	15	R, SE*	46 (27)	N,Y
Apparently life-threatening event (ALTE)/ sudden infant death syndrome (SIDS)	6	SE	48 (33)	N
other	5	SE*	43 (34)	N,Y
C Inborn errors with 3-MGA-uria as discriminative feature	**23**			
3-methylglutaconyl-CoA hydratase deficiency *(AUH)*	3	R	142 (120)***	N**
TAZ defect or Barth syndrome *(TAZ)*	1	R	97 (55)	N
OPA3 defect or Costeff syndrome *(OPA3)*	1	R	43 (43)	N
TMEM70defect *(TMEM70)*	6	R	121 (83)	N
SERAC1 defect or MEGDEL syndrome *(SERAC1)*	9	R	196 (103)	N
NOS 3-MGA-uria	3	R	75 (47)	N
D remaining patients	**100**			
Mt disorder	49	R,SE	60 (29)	N,Y
Hypoglycemia	10	SE	42 (26)	N,Y
Ongoing investigations	41	R,SE	70 (32)	N,Y

Table 2. *Diagnosis and sampling circumstances 227 patients with 3-MGA-uria. Diagnosis and sampling circumstances in 227 patients with 3-MGA-uria. Gene names in italics, 3-MGA-uria = 3-methylglutaconic aciduria, * mmol/mol creatinine, **with exception of 3-Hydroxy-isovaleric aciduria, *** in literature values up to 1000 mmol/mol creatine are reported; P/D = upon presentation or deterioration, R = repetitively, SE = single episode.*

Of the remaining 100 patients (see Table 2D), 49 patients were diagnosed with a mitochondrial disorder. Of them 18 had a genetically proven diagnosis and in the other 31 patients single or multiple OXPHOS enzyme deficiencies were found in muscle. Patients in whom a decreased ATPproduction was found without evidence for single or multiple OXPHOS enzyme deficiency were considered as "possible" mitochondrial disorder, and therefore not included in this group. Ten patients had (mostly isolated) 3-MGA-uria during a single hypoglycaemic episode throughout a febrile illness, mostly of gastroenterological origin, in early childhood. Despite extensive metabolic investigation no underlying metabolic disease was detected in these patients and they are all doing well during follow up of up to 15 years. In 41 patients with isolated or combined presentation of multisystem disorder, psychomotor retardation, leukoencephalopathy,syndromal appearance, myopathy, spastic paraparesis, cataract, neurodegenerative disease, polyneuropathy and/or movement disorders the investigations are ongoing. From the latter group 11 patients showed decreased ATP production without OXPHOS complex deficiencies in a

fresh muscle biopsy, three had biochemically and histologically normal biopsies, the remaining 30 did not undergo muscle biopsy.

	Diagnosis (*affected gene*)	UOA: 3–MGA value(s)*	UOA: other findings
1	Congenital merosin negative muscle dystrophy *(NA)*	32	none
2	Congenital merosin negative muscle dystrophy *(NA)*	24, 25, 23, 17, 8, 13	once ketotic profile, always EMA
3	Congenital Actine Filament aggregation myopathy without nemaline rods *(NA)***	26, 12	none
4	Duchenne Muscular Dystrophy *(DMD)****	23, 13	EMA, lactate, succinic acid
5	Lipid myopathy *(NA)*	22	none
6	Multi-minicore myopathy *(RYR1)*	21	none
7	Multi-minicore myopathy *(RYR1)*	37, 26, 24, 18	TCA intermediates, once ketotic profile
8	SMA *(SMN1)*	41	MMA, EMA
9	SMA *(SMN1)*	23	EMA, mild elevation of dicarbonic acids
10	SMA *(SMN1)*****	23; 18	EMA
11	SMA *(SMN1)*****	27, 27, 25, 25, 19, 19, 19	EMA, adipic and suberic acid, TCA cycle intermediates
12	SMA *(SMN1)*	22	EMA
13	Muscular Dystrophy *(NA)*	50, 46	none

Table 3. *Details on 13 patients with neuromuscular disorders and 3–MGA–uria. EMA = ethylmalonic aciduria, MMA = methylmalonic aciduria, NA = not available, SMA = spinal muscular atrophy, UOA = urinary organic acid analysis, * inmmol/mol creatinine (ref. 0–20) in chronological order; ** low serum citrulline, ***prednisone treatment, **** SCADD excluded genetically.*

Group 2: 3–MGA–uria patients with genetically proven mitochondrial disorders

For a total of 591 patients carrying pathogenic mutations in 50 nuclear genes or the mitochondrial DNA we could retrieve the urinary organic acid results. This encompasses 202 patients from our centre or under the care of one of our co-authors and 389 patients from the literature. The data are summarized in Table 4.

Discussion

3–MGA–uria is a rather common finding in patients suspected of a metabolic disorder

3–MGA–uria was thought to be a rare finding in patients suspected of a metabolic disorder. Unexpectedly, we observed it in nearly 3 % of all samples received for urinary organic acid analysis at our centre in the last 18 years. 3–MGA–uria was frequently seen in association with several metabolic disorders, such as organic acidurias, glycogen storage disorders (GSD), fatty acid oxidation disorders (FAODs), urea cycle disorders.

3-MGA-uria is mostly correlated with mitochondrial dysfunction

A relation with mitochondrial dysfunction undoubtedly accounts for most patients with 3-MGA-uria. Ten percent of all 3-MGA-uria patients were diagnosed with FAODs (see Table 2A), in fact primary mitochondrial disorders. 3-MGA-uria was also found frequently in patients presenting with a metabolic crisis due to an organic aciduria. Propionyl-CoA has been shown to non-competitively inhibit pyruvate dehydrogenase complex (PDHc, [146]), also multiple OXPHOS deficiency in different tissues was detected in organic aciduria patients [147].

Mitochondrial dysfunction also may play a role in urea cycle disorder patients showing 3-MGA-uria. It is proven in rodents, that hyperammonemia inhibits the TCA cycle enzyme α-ketoglutarate-dehydrogenase and activates the N-methyl D-aspartate (NMDA) receptor leading to disturbed calcium homeostasis and secondary mitochondrial dysfunction[148].This theory is supported by the frequent co-finding of TCA cycle intermediates and lactate in our urea cycle disorder patients with 3-MGA-uria.

We also tentatively postulate mitochondrial dysfunction as underlying cause for 3-MGA-uria in a group of 37 patients diagnosed with other non-metabolic disorders (Table 2B). However, we can only partly prove this, as only five of the patients underwent a muscle biopsy which showed disturbed mitochondrial function before the final diagnosis was made. On the other hand often lactic acidosis or alanine elevation pointed towards mitochondrial dysfunction. In 13 of these 37 patients, a muscle biopsy was only investigated histologically leading to the diagnosis of a neuromuscular disorder (see Tables 2B and 3). The consistent finding of 3-MGA-uria in this patient group could be a sign of mitochondrial dysfunction. For two classical neuromuscular disorders mitochondrial dysfunction has recently been reported. In myoblasts of the mdx mouse, a well established mouse model of DMD, an impaired cellular energy metabolism due to abnormal calcium homeostasis, reduced amounts of OXPHOS complexes and ATP synthase as well as disorganized mitochondrial network were observed[149]. Furthermore, energy shortage and increased mitochondrial free radical production leading to cell damage was also recently shown in a neural cellmodel of SMA[150], suggesting mitochondrial dysfunction as important pathology underlying SMA.

3-MGA-uria in correlation with impaired cholesterol biosynthesis

The mevalonate or Popjak shunt links cholesterol biosynthesis with leucine catabolism (Figure 1). In patients with Smith Lemli Opitz syndrome elevated 3-MGA-levels have been reported in seven of 35 patients[12]. We did not detect 3-MGA-uria in eight Smith Lemli Opitz syndrome patients on cholesterol/simvastatin treatment.

However, the earlier reported patients, were untreated patients with very low cholesterol levels (< 0.129 mmol/L, reference range not given [12]), suggesting that it only occurs in untreated patients on the severe end of the Smith Lemli Opitz syndrome -spectrum or with high cholesterol precursors[12]. We also did not detect 3-MGA-uria in three patients with Mevalonate kinase deficiency, another defect of cholesterol biosynthesis. However, the

HMG salvage pathway has recently been proven to account for the elevated 3–MGA production in a zebrafish model of Costeff syndrome. The authors showed, that simvastatin inhibited mevalonate production from extramitochondrial HMG–CoA, which leads to elevated 3–MGA levels (see Figure 1, [54]). This shunt should explain the 3–MGA–uria found in 18 of our patients, later diagnosed with GSD I or IX. The finding of 3–MGA–uria was reported earlier in one patient with GSD 1b[79] An imbalanced homeostasis between disturbed gluconeogenesis and cholesterol synthesis is supposed to increase the shunting towards 3–MGA production. One should keep the differential diagnosis of a GSD in mind when facing a patient with elevated lactate, 3–MGA–uria and hepatomegaly clinically suspected of a mitochondrial disorder. Possibly the 3–MGA–uria in two of the patients with haematological disorders, and the Duchenne patient is also related to cholesterol metabolism as the patients were treated with glucocorticosteroids for a long time.

Differential diagnosis in patients with 3–MGA–uria.

After excluding the described patient groups (see Table 2A, B, C) a group of 100 patients with 3–MGAuria (Table 2D) remained. Primary mitochondrial dysfunction defined by either single or multiple OXPHOS deficiency or genetically proven mitochondrial disorder was found in half of the patients. No disorder could be established in spite of extensive investigations in ten patients with a single hypoglycaemia during febrile illness in early childhood and in four patients with ALTE. These children are all doing well during long years of follow up. One may postulate an underlying disorder in (energy) metabolism which is only clinically significant in a limited time window in early childhood. The remaining group of 41 patients, mostly presenting with progressive neurodegenerative disorders, in whom investigations are ongoing is surely an interesting and challenging group. However, this group is clinically very heterogeneous, and most of the patients only showed 3–MGA–uria occasionally and mildly elevated. One should therefore not overrate the diagnostic value of 3–MGA–uria in these patients, but keep an eye open for all diagnostic features of a patient (e.g. physical examination, dysmorphic features, biochemical results, radiological results).

Correlation of 3–MGA–uria with specific mitochondrial disorders

Mutations in TAZ, OPA3, TMEM70 and SERAC1, respectively, are virtually always associated with 3–MGA–uria (88–100% of cases see Table 4). These patients show repetitively and consistently increased urinary 3–MGA, which is also substantially higher as in other disorders (see Table 2). There are no other diagnostic urinary metabolites found beside 3–methylglutaric acid. Hence, the 3–MGA–uria is a major finding, a hallmark of the phenotype and often the key to the diagnosis. These disorders, as well as 3–methylglutaconyl–CoA hydratase deficiency (AUH defect), should be referred to as IEM with 3–MGAuria as discriminative feature. Interestingly, they are all related tomitochondrialmembrane pathology in the broadest sense. 3- MGA-uria is frequently seen in patients with mutations in AGK (70 %). In most cases the excretion is <40 mmol/mol

creatinine. One should not label these patients IEM with 3- MGA-uria as discriminative feature as the clinical and biochemical phenotype is too diverse. Three patients presented with isolated cataract [151], and all turned out to have 3–MGA–uria (F. Alkuraya, personal information). The other end of the spectrum of patients with AGK mutations is Sengers syndrome with cataracts and (cardio)myopathy with four out of seven patients being reported with 3–MGA–uria.

We found 3–MGA–uria in 11 % of all patients with a proven ("primary") mitochondrial disorder. There are three subgroups of patients in which 3–MGA–uria could be helpful in the diagnostic work up.

Gene function	MtDNA	Nuclear DNA	Own	Lit.***	All
Structure and assembly of C I	*MTND2 (1/3); MTND3; MTND4; MTND5; MTND6*	*NDUFS2; NDUFS6; NDUFS7 (1/3); NDUFS8; NDUFV1; NDUFAF2; C20orf7; ACAD9*	2/20	0/15	2/35=5.7%
Structure and assembly of C II	-	*SDHA*	0/1	NR	0/1
Structure and assembly of C III		*BCS1L*	-	0/6	0/6
Structure and assembly of C IV	*MTCO1;MTCO2*	*COX10; COX15; COX6B1; FASTKD2; SCO1; SCO2; SURF1*	0/3	0/11	0/14
Structure and assembly of C V	*MTATP6 (1/8); MTATP8*	*ATP5E (1/1); ATP12(1/1)*	1/11	2/18	3/29=10.3%
		TMEM70	**7/7**	**55/58**	**62/65=95%**
MtDNA replication, nucleotide synthesis and transport		*POLG (6/41); DGUOK; TK2; TYMP; SLC25A3; SUCLG1(2/12)*; SUCLA2(5/6)*; TWINKLE (1/21); RRM2B; MPV17*	13/80	1/36	14/116=12%
MtDNA translation	*MTTL (m.3243A>G (4/26)),MTTS*	*EFG1; MRPS22; PUS1; TRMU; DARS2; RARS2*	3/26	1/35	4/61=6.5%
Mt protein import		*TIMM8A*	0/5	NR	0/5
		DNAJC19	**-**	**19/19**	**19/19=100%**
Mt membrane phospholipid remodelling		***TAZ***	**3/3**	**46/53**	**49/56=88%**
		SERAC1	**18/18**		**18/18=100%**
Mt membrane biogenesis and maintenance		*OPA1*	0/2	0/31	0/33
		OPA3	**1/1**	**44/44**	**45/45=100%**
		AGK	6/9	1/1	7/10=70%
Mt other	*Deletion (8/24)*		0/5	8/19	8/24=30%
CoQ10 related		*COQ2; PDSS1; ETFDH (3/35)*	1/7	2/34	3/41=7.3%
Pyruvate metabolism		*PDHA1; PDP1*	0/2	0/2	0/4
TCA cycle related		*FH;* alpha-ketoglutarate DH***	-	0/7	0/7
IEM with 3-MGA-uria as discriminative feature			**31/31**	**164/174**	**195/205=95%**
Other			26/171	15/215	41/386=11%
All			57/202	179/389	236/591

Table 4 *Presence of 3-MGA-uria in 591 patients with known mutations. 3-MGA= 3-methylglutaconic acid, 3-MGA-uria= 3-methylglutaconic aciduria, DH= dehydrogenase, IEM = inborn error of metabolism, C = complex of the respiratory chain, CoQ= Coenzyme Q10, Mt =mitochondrial, NR = not reported in literature, TCA= Tricarboxylic acid cycle* part of TCA cycle, but clinical and biochemical phenotype of mtDNA depletion syndrome, ** gene unknown, maps to 7q14-1. ***References are presented in the supplementary data. Gene names in italics. IEM with 3-MGA-uria as discriminative feature in bold.*

The first subgroup with a high correlation of disease mechanism and 3–MGA–uria, are the patients with mitochondrial deletion leading to the Pearson phenotype. Of these patients 30 % are reported with 3–MGA–uria[72-74, 152, 153]. Curiously, mitochondrial deletions presenting with the Kearns-Sayre phenotype do not lead to 3–MGA–uria. The finding of 3–MGA–uria in a patient presenting with refractory anemia should lead the physician to mitochondrial DNA deletion screening in several tissues, hence sparing the patient a bone marrow aspiration.

Two other patient subgroups show 3–MGA–uria in 10.3 and 12 % of patients, respectively. These are patients with ATPase deficiency related pathology and patients with mitochondrial depletion syndromes.

3–MGA–uria is seen less frequently in patients with complex I-related mutations (5.7 %) and until now not found in relation with complex II, III or IV mutations. In contrast, both patients with ATPase related mutations (ATP5E, ATP12) did have 3–MGA–uria, as had one of the MTATP6 patients. Combining this with the consistent 3–MGA–uria found in 95% of patients with TMEM70 defect, this makes a link of 3–MGAuria and ATPase-dysfunction or -related processes affecting the mitochondrial membrane more likely. One should still keep in mind, that the investigated mutations are very rare and often only one patient in each category is reported. Furthermore, patients with mitochondrial depletion syndromes (POLG, SUCLG1, SUCLA2 and TWINKLE mutations) more often show 3–MGA–uria. Strictly SUCLG1 and SUCLA2 are genes involved in the TCA cycle, given the fact that they lead to a typicial mitochondrial depletion syndrome, we chose to group the patients here [104]. In patients with a phenotype suggestive for a mitochondrial depletion syndrome 3–MGA–uria makes this suspicion stronger. One limitation of this group is, that 3–MGA–uria was mainly found in the patient population of the contributing authors. This could be due to the fact, that these Laboratories are able to quantify 3–MGA in urine and therefore are able to detect slight elevations (20–40 mmol/mol creatinine). Other laboratories may often report 3–MGA–uria only if more substantial (>40 mmol/mol creatinine) as is the case in the IEM with 3–MGA–uria as discriminative feature. Furthermore, there is again a limited number of patients reported, often in genetic or neurological journals without describing the metabolic findings beside lactic acidosis. In addition there are depletion syndromes with pure myopathic presentation in which a muscle biopsy rather than metabolic work-up is chosen as diagnostic approach. However, the correlation could help the physician in search for the diagnosis.

3–MGA–uria has not been found in association with defects in mitochondrial translation, again with the limitation of small patient numbers of these newly found group of diseases. Mutations in DNAJC19 underlie DCMA syndrome. All described 19 patients had 3–MGA–uria. DNAJC 19 is suspected to be involved in mitochondrial protein import. In contrast, we did not find 3–MGA–uria in five patients with Mohr-Tranebjaerg syndrome (TIMM8A), a dystonia-deafness syndrome in which a similar pathomechanism is suspected.

TAZ and OPA3 defect are both suspected to alter mitochondrial membrane biogenesis and maintenance ("fusion/fission"). Contradictory no patients with 3–MGA–uria and OPA1 mutations, also leading to a defective fusion/fission, have been found.
3–MGA–uria is seen in multiple acyl-CoA dehydrogenase deficiency (MADD, Glutaric aciduria IIc) patients with mutations in ETFDH. The defect affects fatty acid, amino acid and choline metabolism, but certainly mitochondrial dysfunction is present in this complex disorder.

Conclusions

3–MGA–uria is a rather common finding in patients suspected of a metabolic disorder. In most patients it is seen in association with mitochondrial dysfunction. The majority of patients can be diagnosed upon routine metabolic screening including urine oligosaccharide screening for the differential diagnosis of GSD. In the latter the 3–MGA probably stems from the cholesterol biosynthesis. The minority of patients suffers an IEM with 3–MGA–uria as discriminative feature, a diagnostic flowchart and more details on a pathomechanism based classification and nomenclature of these disorders is presented in an accompanying article in this issue of JIMD [154].

Supplementary results

Group 1A: Classical metabolic disorders

61 patients were diagnosed with classical metabolic disorders (see Table 2A).

22 patients had 3–MGA–uria during crisis, based on which the following fatty acid oxidation (FAO) disorders were diagnosed: i.e. two carnitine palmitoyltransferase II deficiency (CPT2D), four very long-chain acyl-CoA dehydrogenase deficiency (VLCADD), four long-chain hydroxyacyl-CoA dehydrogenase deficiency (LCHADD), three medium-chain acyl-CoA dehydrogenase deficiency (MCADD), four short-chain acyl-CoA dehydrogenase deficiency (SCADD), four multiple acyl-CoA dehydrogenase deficiency (MADD), one 3–hydroxy–3–methylglutary–CoA(HMG–CoA) synthase deficiency. Ten patients had 3–MGA–uria upon presentation with an organic aciduria (four methylmalonic aciduria (MMA), six propionic aciduria (PA)). In one of the MMA and all of the PA patients, 3–MGA–uria was repeatedly seen upon metabolic derangement. The urine samples also exhibited the classical signs of MMA or PA, such as propionylglycine and 3-OH-propionic acid (PA patients), methylmalonic acid (MMA patients), 2-methylcitric acid (in both organic acidurias). Most of the urines also contained intermediates of the TCA cycle and elevated lactate. In 18 patients, a glycogen storage disorder (GSD) was diagnosed. The samples were taken randomly during the disease course of eight patients with GSD IX and upon presentation or metabolic crisis of ten GSD Ia/b patients. Often, also a mild to severe ketosis was seen, in nine samples elevated lactate and in six samples TCA cycle intermediates were reported in addition. Six patients with urea cycle disorders (UCD; i.e. two carbamoylphosphate synthase I deficiency (CPS1D), two argininosuccinate lyase deficiency (ASLD), two ornithine transcarbamylase deficiency (OTCD) showed 3–MGA–uria upon disease presentation or metabolic deterioration during the course of disease. Besides the typical UCD pattern, lactate was detected in all patient samples and TCA cycle intermediates in three. Five patients were diagnosed with other metabolic disorders, i.e. guanidinoacetate methyltransferase (GAMT) deficiency, lipoproteinlipase deficiency, tyrosine hydroxylase deficiency, peroxisomal biogenesis disorder and cystinosis.

Group 1B: Classical non-metabolic disorders

43 Patients were diagnosed with other, non-metabolic disorders (see Table 2 B). Four patients with 3–MGA–uria were diagnosed with haematological disorders. Two patients with hemophagocytic lymphohistiocytosis (HLH) whose samples were taken during evaluation of short stature after bone marrow transplantation and extensive glucocorticosteroid treatment. One patients with acute lymphatic leucemia (ALL) was tested for a suspected inborn error of metablism because of extremely high cholesterol levels during partial parenteral nutrition including intravenous lipids. One patient, presenting with hepatomegaly and pancytopenia was later diagnosed with Myelodysplastic syndrome (MDS). 13 patients were diagnosed with a neuromuscular

disorder (for details see Table 3). In most of the patients 3–MGA was consistently elevated in the urine. Seven of the patients also showed ethylmalonic aciduria (EMA-uria), in two of them SCADD was excluded genetically. Two of these seven patients had lactic acidemia, none had elevated serum alanine. The patient with Duchenne muscular dystrophy was treated with prednisone upon sampling. A total of 15 patients were diagnosed with genetic disorders, i.e. cardiofaciocutaneous (CFC) Syndrome, Sphrintzen-Goldberg Syndrome, Pelizaeus-Merzbacher Syndrome, Kabuki, CHARGE, Noonan and ter Haar Syndrome (each in one patient, respectively), eight with (multiple) chromosomal abnormalities. In five of these patients mitochondrial dysfunction in muscle (defined as: decreased ATP production and/or single or multiple OXPHOS enzyme deficiencies) was reported. In the other 10 patients, the final diagnosis was made without a muscle biopsy, hence it is unknown if they have a mitochondrial dysfunction.

Group 2: 3–MGA–uria patients with genetically proven mitochondrial disorders

For a total of 591 patients carrying pathogenic mutations in 50 nuclear genes or the mitochondrialDNA we could retrieve the urinary organic acid results. This encompasses 202 patients from our centre or under the care of one of our co-authors and 591 patients from the literature. The data are summarized in Table 4.

Five patients were diagnosed with other disorders, i.e. celiac disease, glucose galactose malabsorption syndrome, juvenile idiopathic arthritis (JIA), cystic fibrosis were each observed in one of these patients, respectively. One female patient was pregnant at the moment of testing, a condition in which 3–MGA–uria is known to occur[81].

Six patients had suffered from an apparently life threatening event (ALTE), two died of sudden infant death syndrome (SIDS) just before sampling. Beside the 3–MGA–uria, the urinary organic acid pattern did not show other metabolites pointing towards a specific inborn error of metabolism.

In patients with mutations in genes encoding for the biogenesis and assembly of OXPHOS complexes, 3–MGA–uria was found in relation with the nuclear genes *NDUFS7* (one out of three, 1/3), *ATP5E* (1/1), *ATP12* (1/1), *TMEM70* (57/60) and the mitochondrial DNA genes MTND2 (1/3) and MTATP6 (m.8993T>G, 1/8). In patients with mutations in genes involved in mitochondrial DNA replication, six *POLG* (6/41) and one *TWINKLE* (1/21) patients had elevated urinary 3–MGA. In correlation with genes encoding for mitochondrial nucleotide synthesis and transport 3–MGA–uria was seen in *SUCLG1* (2/12) and *SUCLA2* (5/6) patients. 3–MGA–uria was not found in other mitochondrial depletion syndromes (mutations in *RRM2B 0/3, DGUOK 0/9, TK2 0/10, TYMP 0/9, MPV17 0/3*).

In patients with mutations in nuclear genes involved in mitochondrial translation, elevated levels of 3–MGA were not found, but it was seen in four patients with mitochondrial DNA mutations in MTTL (tRNA Leu, m.3243A>G, 4/26). Furthermore 3–MGA–uria was seen in eight of sixteen patients with Pearson syndrome due to deletions in DNA, but not in other clinical phenotypes (e.g. Kearns Sayre syndrome, total 8/24). In patients with *SPG7* mutations, a gene involved in mitochondrial protein processing and quality control, no

urinary organic acid profiles were available. In patients with mutations in genes involved in mitochondrial protein import, 3–MGA–uria was reported in all patients with *DNAJC19* syndrome (*DNAJC19*, 17/17 = 100%) but not in patients with *TIMM8A* (0/5) mutations. 3–MGA–uria is seen in most patients with *TAZ* syndrome 49/56 = 88%) and in all patients with mutations in *SERAC1* (18/18 = 100%), both phospholipid remodelling disorders.

In patients with defects in genes involved in mitochondrial membrane biogenesis and maintenance, 3–MGA–uria was a consistent feature in patients *OPA3* syndrome (*OPA3*, 45/45 = 100%) but not in patients harbouring *OPA1* mutations (0/33). It was also a hallmark of patients with *TMEM70* mutations (*TMEM70*, 57/60 = 95%) and frequently, but less often in patients with mutations in *AGK* (7/10). AGK mutations can lead to Sengers syndrome (4/7), but also to isolated cataracts[151].

Furthermore 3–MGA–uria was found in patients with *ETFDH* mutations (3/35). 3–MGA–uria was not found in relation with TCA cycle (0/7) or pyruvate metabolism (0/4) disorders.

Taken together, 3–MGA–uria is seen as a consistent feature in the 3–MGA syndromes and in a high percentage of patients with *AGK* mutations. In the remaining 386 patients, harbouring mutations in 45 nuclear genes or the mitochondrial DNA, 3–MGA–uria is found in 42 patients (11%).

We did not detect 3–MGA–uria in eight patients with Smith Lemli Opitz Syndrome (SLOS), neither in three patients with mevalonate kinase deficiency

Structure and assembly of C I	**155-164**
Structure and assembly of C III	165-170
Structure and assembly of C IV	171-179
Structure and assembly of C V	64-67, 180-184
Mitochondrial DNA replication, nucleotide synthesis and transport	185-210
Mitochondrial DNA translation	60, 211-223
Mitochondrial protein import	75, 224
Mitochondrial membrane phospholipid remodelling	3, 10, 34, 39, 225-246
Mitochondrial membrane biogenesis and maintenance	1, 45, 46, 48, 151, 247-250
Mitochondrial other	72-74, 152, 153, 251-260
CoQ10 related	78, 261-267
Pyruvate metabolism	268, 269
TCA cycle related	270-272

Supplementary reference list for table 4.

Chapter 8

Inborn errors of metabolism with 3–methylglutaconic aciduria asdiscriminative feature: proper classification and nomenclature.

S. Wortmann[1+], M. Duran[2], Y. Anikster[3], P. Barth[4], W. Sperl[5], J. Zschocke[6]*, E. Morava[1]*, R. Wevers[7]*

[1]Nijmegen Centre for Mitochondrial Disorders at the Department of Pediatrics and the Institute of Genetic and Metabolic Disease and [7]Laboratory of Genetic, Endocrine and Metabolic Diseases (LGEM), Department of Laboratory Medicine, Radboud University Medical Centre, Nijmegen, The Netherlands. [2]Laboratory Genetic Metabolic Diseases and [4]Emeritus Professor of Pediatric Neurology, Emma Children's Hospital/Academic Medical Centre, University of Amsterdam, Amsterdam, The Netherlands. [3]Metabolic Disease Unit, Edmond and Lily Safra Children's Hospital, Sheba Medical Center, Sackler Faculty of Medicine, Tel Aviv University, Tel Aviv, Israel. [5]Department of Paediatrics, Paracelsus Medical University, Salzburg, Austria. [6]Division of Human Genetics, Innsbruck Medical University, Innsbruck, Austria. *Equal contribution.

J Inherit Metab Dis. 2013, DOI 10.1007/s10545-012-9580-0.

Abstract

Increased urinary 3–methylglutaconic acid excretion is a relatively common finding in metabolic disorders, especially in mitochondrial disorders. In most cases 3–methylglutaconic acid is only slightly elevated and accompanied by other (disease specific) metabolites. There is, however, a group of disorders with significantly and consistently increased 3–methylglutaconic acid excretion, where the 3–methylglutaconic aciduria is a hallmark of the phenotype and the key to diagnosis. Until now these disorders were labelled by roman numbers (I–V) in the order of discovery regardless of pathomechanism. Especially, the so called "unspecified" 3–methylglutaconic aciduria type IV has been ever growing, leading to biochemical and clinical diagnostic confusion. Therefore, we propose the following pathomechanism based classification and a simplified diagnostic flow chart for these "inborn errors of metabolism with 3–methylglutaconic aciduria as discriminative feature". One should distinguish between "primary 3–methylglutaconic aciduria" formerly known as type I (3-methylglutaconyl-CoA hydratase deficiency, AUH defect) due to defective leucine catabolism and the—currently known—three groups of "secondary 3–methylglutaconic aciduria". The latter should be further classified and named by their defective protein or the historical name as follows: i) defective phospholipid remodelling (TAZ defect or Barth syndrome, SERAC1 defect or MEGDEL syndrome) and ii) mitochondrial membrane associated disorders (OPA3 defect or Costeff syndrome, DNAJC19 defect or DCMA syndrome, TMEM70 defect). The remaining patients with significant and consistent 3–methylglutaconic aciduria in whom the above mentioned syndromes have been excluded, should be referred to as "not otherwise specified (NOS) 3–MGA uria" until elucidation of the underlying pathomechanism enables proper (possibly extended) classification.

Introduction

In the urine of healthy individuals 3–methylglutaconic acid (3–MGA) is found only in traces (0–10 mmol/mol creatinine). Increased urinary excretion of 3–methylglutaconic acid (3–MGA–uria), often associated with 3–methylglutaric aciduria, is a relatively common finding in patients with metabolic disorders in general[273]. In these cases, 3–MGA–uria is mostly found occasionally, e.g. upon presentation or during severe metabolic decompensation of e.g. propionic aciduria. It is not isolated but only an accompanying finding beside several other, more disease specific, urinary metabolites. Another patient group in whom 3–MGA–uria is seen in approximately 11 % of all patients (isolated or together with e.g. Krebs cycle intermediates), are patients with disorders of the oxidative phosphorylation (e.g. due to mutations in POLG[273]). In these patient groups 3–MGAuria is mostly mild (20–40 mmol/mol creatinine), only a minor finding and not the hallmark of the phenotype. Also patients with the mitochondrial AGK defect (or Sengers syndrome) may have increased 3–MGA in their urine[249].

This is different in another group of patients with significantly and consistently increased 3–MGA excretion (40- >1000 mmol/mol creatinine). Here, the 3–MGA–uria is a major finding, a hallmark of the phenotype and often the key to the diagnosis. Consider e.g. the differential diagnosis of optic atrophy, which is very long, but the finding of 3–MGA–uria reduces the differential diagnosis to Costeff syndrome. The same holds even more so for patients with cardiomyopathy.

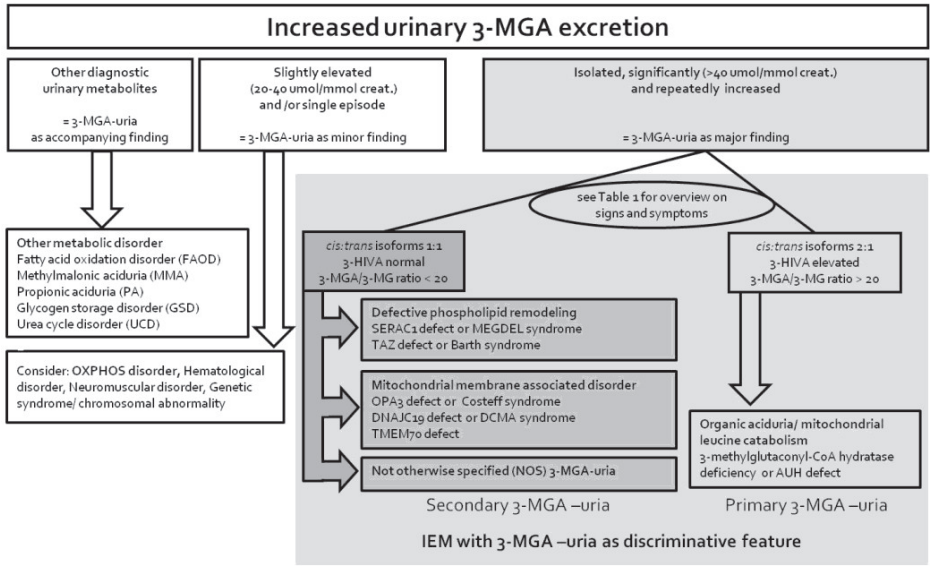

Figure 1. *Diagnostic flowchart for patients with increased urinary 3–methylglutaconic acid excretion 3–HIVA = 3–hydroxyisovaleric acid, 3–MGA = 3–methylglutaconic acid, 3–MGA–uria = 3–methylglutaconic aciduria, IEM = inborn error of metabolism, NOS = not otherwise specified, OXPHOS = oxidative phosphorylation system.*

Therefore we propose to refer to this group of disorders as **"inborn errors of metabolism with 3-methylglutaconic aciduria as discriminative feature".**

Until now the different disorders with significantly elevated urinary 3-MGA excretion were randomly given roman numbers (I-V), without taking the underlying pathomechanism into account for a proper classification. Especially "the unspecified" 3-MGA-uria type IV was ever growing, as was the confusion it caused. Therefore we propose to use the following classification based upon the underlying pathomechanism (see Table 1 and Figure 1) for this group of "inborn errors of metabolism with 3-methylglutaconic aciduria as discriminative feature".

The former type I, 3-methylglutaconyl-CoA hydratase deficiency, is the only "primary 3-methylglutaconic aciduria" due to the hydratase defect in leucine catabolism[22, 90]. In all other types the exact mechanism leading to 3-MGA-uria is unknown, but not directly related to leucine breakdown, therefore one should refer to them as "secondary 3-methylglutaconic aciduria(s)". Most of these disorders are recognizable, distinctive clinical associations, that have been described before the molecular defect had been found and therefore classify as syndromes (e.g. Barth syndrome, Costeff syndrome, MEGDEL syndrome, DCMA syndrome). Though patients with mutations in TMEM70 also show 3-MGA-uria as consistent feature but do have a variable (and still expanding) phenotype one should avoid to refer to 3-MGA-syndromes when dealing with this group of disorders. The patients can be further subdivided and classified correctly based on the underlying pathomechansim as follows: i) defective phospholipid remodelling (TAZ defect or Barth syndrome, SERAC1 defect or MEGDEL syndrome) or ii) mitochondrial membrane associated disorders (OPA3 defect or Costeff syndrome, DNAJC19 defect or DCMA syndrome, TMEM70 defect). The remaining patients with significant and consistent 3-MGA-uria (>40 µmol/mmol creatinine) in whom the above mentioned defects have been excluded, should be referred to as "not otherwise specified (NOS) 3-MGA-uria" until the underlying pathomechanism is elucidated leading to a more precise classification.

This nomenclature also simplifies the diagnostic approach (see Figure 1). When facing a patient with increased urinary excretion of 3-MGA one should first discriminate whether the 3-MGA-uria is just a minor or accompanying finding or a major finding.

Primary 3-MGA-uria

If 3-MGA-uria is significantly and consistently elevated (>40 mmol/mol creatinine), the "Primary 3-MGA-uria" **3-methylglutaconyl-CoA hydratase deficiency or AUH defect (MIM #250950, former type I)** can be easily diagnosed upon the finding of increased 3-hydroxyisovaleric acid (3-HIVA) and the 2:1 ratio for cis:trans isoforms[19]. Furthermore the ratio between 3-MGA/3-MG in general is>20 in AUH defect patients and<20 in all other inborn errors of metabolism with 3-methylglutaconic aciduria as discriminative feature (personal communication R. Duran). The ratio of the two isoforms can be determined with proton NMR spectroscopy (Engelke et al 2006) as well as by conventional GC-MS analysis of organic acids in urine as the two forms appear as separate peaks in the chromatogram[19].

We propose to use 3–methylglutaconyl–CoA hydratase deficiency or AUH defect as disease name, as it directly links to the underlying defective leucine catabolism. The patients show an adult onset of disease with progressive spasticity and dementia with a characteristic slowly developing radiological picture of extensive leucoencephalopathy [26].
In all other types, "the secondary 3–MGA–urias", the cis:trans isoforms show a 1:1 ratio and 3–HIVA is normal. The excretion level of 3–MGA in the urine can also be helpful for the differential diagnosis (see Figure 2). A thorough clinical examination and a multi-organ screening are necessary to further subdivide the different disorders. A detailed review of the clinical, radiological and biochemical phenotypes of the different syndromes is beyond the scope of this article. We refer the interested reader to a recent review[103]. Table 1 provides a short overview on the clinical, biochemical and radiological findings.

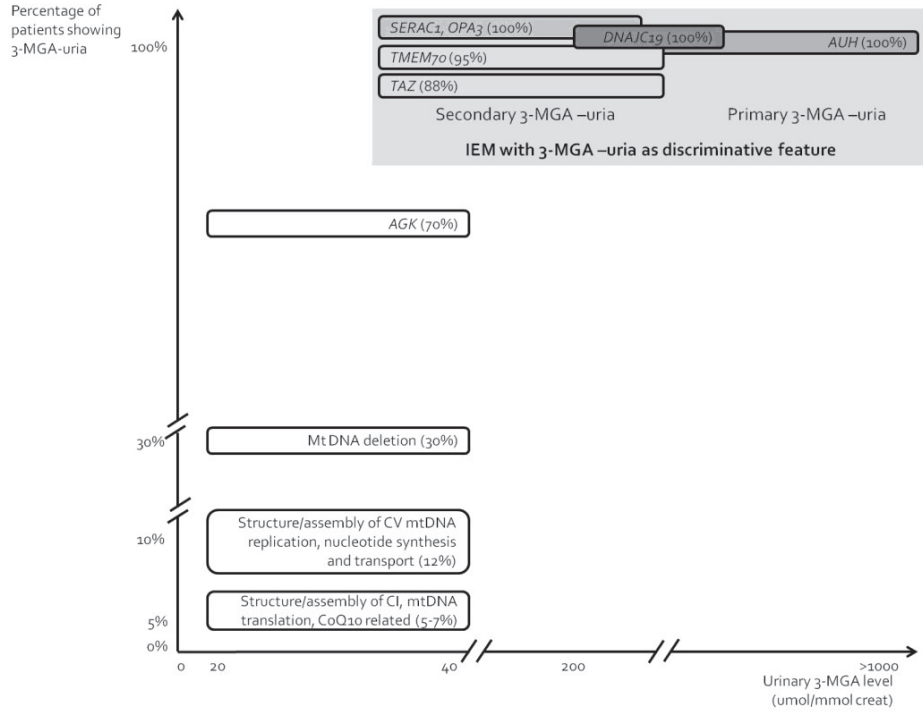

Figure 2. *3–methylglutaconic aciduria in different metabolic disorders: How high? How frequent? Excretion levels of urinary 3–methylglutaconic acid (3–MGA) and percentage of patients showing this finding in patients with inborn errors of metabolism (IEM) with 3–methylglutaconic aciduria (3- MGA-uria) as discriminative feature and patients with different types of oxidative phosphorylation system (OXPHOS) disorders. All disorders are represented by the abbreviations of the underlying genetic defect. Mt = Mitochondrial. C = Complex of the respiratory chain. CoQ = Coenzyme Q10.*

Secondary 3-MGA-uria

Secondary 3-MGA-uria due to defective phospholipid remodelling

The only known X-linked disorder is **TAZ defect or Barth syndrome** (MIM #302060, former type II) presenting in males with 3-MGA-uria, (left ventricular non-compaction) cardiomyopathy, neutropenia, myopathy, typical facial features, hypocholesterolemia and a cognitive phenotype [32, 44]. The TAZ gene encodes taffazin, which is involved in cardiolipin remodelling in the mitochondrial membrane. Disturbed cardiolipin remodelling leads to oxidative phosphorylation defects and is involved in apoptosis and mitochondrial membrane dynamics. Patients with SERAC1 defect or MEGDEL syndrome (MIM # 614739) present during early childhood with the unique combination of 3-MGA-uria, deafness, progressive spasticity and dystonia, psychomotor retardation and Leigh like syndrome on MRI[68, 232]. Mutations are found in SERAC1, encoding an enzyme involved in phosphatidylglycerol remodelling. The enzyme is essential for both mitochondrial function and intracellular cholesterol trafficking[232].

Secondary 3-MGA-uria due to mitochondrial membrane associated disorders

Patients with **OPA3 defect or Costeff syndrome (MIM #258501, former type III)** present in infancy with the classical trias of 3-MGA-uria, optic atrophy and movement disorder (ataxia or extrapyramidal disorder)[45, 46]. Mutations were found in OPA3, the function of its gene product OPA3 is not fully elucidated, but a protective function for the respiratory chain has been shown recently[54]. Hutterite patients with **DNJAC19 defect or DCMA syndrome** (MIM #610198, former type V) show the characteristic combination of childhood onset dilated cardiomyopathy, non-progressive cerebellar ataxia, testicular dysgenesis, growth failure, and 3-MGA-uria[75]. Mutations are found in DNAJC19 encoding a protein showing homology with TIMM8A, which is involved in mitochondrial protein import. **TMEM70 defect** (#604273, no former type) patients mostly present in the neonatal period with a muscular hypotonia, hypertrophic cardiomyopathy, psychomotor retardation, 3-MGA-uria, hyperammonemia and lactic acidosis. Patients surviving the neonatal period later show developmental delay. The cardiomyopathy is not progressive[61, 64, 65]. However, the phenotypic spectrum is variable and broadening and there seems to be no syndromic presentation. All patients show a deficiency of the ATPase (complex V) of the oxidative phosphorylation (OXPHOS) system, however TMEM70 seems to be neither a subunit nor an assembly factor of the ATPase. A role in insertion of ATPase into the mitochondrial membrane is speculated.

Secondary 3-MGA-uria due to unknown pathomechanism: the "not otherwise specified (NOS) 3-MGA-uria"

Some patients with significant and consistent 3-MGA-uria remain unexplained after ruling out all currently known causes[273]. This means that new inborn errors of metabolism with 3-methylglutaconic aciduria as discriminative feature will certainly be encountered in the future. This may concern individual patients with significant 3-MGA-uria or patient groups

with a distinctive phenotype and 3–MGA–uria as a hallmark of this phenotype. We propose to diagnose these patients as **not otherwise specified (NOS) 3–MGA–uria** until the underlying genetic defect and pathomechanism is elucidated. It may occur that a causative gene of a new inborn error of metabolism with 3–methylglutaconic aciduria as discriminative feature is found, but the function of the protein is still unknown. In this case, the nomenclature consisting of the gene name followed by syndrome should already be used, but the new disorder should be classified as "NOS" until the pathomechanism is (roughly) understood.

The proposed classification is the first to take the underlying pathomechanism of 3–MGA–uria into account and furthermore simplifies the diagnostic approach. We would like to stress once again, that the term inborn error of metabolism with 3–methylglutaconic aciduria as discriminative feature should be reserved for disorders in which urinary 3–MGA is found significantly and consistently elevated.

Group	Patho-mechanism	Disease name	*old type*	Hallmarks of phenotype (beside 3-MGA-uria)	Affected *gene*, protein, subcellular localization, proposed function
Primary 3-MGA-uria	Organic aciduria	3-methylglutaconyl-CoA hydratase deficiency or AUH defect	*I*	Adult onset leuco-encephalopathy, dementia, progressive spasticity	*AUH*, 3-methylglutaconyl-CoA hydratase, mitochondrial matrix, leucine catabolism
Secondary 3-MGA-uria	Defective phospholipid remodeling	TAZ defect or Barth syndrome	*II*	X-linked, (cardio)myopathy, short stature, neutropenia, OXPHOS dysfunction, hypocholesterolemia, cognitive phenotype, mild dysmorphic features,	*TAZ*, Tafazzin, (inner) mitochondrial membrane, cardiolipin remodeling
		SERAC1 defect or MEGDEL syndrome	*IV*	Progressive spasticity, dystonia, deafness, Leigh like MRI, severe PMR, hypocholesterolemia, OXPHOS dysfunction	*SERAC1*, SERAC1, mitochondria associated membranes fraction, phosphatidyl-glycerol remodeling, cardiolipin composition
	Mitochondrial membrane associated disorder	OPA3 defect or Costeff syndrome	*III*	Ataxia/extrapyramidal dysfunction, optic atrophy	*OPA3*, OPA3, outer mitochondrial membrane, ?protective function for respiratory chain
		DNAJC19 defect or DCMA syndrome	*V*	Dilated cardiomyopathy, ECG abnormalities, non-progressive cerebellar ataxia, testicular dysgenesis, growth failure, anemia, steatosis hepatis	*DNAJC19*, DNAJC19, ?inner mitochondrial membrane, ?mitochondrial protein import
		TMEM70 defect	*IV*	Broad phenotypical variety, hypertrophic cardiomyopathy, ATPase deficiency, myopathy, dysmorphic features, cataracts, PMR, lactic acidosis, hyperammonemia	*TMEM70*, TMEM70, inner mitochondrial membrane, ?complex V assembly and insertion in mitochondrial membrane
	Unknown	NOS 3-MGA-uria	*IV*	Variable, mostly progressive neurological disease	unknown

Table 1 *Classification of "Inborn errors of metabolism with 3-methylglutaconic aciduria as discriminative feature". 3-MGA-uria = 3-methylglutaconic aciduria, NOS = not otherwise specified; OXPHOS = oxidative phosphorylation, PMR = psychomotor retardation.*

Chapter 9

Summary and outlook

With the exponential growth of knowledge we discover new disorders every day. Still many patients in the clinical practice miss an exact diagnosis and pathophysiologic explanation for his of her disease, which lies at the basis of any possible treatment. The physician, together with the biochemist and geneticist, are challenged to combine their findings, to recognize a distinctive disease pattern in order to finally come to the correct diagnosis. In this process biochemical markers are helpful tools. In this thesis we show, that 3-methylglutaconid acid (3–MGA) is one of those useful markers.

Chapter 1 summarizes the current knowledge about the 3–methylglutaconic acidurias (3–MGA–urias). In the urine of healthy individuals the organic acid 3–MGA is found only in trace amountss (0-20 µmol/mmol creatinine). Increased urinary excretion of 3–MGA is often associated with 3–methylglutaric aciduria, which is a powerful diagnostic clue for several rare, but highly characteristic neurometabolic syndromes like Barth syndrome or Costeff syndrome (MIM #250950).

The most prominent clinical feature of the X-linked Barth syndrome or *TAZ* defect (3–MGA–uria type II, MIM # 302060) is cardiomyopathy, which is often dilated with signs of left ventricular noncompaction. The cardiomyopathy can have a fetal onset and finally necessitate heart transplantation. Patients present with (cyclic) neutropenia and skeletal myopathy. Typical facial features and a cognitive phenotype with normal IQ but with problems with visual spatial tasks and mathematics are reported. Serum hypocholesterinemia and oxidative phosphorylation system (OXPHOS) dysfunction in muscle is found frequently. The disease is caused by underlying mutations in *TAZ*, which encodes the (inner) mitochondrial membrane protein tafazzin, a remodeler of cardiolpin. Cardiolipin is a phospholipid specifically found in the mitochondrial inner membrane and therefore is present in high quantities in mitochondria-enriched tissues, such as heart and skeletal muscle. It is reported to function in the stabilization of the individual respiratory chain complexes, as well as in the OXPHOS supercomplex forming. This explains the OXPHOS dysfunction. A role in apoptosis has been suggested as well.

Costeffsyndrome or *OPA3* defect (3–MGA–uria type III, MIM #258501) is an autosomal recessive disorder with infantile bilateral optic atrophy, extrapyramidal signs, spasticity, ataxia, dysarthria, and cognitive deficit in decreasing order of frequency. As in the other 3–MGA–uria syndromes there is a strong relation with OXPHOS (dys)function. Mutations are found in *OPA3* encoding for the OPA3 protein, which is enriched in the outer mitochondrial membrane. In a zebrafish model of Costeff syndrome OPA3 has recently been shown to have protective effects for the respiratory chain.

In both syndromes 3–MGA–uria is the key feature leading the physician to the correct diagnosis, however, the pathomechanism underlying 3–MGA–uria is unknown.

This is the case in all conditions in which 3–MGA–uria is seen with an exception of 3–methylglutaconyl–CoA hydratase (3–MGH) deficiency or *AUH* defect (former 3–MGA–uria type I, MIM #250950) where it stems from leucine degradation (Chapter 1,

Figure 1). However, mitochondrial dysfunction seems appears to link the disorders together as the common denominator.

3–MGH deficiency or *AUH* defect is biochemically a classical inborn error of metabolism. The defect is situated in a known pathway, the degradation of leucine. The affected enzyme 3–MGH, catalyzes the fifth step of leucine catabolism, the conversion of 3–methylglutaconyl–CoA to 3-hydroxy-3-methylglutaryl-CoA. This explains the finding of the different metabolites in urine: 3–MGA, 3–methylglutaconic acid (3–MG) and 3–hydroxyisovaleric acid (3–HIVA). Increased 3–HIVA excretion distinguishes 3–methylglutaconyl–CoA hydratase deficiency from the other types of 3–MGA syndromes. For a long time it remained unclear which clinical presentation belongs to this inborn error of metabolism. It was even speculated to be a non-disease. In **Chapter 2** we show, that it is definitely not a non-disease. Instead, it is a very slowly progressive disorder leading to an adult onset of clinical symptoms. Clinically the patients present with progressive ataxia, which can be combined with dementia, spasticity or optic atrophy. When this finding leads to cerebral imaging, one will find an impressive white matter disease (Chapter 2, Figure 1). One could speculate that this is the consequence of a long term auto-intoxication by one of the accumulating metabolites and therefore a leucine restricted diet or a protein restriction as treatment could be considered. On the other hand, the clinical course is not characterised by episodes of metabolic derangement, so that, also in this case 3–MGA uria is only a marker of a yet unknown pathomechanism secondary to the disturbance in the leucine catabolic pathway. Disturbances in mitochondrial membrane dynamics and OXPHOS function may play a role in the pathomechanism as well.

Besides these three well defined disorders there was an ever growing group of patients with more or less significantly and more or less consistently increased 3–MGA excretion. The different disorders were labelled by roman numbers (I-V) in the order of discovery, without including the underlying pathomechanism in the classification. The so called "unspecified" 3–MGA–uria type IV (MIM 250951) encompassing patients with various organ involvement and mostly progressive neurological impairment has been ever growing since, leading to biochemical and clinical diagnostic confusion. From **Chapter 3** onwards we focus on this heterogeneous group of patients and disorders and re-establish order.

Chapter 3 describes the clinical and biochemical phenotype of 18 children with 3–MGA–uria type IV and defines four clinical subgroups (encephalomyopathic, hepatocerebral, cardiomyopathic, myopathic). By delineating patient-groups we elucidated the genetic defect (mutations in *POLG, SUCLA2, TMEM70, RYR1*) in 10 out of 18 children.

This is a much higher yield than the 20% of patient for which the genetic basis is found in the general OXPHOS patient population. This underlines the feasibility of 3–MGA–uria as a marker for OXPHOS dysfunction.

In **Chapter 4** we show, that dysmorphic features are commonly present in 3–MGA–uria type IV. Most of these appear during the course of disease, secondary to basal ganglia involvement (mask-like facial features), muscle wasting of the facial musculature, and hypotonia, leading to an elongation of the face and long prominent ears. Some of these

facial features are comparable with those in patients with Barth syndrome (broad and tall forehead, curved eyebrows; Chapter 4, Figure 1).

In **Chapter 5** we describe the association of 3-MGA-uria with sensori-neural deafness, encephalopathy, and Leigh-like syndrome (MEGDEL or *SERAC1* syndrome, MIM #614739) in four patients with a disorder of the oxidative phosphorylation. In **Chapter 6** we elucidate the genetic and functional background. MEGDEL or *SERAC1* syndrome is a clinically highly characteristic dystonia-deafness syndrome. In the neonatal period children often are admitted due to suspicion of infection, however very often no infectious agent can be detected. Furthermore the patients often have hypoglycaemias. In infancy feeding problems leading to failure to thrive and delayed achievement of milestones bring the children under attention of the paediatrician. A certain percentage of patients also has (intermittently) elevated liver enzymes, cholestasis or even liver failure, mostly during the first year of life. Upon physical examination an axial hypotonia with hypertonia of the extremities is noted, as well as dystonia of the hands. The features progress significantly over time. Deafness is often difficult to evaluate clinically due to the severe psychomotor retardation and necessitates specific testing. Most children have little or no speech development. The cerebral MRI shows features reminiscent of Leigh syndrome (subacute necrotizing encephalopathy) with hyperintensities in the basal ganglia and cerebral and cerebellar atrophy.

Laboratory investigations reveal significantly and consistently elevated urinary 3-MGA (and 3-methylglutaric aciduria). Together with the elevated lactate and alanine levels found in most of the patients these observations lead to the suspicion of an OXPHOS disorder. Investigations of the OXPHOS system in fresh muscle often show a diminished ATP production capacity, sometimes combined with respiratory chain complex deficiencies. The same holds for evaluation of OXPHOS in fibroblasts.

However, the alterations are mostly only mild and do not have a specific pattern. This is comparable to the findings in patients with Barth syndrome, yet the OXPHOS dysfunction is more outspoken in Barth syndrome. The clinical, biochemical and radiological findings are described in Chapter 5 (also Chapter 6, Supplementary Table 1 summarizes the findings).

Using exome sequencing in two unrelated patients, we identified mutations in *SERAC1,* a gene of unknown function. Little was known about *SERAC1* , other than the presence of a lipase domain. This, taken together with the overlapping clinical signs and symptoms between Barth and MEGDEL syndrome (3-MGA-uria, OXPHOS dysfunction, hypocholesterinemia) lead us to perform phospholipid analysis in patients' fibroblasts.

This revealed elevated concentrations of phosphatidylglycerol-34:1 and decreased concentrations of phosphatidylglycerol-36:1 species (Chapter 6, Figure 3A,B). This identifies SERAC1 as the second known phospholipid remodeller beside tafazzin that is deficient in Barth syndrome. Cardiolipin is present in the inner mitochondrial membrane and has been reported to stabilize the individual respiratory chain complexes, as well as in the OXPHOS supercomplex forming. This explains the OXPHOS dysfunction in Barth

syndrome. In MEGDEL syndrome the total amount of cardiolipin is normal, while the subspecies composition is disturbed, which explains the OXPHOS dysfunction in MEGDEL syndrome (Chapter 6, Figure 4). We localized SERAC1 at the interface between the mitochondria and the endoplasmic reticulum in the mitochondria-associated membrane (MAM) fraction that is essential for phospholipid exchange between these organelles (Chapter 6, Figure 6, 7).

Furthermore, we also detected low concentrations of bis(monoacyl-glycerol)-phosphate, suggesting that SERAC1 catalyses the first enzymatic reaction in the as yet unknown bis(monoacyl-glycerol)-phosphate biosynthetic pathway (Chapter 6, Figure 2). Low bis(monoacylglycerol)phosphate concentrations are known to lead to intracellular accumulation of free cholesterol, a phenomenon known from Niemann Pick C disease, a lysosomal storage disorder. By filippin staining of MEGDEL fibroblasts we could indeed show intracellular cholesterol accumulation (Chapter 6, Figure 5). This makes MEGDEL syndrome also the second known intracellular cholesterol trafficking disorder.

Complementation of patient fibroblasts with wild-type human SERAC1 by lentiviral infection lead to a partial normalization of the mean ratio of phosphatidylglycerol-34:1 to phosphatidylglycerol-36:1, thereby proving the ascribed function (Chapter 6, Figure 9).

As shown in the Chapters 1-6, 3–MGA–uria is a useful biomarker, which can lead the physician to the right diagnosis. However a proper classification of the growing group of disorders associated with 3–MGA–uria was lacking.

In **Chapter 7** we show, that 3–MGA–uria is a relatively common finding in patients with suspicion of metabolic disorders in general. We found it in 3% of all urine samples (nearly 20000) sent to our laboratory in an eight year period. We therefore reviewed the biochemical, clinical and genetic data of all patients with 3–MGA–uria who were referred to our centre under the suspicion of a metabolic disorder (Chapter 7, Table 2 summarizes the findings). We could confirm OXPHOS dysfunction as common denominator.

In a further approach we therefore evaluated in which specific OXPHOS disorders 3–MGA–uria can be found. Taken together this enabled us to subdivide disorders with 3–MGA–uria into three subgroups (see Chapter 8, Figure 1 and Table 1). In Chapter 7 we present this in-depth evaluation and come to a classification based on the underlying pathomechanisms as shown in brief below, which is presented in **Chapter 8.**

1. Disorders with 3–MGA–uria as an accompanying finding

In patients suffering from classical metabolic disorders (e.g. fatty acid oxidation disorders, organic acidurias, urea cycle disorders, glycogen storage disorders) 3–MGA–uria is mostly found occasionally, e.g. upon presentation or during severe metabolic decompensation. Furthermore, 3–MGA–uria is not isolated but only an accompanying finding beside several other, more disease specific, urinary metabolites. Indeed OXPHOS dysfunction seems to be the common denominator.

2. *Disorders with 3–MGA–uria as a minor finding*

In this patient group 3–MGA–uria is mostly mild (20-40 µmol/mmol creatinine), only a minor finding and not the hallmark of the phenotype. Mostly patients suffer from OXPHOS

disorders, but one should not forget to take hematological disorders, neuromuscular disorder, genetic syndromes or chromosomal abnormalities into account. Investigation of nearly 600 patients with 50 different, genetically proven, OXPHOS disorders for the presence or absence of 3-MGA-uria revealed, that 11% of these patient presented 3-MGA-uria. There is no strong relation between 3-MGA-uria and specific genes, however there are some subgroups which seem to exhibit 3-MGA-uria more often than others. It was more frequently seen in complex V (ATPase) related disorders, with mitochondrial DNA depletion or deletion, but not in patients with single respiratory chain complex deficiencies (Chapter 7a, Table 4).

3. Inborn errors with 3-MGA-uria as discriminative feature

In this group of disorders 3-MGA-uria is a major finding, the hallmark of the phenotype and often the key to the diagnosis. Patients show significantly and consistently increased 3-MGA excretion (40- >1000 µmol/mmol creatinine) which is mostly isolated.

Therefore, we propose the following pathomechanism based classification for these "Inborn errors of metabolism with 3-MGA-uria as discriminative feature". One should distinguish between "Primary 3-MGA-uria" formerly known as type I (3-methylglutaconyl-CoA hydratase deficiency, AUH defect) due to defective leucine catabolism and the – currently known - three groups of "Secondary 3-MGA-uria". The latter should be further classified and named by their defective protein or the historical name as follows: i) defective phospholipid remodelling (TAZ defect or Barth syndrome, SERAC1 defect or MEGDEL syndrome) and ii) mitochondrial membrane associated disorders (OPA3 defect or Costeff syndrome, DNAJC19 defect or DCMA syndrome, TMEM70 defect). The remaining patients with significant and consistent 3-MGA-uria in whom the above mentioned syndromes have been excluded, should be referred to as "not otherwise specified (NOS) 3-MGA-uria" until elucidation of the underlying pathomechanism enables proper (possibly extended) classification.

We have shown, that 3-MGA-uria is a useful marker for OXPHOS dysfunction in general and for several highly characteristic neurometabolic syndromes in particular. Exome sequencing studies in patients with NOS 3-MGA-uria will identify new players in the hitherto poorly characterised pathways related to phospholipid remodelling and intracellular cholesterol trafficking. Increasing knowledge on these pathways and their correlation with the OXPHOS will identify possible future treatment targets and improve counselling. Further studies should also aim to answer *THE* question: where does 3-MGA-uria stem from?

Samenvatting

Met de exponentiële groei van kennis worden vrijwel iedere dag nieuwe ziektebeelden ontdekt. Maar nog steeds zijn artsen vaak niet in staat om bij een individuele patiënt een exacte diagnose te stellen. Een juiste diagnose moet aan iedere behandeling ten grondslag liggen. Veelal is er onvoldoende kennis over de onderliggende ziekteprocessen. Dit verklaart waarom voor zoveel (stofwisselings-)ziekten nog geen behandeling beschikbaar is. Door de vele verschillende ziektebeelden wordt het voor artsen steeds moeilijker deze van elkaar te onderscheiden. De arts moet uit een overvloed aan informatie (klinische verschijnselen, laboratoriumuitslagen, radiologische bevindingen etc.) een ziektepatroon destilleren om tot de juiste diagnose te komen. Hierbij kan een biomarker helpen. Verhoogde uitscheiding van 3–methylglutaconzuur (3–MGA) in de urine is zo'n biomarker. Bij gezonde personen komt dit zuur nagenoeg niet in de urine voor. Bij patiënten met enkele zeldzame stofwisselingsziekten is dit juist een kenmerk van hun ziekte.

Hoofdstuk 1 geeft een overzicht van de huidige kennis van ziektebeelden met een verhoogde concentratie van 3–methylglutaconzuur in de urine (3–MGA–uria). Een syndroom is een verzameling van steeds tezamen voorkomende klinische verschijnselen. Er zijn meerdere syndromen bekend die als kenmerk een 3–MGA–uria hebben. Bijvoorbeeld het Barth syndroom, waarbij de ziekteverschijnselen 3–MGA–uria, cardiomyopathie en te weinig witte bloedcellen (neutropenie) zijn. Dit ziektebeeld wordt veroorzaakt door foutjes (mutaties) in het *TAZ* gen. *TAZ* codeert voor het eiwit tafazzine en is verantwoordelijk voor het hermodelleren van cardiolipine. Cardiolipine is een stofje dat specifiek in de mitochondria wordt gevonden en belangrijk is voor het juist functioneren van de ademhalingsketen. Bij deze patiënten functioneert de ademhalingsketen niet goed, ze hebben een tekort aan energie, een energiestofwisselingsziekte.

Bij het Barth syndroom wordt de arts door de unieke bevinding van 3–MGA in de urine op het juiste spoor gezet. Er zijn bijvoorbeeld veel verschillende vormen van cardiomyopathie, maar er bestaan slechts twee vormen van cardiomyopathie met 3–MGA–uria.

Hoe de verhoogde uitscheiding van 3–MGA in de urine ontstaat is voor de meeste ziektebeelden onbekend. Uitzondering vormt het ziektebeeld 3–methylglutaconyl-CoA hydratase (3-MGH) deficiëntie. Bij deze ziekte komt het 3–MGA uit de afbraak van het eiwitbouwsteen (aminozuur) leucine (Hoofdstuk 1, figuur 1). Biochemisch gezien is dit een klassieke aangeboren stofwisselingsziekte. Lange tijd was het onduidelijk welke klinische symptomen bij deze aangeboren stofwisselingsziekte horen. Er waren zelfs speculaties of het überhaupt wel een echte ziekte was. In **hoofdstuk 2** laten we zien, dat 3–MGH deficientie zeker een ziektebeeld is. Het is een zeer langzaam progressieve aandoening waarbij de klinische verschijnselen van deze aangeboren ziekte pas op volwassen leeftijd zichtbaar worden. De patiënten presenteren zich met een opvallend (ataktisch) looppatroon, vaak gecombineerd met spasticiteit en dementie. Op de MRI van de hersenen is een zeer uitgebreide witte stofziekte te zien (Hoofdstuk 2, figuur 1).

Naast deze twee goed gekarakteriseerde ziektebeelden is er een groeiende groep van patiënten met meer of minder uitgesproken en meer of minder consistente 3–MGA–uria. Tot op heden werden de verschillende ziektebeelden met romeinse getallen aangeduid, zonder bij deze indeling met de onderliggende pathofysiologie rekening te houden. Het "ongeclassificeerde type IV" was een steeds groter wordende groep van patiënten met een multi-systeem ziekte veelal met neurologische verschijnselen. De diversiteit van klinische verschijnselen in deze groep zaaide veel verwarring bij artsen en biochemici. Vanaf hoofdstuk 3 zullen we deze "verzamelbak" evalueren en de ziektebeelden met 3–MGA–uria opnieuw indelen.

Hoofdstuk 3 beschrijft de klinische en biochemische ziekteverschijnselen van 18 kinderen met 3–MGA–uria, welke op basis van deze bevindingen in vier groepen kunnen worden onderverdeeld. Door deze indeling konden we bij 10 van 18 patiënten tot een genetische diagnose komen. Dit is een hoger oplossingspercentage dan bij patiënten met een energiestofwisselingziekte. Bij hen kan gemiddeld in slechts 20% van de gevallen een genetische diagnose gesteld worden. 3–MGA–uria is dus een zinvolle biomarker, die de arts helpt om tot de juiste diagnose te komen.

In **hoofdstuk 4** laten we zien, dat patiënten met 3–MGA–uria type IV vaak opvallende gelaatskenmerken hebben. Dit kan naast de 3–MGA–uria een bijzonder kenmerk van een syndroom zijn en daarmee ook in de diagnostiek helpen.

In **hoofdstuk 5** beschrijven we een nieuwe ziekte, het MEGDEL syndroom. Dit is een zeer karakteristiek ziektebeeld, gekenmerkt door 3–MGA–uria, doofheid, progressieve spasticiteit en bewegingsstoornis (dystonie) beginnend op de kinderleeftijd. Tevens hebben alle patienten specifieke afwijkingen op de MRI van de hersenen die wij kennen van kinderen met energiestofwisselingsziekten. In **hoofdstuk 6** ontrafelen we de genetische oorzaak en de onderliggende pathofysiologie van dit ziektebeeld. *Exome sequencing* is een nieuwe genetische methode waardoor alle genen van de mens in een onderzoek op foutjes nagekeken kunnen worden. Bij twee patiënten met het MEGDEL syndroom vonden wij foutjes (mutaties) in hetzelfde gen, *SERAC1.* Het was dus aannemelijk dat mutaties in dit gen leiden tot het MEGDEL syndroom. De functie van het SERAC1 eiwit was op dat moment volledig onbekend. Om te bewijzen, dat MEGDEL syndroom door mutaties in *SERAC1* onstaat, moesten wij de functie van dit eiwit vinden. Dit onderzoek leidde tot meerdere baanbrekende inzichten. Wij konden aantonen dat SERAC1 een zeer belangrijke rol speelt bij zowel de energiestofwisseling als ook bij het transport van cholesterol in de cel. Er zijn enkele overlappingen met het Barth syndroom, maar een soortgelijke ziekte was tot op heden onbekend. Ook over de aangetaste stofwisselingsroutes was eerder heel weinig bekend.

In **hoofdstuk 7** onderzoeken we bij bijna 400 patiënten met de biomarker 3–MGA–uria welke ziektebeelden zij hebben. Wij concluderen, dat de biomarker 3–MGA–uria een marker is voor een gestoorde energiestofwisseling. Er lijken zelfs enkele types van energiestofwisselingsziekten te bestaan waarbij deze marker vaker voorkomt. Beide bevindingen kunnen de arts op het juiste spoor zetten bij zijn zoektocht naar een diagnose.

Met alle kennis opgedaan in het kader van dit proefschrift stellen wij in **hoofdstuk 8** een nieuwe indeling van ziektebeelden met 3–MGA–uria als kenmerk op met een bijbehorende nieuwe nomenclatuur voor deze groep ziekten.

Reference List

1. Elpeleg,O.N. *et al.* 3-Methylglutaconic aciduria in the Iraqi-Jewish 'optic atrophy plus' (Costeff) syndrome. *Dev. Med. Child Neurol.* **36,** 167-172 (1994).
2. Christodoulou,J. *et al.* Barth syndrome: clinical observations and genetic linkage studies. *Am. J. Med. Genet.* **50,** 255-264 (1994).
3. Cantlay,A.M. *et al.* Genetic analysis of the G4.5 gene in families with suspected Barth syndrome. *J. Pediatr.* **135,** 311-315 (1999).
4. Schmidt,M.R., Birkebaek,N., Gonzalez,I., & Sunde,L. Barth syndrome without 3-methylglutaconic aciduria. *Acta Paediatr.* **93,** 419-421 (2004).
5. Ensenauer,R. *et al.* 3-Methylglutaconyl-CoA hydratase deficiency: a new patient with speech retardation as the leading sign. *J. Inherit. Metab Dis.* **23,** 341-344 (2000).
6. Duran,M. *et al.* Inherited 3-methylglutaconic aciduria in two brothers--another defect of leucine metabolism. *J. Pediatr.* **101,** 551-554 (1982).
7. Kelley,R.I. *et al.* X-linked dilated cardiomyopathy with neutropenia, growth retardation, and 3-methylglutaconic aciduria. *J. Pediatr.* **119,** 738-747 (1991).
8. Christodoulou,J. *et al.* Barth syndrome: clinical observations and genetic linkage studies. *Am. J. Med. Genet.* **50,** 255-264 (1994).
9. Chitayat,D. *et al.* 3-Methylglutaconic aciduria: a marker for as yet unspecified disorders and the relevance of prenatal diagnosis in a 'new' type ('type 4'). *J. Inherit. Metab Dis.* **15,** 204-212 (1992).
10. Schmidt,M.R., Birkebaek,N., Gonzalez,I., & Sunde,L. Barth syndrome without 3-methylglutaconic aciduria. *Acta Paediatr.* **93,** 419-421 (2004).
11. Wortmann,S.B. *et al.* Biochemical and genetic analysis of 3-methylglutaconic aciduria type IV: a diagnostic strategy. *Brain* **132,** 136-146 (2009).
12. Kelley,R.I. & Kratz,L. 3-methylglutaconic acidemia in Smith-Lemli-Opitz syndrome. *Pediatr. Res.* **37,** 671-674 (1995).
13. Edmond,J. & Popjak,G. Transfer of carbon atoms from mevalonate to n-fatty acids. *J. Biol. Chem.* **249,** 66-71 (1974).
14. Schroepfer,G.J., Jr. Sterol biosynthesis. *Annu. Rev. Biochem.* **50,** 585-621 (1981).
15. Walsh,R., Conway,H., Roche,G., & Mayne,P.D. What is the origin of 3-methylglutaconic acid? *J. Inherit. Metab Dis.* **22,** 251-255 (1999).
16. Hughes-Fulford,M. *et al.* Role of the kidneys in the metabolism of circulating mevalonate in humans. *J. Clin. Endocrinol. Metab* **62,** 1227-1231 (1986).
17. Weinstock,S.B. *et al.* The shunt pathway of mevalonate metabolism in the isolated perfused rat liver. *J. Biol. Chem.* **259,** 8939-8944 (1984).
18. Goldstein,J.L. & Brown,M.S. Regulation of the mevalonate pathway. *Nature* **343,** 425-430 (1990).
19. Engelke,U.F. *et al.* NMR spectroscopic studies on the late onset form of 3-methylglutaconic aciduria type I and other defects in leucine metabolism. *NMR Biomed.* **19,** 271-278 (2006).

20. Brennan,L.E., Nakagawa,J., Egger,D., Bienz,K., & Moroni,C. Characterisation and mitochondrial localisation of AUH, an AU-specific RNA-binding enoyl-CoA hydratase. *Gene* **228**, 85-91 (1999).
21. Narisawa,K. *et al.* Deficiency of 3-methylglutaconyl-coenzyme A hydratase in two siblings with 3-methylglutaconic aciduria. *J. Clin. Invest* **77**, 1148-1152 (1986).
22. IJlst,L. *et al.* 3-Methylglutaconic aciduria type I is caused by mutations in AUH. *Am. J. Hum. Genet.* **71**, 1463-1466 (2002).
23. Ly,T.B. *et al.* Mutations in the AUH gene cause 3-methylglutaconic aciduria type I. *Hum. Mutat.* **21**, 401-407 (2003).
24. LYNEN,F. *et al.* [On the biochemical function of biotin. II. Purification and mode of action of beta-methyl-crotonyl-carboxylase]. *Biochem. Z.* **335**, 123-167 (1961).
25. Gibson,K.M. *et al.* Variable clinical presentation in three patients with 3-methylglutaconyl-coenzyme A hydratase deficiency. *J. Inherit. Metab Dis.* **21**, 631-638 (1998).
26. Wortmann,S.B. *et al.* 3-Methylglutaconic aciduria type I redefined: a syndrome with late-onset leukoencephalopathy. *Neurology* **75**, 1079-1083 (2010).
27. Illsinger,S., Lucke,T., Zschocke,J., Gibson,K.M., & Das,A.M. 3-methylglutaconic aciduria type I in a boy with fever-associated seizures. *Pediatr. Neurol.* **30**, 213-215 (2004).
28. Matsumori,M., Shoji,Y., Takahashi,T., Shoji,Y., & Takada,G. A molecular lesion in a Japanese patient with severe phenotype of 3-methylglutaconic aciduria type I. *Pediatr. Int.* **47**, 684-686 (2005).
29. Eriguchi,M. *et al.* 3-Methylglutaconic aciduria type I causes leukoencephalopathy of adult onset. *Neurology* **67**, 1895-1896 (2006).
30. Leipnitz,G. *et al.* Induction of oxidative stress by the metabolites accumulating in 3-methylglutaconic aciduria in cerebral cortex of young rats. *Life Sci.* **82**, 652-662 (2008).
31. Duran,M. *et al.* Cerebrospinal fluid organic acids in biotinidase deficiency. *J. Inherit. Metab Dis.* **16**, 513-516 (1993).
32. Barth,P.G. *et al.* An X-linked mitochondrial disease affecting cardiac muscle, skeletal muscle and neutrophil leucocytes. *J. Neurol. Sci.* **62**, 327-355 (1983).
33. Barth,P. *et al.* An X-linked mitochondrial disease affecting cardiac muscle, skeletal muscle and neutrophil leukocytes. 161-164 (Beesterzwaag, The Netherlands: Mefar (pub.), 1981).
34. Yen,T.Y. *et al.* Acute metabolic decompensation and sudden death in Barth syndrome: report of a family and a literature review. *Eur. J. Pediatr.* **167**, 941-944 (2008).
35. Adwani,S.S. *et al.* Heart transplantation for Barth syndrome. *Pediatr. Cardiol.* **18**, 143-145 (1997).
36. Mangat,J., Lunnon-Wood,T., Rees,P., Elliott,M., & Burch,M. Successful cardiac transplantation in Barth syndrome--single-centre experience of four patients. *Pediatr. Transplant.* **11**, 327-331 (2007).
37. Barth,P.G. *et al.* X-linked cardioskeletal myopathy and neutropenia (Barth syndrome): an update. *Am. J. Med. Genet. A* **126A**, 349-354 (2004).

38. Dale,D.C. *et al.* The Severe Chronic Neutropenia International Registry: 10-Year Follow-up Report. *Support. Cancer Ther.* **3,** 220-231 (2006).
39. Hastings,R., Steward,C., Tsai-Goodman,B., & Newbury-Ecob,R. Dysmorphology of Barth syndrome. *Clin. Dysmorphol.* **18,** 185-187 (2009).
40. Mazzocco,M.M., Henry,A.E., & Kelly,R.I. Barth syndrome is associated with a cognitive phenotype. *J. Dev. Behav. Pediatr.* **28,** 22-30 (2007).
41. Houtkooper,R.H. *et al.* The enigmatic role of tafazzin in cardiolipin metabolism. *Biochim. Biophys. Acta* **1788,** 2003-2014 (2009).
42. Valianpour,F. *et al.* Cardiolipin deficiency in X-linked cardioskeletal myopathy and neutropenia (Barth syndrome, MIM 302060): a study in cultured skin fibroblasts. *J. Pediatr.* **141,** 729-733 (2002).
43. Houtkooper,R.H. & Vaz,F.M. Cardiolipin, the heart of mitochondrial metabolism. *Cell Mol. Life Sci.* **65,** 2493-2506 (2008).
44. Bione,S. *et al.* A novel X-linked gene, G4.5. is responsible for Barth syndrome. *Nat. Genet.* **12,** 385-389 (1996).
45. Costeff,H., Gadoth,N., Apter,N., Prialnic,M., & Savir,H. A familial syndrome of infantile optic atrophy, movement disorder, and spastic paraplegia. *Neurology* **39,** 595-597 (1989).
46. Anikster,Y., Kleta,R., Shaag,A., Gahl,W.A., & Elpeleg,O. Type III 3-methylglutaconic aciduria (optic atrophy plus syndrome, or Costeff optic atrophy syndrome): identification of the OPA3 gene and its founder mutation in Iraqi Jews. *Am. J. Hum. Genet.* **69,** 1218-1224 (2001).
47. Kleta,R. *et al.* 3-Methylglutaconic aciduria type III in a non-Iraqi-Jewish kindred: clinical and molecular findings. *Mol. Genet. Metab* **76,** 201-206 (2002).
48. Neas,K. *et al.* OPA3 mutation screening in patients with unexplained 3-methylglutaconic aciduria. *J. Inherit. Metab Dis.* **28,** 525-532 (2005).
49. Ho,G., Walter,J.H., & Christodoulou,J. Costeff optic atrophy syndrome: new clinical case and novel molecular findings. *J. Inherit. Metab Dis.* **31 Suppl 2,** S419-S423 (2008).
50. Reynier,P. *et al.* OPA3 gene mutations responsible for autosomal dominant optic atrophy and cataract. *J. Med. Genet.* **41,** e110 (2004).
51. Verny,C. *et al.* [An OPA3 gene mutation is responsible for the disease associating optic atrophy and cataract with extrapyramidal signs]. *Rev. Neurol. (Paris)* **161,** 451-454 (2005).
52. Huizing,M. *et al.* OPA3, mutated in 3-methylglutaconic aciduria type III, encodes two transcripts targeted primarily to mitochondria. *Mol. Genet. Metab* **100,** 149-154 (2010).
53. Ryu,S.W., Jeong,H.J., Choi,M., Karbowski,M., & Choi,C. Optic atrophy 3 as a protein of the mitochondrial outer membrane induces mitochondrial fragmentation. *Cell Mol. Life Sci.* **67,** 2839-2850 (2010).
54. Pei,W. *et al.* A model of Costeff Syndrome reveals metabolic and protective functions of mitochondrial OPA3. *Development* **137,** 2587-2596 (2010).
55. Gunay-Aygun,M. 3-Methylglutaconic aciduria: a common biochemical marker in various syndromes with diverse clinical features. *Mol. Genet. Metab* **84,** 1-3 (2005).
56. Holme,E. *et al.* Mitochondrial ATP-synthase deficiency in a child with 3-methylglutaconic aciduria. *Pediatr. Res.* **32,** 731-735 (1992).

57. Ibel,H. *et al.* Multiple respiratory chain abnormalities associated with hypertrophic cardiomyopathy and 3-methylglutaconic aciduria. *Eur. J. Pediatr.* **152**, 665-670 (1993).
58. Besley,G.T. *et al.* Mitochondrial complex deficiencies in a male with cardiomyopathy and 3-methylglutaconic aciduria. *J. Inherit. Metab Dis.* **18**, 221-223 (1995).
59. Ruesch,S. *et al.* Combined 3-methylglutaconic and 3-hydroxy-3-methylglutaric aciduria with endocardial fibroelastosis and dilatative cardiomyopathy in male and female siblings with partial deficiency of complex II/III in fibroblasts. *Enzyme Protein* **49**, 321-329 (1996).
60. De Kremer,R.D. *et al.* Barth's syndrome-like disorder: a new phenotype with a maternally inherited A3243G substitution of mitochondrial DNA (MELAS mutation). *Am. J. Med. Genet.* **99**, 83-93 (2001).
61. Sperl,W. *et al.* Deficiency of mitochondrial ATP synthase of nuclear genetic origin. *Neuromuscul. Disord.* **16**, 821-829 (2006).
62. Morava,E. *et al.* Congenital hypertrophic cardiomyopathy, cataract, mitochondrial myopathy and defective oxidative phosphorylation in two siblings with Sengers-like syndrome. *Eur. J. Pediatr.* **163**, 467-471 (2004).
63. Di Rosa G. *et al.* Hypertrophic cardiomyopathy, cataract, developmental delay, lactic acidosis: a novel subtype of 3-methylglutaconic aciduria. *J. Inherit. Metab Dis.* **29**, 546-550 (2006).
64. Cizkova,A. *et al.* TMEM70 mutations cause isolated ATP synthase deficiency and neonatal mitochondrial encephalocardiomyopathy. *Nat. Genet.* **40**, 1288-1290 (2008).
65. Honzik,T. *et al.* Mitochondrial encephalocardio-myopathy with early neonatal onset due to TMEM70 mutation. *Arch. Dis. Child* **95**, 296-301 (2010).
66. Mayr,J.A. *et al.* Mitochondrial ATP synthase deficiency due to a mutation in the ATP5E gene for the F1 epsilon subunit. *Hum. Mol. Genet.* **19**, 3430-3439 (2010).
67. De Meirleir L. *et al.* Respiratory chain complex V deficiency due to a mutation in the assembly gene ATP12. *J. Med. Genet.* **41**, 120-124 (2004).
68. Wortmann,S.B. *et al.* Association of 3-methylglutaconic aciduria with sensori-neural deafness, encephalopathy, and Leigh-like syndrome (MEGDEL association) in four patients with a disorder of the oxidative phosphorylation. *Mol. Genet. Metab* **88**, 47-52 (2006).
69. de Vries,M.C. *et al.* Multiple oxidative phosphorylation deficiencies in severe childhood multi-system disorders due to polymerase gamma (POLG1) mutations. *Eur. J. Pediatr.* **166**, 229-234 (2007).
70. Figarella-Branger,D., Pellissier,J.F., Scheiner,C., Wernert,F., & Desnuelle,C. Defects of the mitochondrial respiratory chain complexes in three pediatric cases with hypotonia and cardiac involvement. *J. Neurol. Sci.* **108**, 105-113 (1992).
71. Scaglia,F. *et al.* Mitochondrial DNA depletion associated with partial complex II and IV deficiencies and 3-methylglutaconic aciduria. *J. Child Neurol.* **16**, 136-138 (2001).
72. Jakobs,C., Danse,P., & Veerman,A.J. Organic aciduria in Pearson syndrome. *Eur. J. Pediatr.* **150**, 684 (1991).

73. Gibson,K.M. *et al.* 3-Methylglutaconic aciduria associated with Pearson syndrome and respiratory chain defects. *J. Pediatr.* **121,** 940-942 (1992).
74. Lichter-Konecki,U. *et al.* 3-Methylglutaconic aciduria in a patient with Pearson syndrome. *Eur. J. Pediatr.* **152,** 378 (1993).
75. Davey,K.M. *et al.* Mutation of DNAJC19, a human homologue of yeast inner mitochondrial membrane co-chaperones, causes DCMA syndrome, a novel autosomal recessive Barth syndrome-like condition. *J. Med. Genet.* **43,** 385-393 (2006).
76. Roesch,K., Curran,S.P., Tranebjaerg,L., & Koehler,C.M. Human deafness dystonia syndrome is caused by a defect in assembly of the DDP1/TIMM8a-TIMM13 complex. *Hum. Mol. Genet.* **11,** 477-486 (2002).
77. Faull,K. *et al.* Letter: Patient with defect in leucine metabolism. *N. Engl. J. Med.* **294,** 1013 (1976).
78. Liang,W.C. *et al.* ETFDH mutations, CoQ10 levels, and respiratory chain activities in patients with riboflavin-responsive multiple acyl-CoA dehydrogenase deficiency. *Neuromuscul. Disord.* **19,** 212-216 (2009).
79. Law,L.K., Tang,N.L., Hui,J., Lam,C.W., & Fok,T.F. 3-methyglutaconic aciduria in a Chinese patient with glycogen storage disease Ib. *J. Inherit. Metab Dis.* **26,** 705-709 (2003).
80. de Koning Tj, Duran,M., Dorland,L., Berger,R., & Poll-The BT Maternal 3-methylglutaconic aciduria associated with abnormalities in offspring. *Lancet* **348,** 887-888 (1996).
81. Walsh,R., Conway,H., Roche,G., Naughten,E., & Mayne,P.D. 3-Methylglutaconic aciduria in pregnancy. *Lancet* **349,** 776 (1997).
82. Jooste,S., Erasmus,E., Mienie,L.J., de Wet,W.J., & Gibson,K.M. The detection of 3-methylglutarylcarnitine and a new dicarboxylic conjugate, 3-methylglutaconylcarnitine, in 3-methylglutaconic aciduria. *Clin. Chim. Acta* **230,** 1-8 (1994).
83. Wilcken,B. *et al.* Expanded newborn screening: outcome in screened and unscreened patients at age 6 years. *Pediatrics* **124,** e241-e248 (2009).
84. Loupatty,F.J., Ruiter,J.P., IJlst,L., Duran,M., & Wanders,R.J. Direct nonisotopic assay of 3-methylglutaconyl-CoA hydratase in cultured human skin fibroblasts to specifically identify patients with 3-methylglutaconic aciduria type I. *Clin. Chem.* **50,** 1447-1450 (2004).
85. Wolf,N.I. & Smeitink,J.A. Mitochondrial disorders: a proposal for consensus diagnostic criteria in infants and children. *Neurology* **59,** 1402-1405 (2002).
86. Holden,H.M., Benning,M.M., Haller,T., & Gerlt,J.A. The crotonase superfamily: divergently related enzymes that catalyze different reactions involving acyl coenzyme a thioesters. *Acc. Chem. Res.* **34,** 145-157 (2001).
87. Bell,A.F., Wu,J., Feng,Y., & Tonge,P.J. Involvement of glycine 141 in substrate activation by enoyl-CoA hydratase. *Biochemistry* **40,** 1725-1733 (2001).
88. Kurimoto,K., Fukai,S., Nureki,O., Muto,Y., & Yokoyama,S. Crystal structure of human AUH protein, a single-stranded RNA binding homolog of enoyl-CoA hydratase. *Structure.* **9,** 1253-1263 (2001).
89. Shoji,Y. *et al.* 3-Methylglutaconic aciduria type I: clinical heterogeneity as a neurometabolic disease. *J. Inherit. Metab Dis.* **22,** 1-8 (1999).

90. Duran,M. *et al.* Inherited 3-methylglutaconic aciduria in two brothers--another defect of leucine metabolism. *J. Pediatr.* **101,** 551-554 (1982).
91. Morava,E. *et al.* Mitochondrial disease criteria: diagnostic applications in children. *Neurology* **67,** 1823-1826 (2006).
92. Engelke,U.F. *et al.* N-acetylated metabolites in urine: proton nuclear magnetic resonance spectroscopic study on patients with inborn errors of metabolism. *Clin. Chem.* **50,** 58-66 (2004).
93. Janssen,A.J. *et al.* Measurement of the energy-generating capacity of human muscle mitochondria: diagnostic procedure and application to human pathology. *Clin. Chem.* **52,** 860-871 (2006).
94. Nijtmans,L.G., Henderson,N.S., & Holt,I.J. Blue Native electrophoresis to study mitochondrial and other protein complexes. *Methods* **26,** 327-334 (2002).
95. Carrozzo,R. *et al.* SUCLA2 mutations are associated with mild methylmalonic aciduria, Leigh-like encephalomyopathy, dystonia and deafness. *Brain* **130,** 862-874 (2007).
96. Woods,C.G. *et al.* Quantification of homozygosity in consanguineous individuals with autosomal recessive disease. *Am. J. Hum. Genet.* **78,** 889-896 (2006).
97. Cizkova,A. *et al.* TMEM70 is a novel factor of mitochondrial ATPase biogenesis and its mutations cause isolated enzyme deficiency and neonatal encephalocardiomyopathy. Abstractbook of the Euromit 7, Stockholm 2008 A:137 . 2008.
Ref Type: Abstract
98. Monnier,N. *et al.* Null mutations causing depletion of the type 1 ryanodine receptor (RYR1) are commonly associated with recessive structural congenital myopathies with cores. *Hum. Mutat.* **29,** 670-678 (2008).
99. Gibson,K.M. *et al.* Phenotypic heterogeneity in the syndromes of 3-methylglutaconic aciduria. *J. Pediatr.* **118,** 885-890 (1991).
100. Bene,J., Nadasi,E., Kosztolanyi,G., Mehes,K., & Melegh,B. Congenital cataract as the first symptom of a neuromuscular disease caused by a novel single large-scale mitochondrial DNA deletion. *Eur. J. Hum. Genet.* **11,** 375-379 (2003).
101. Sarzi,E. *et al.* Mitochondrial DNA depletion is a prevalent cause of multiple respiratory chain deficiency in childhood. *J. Pediatr.* **150,** 531-4, 534 (2007).
102. Sengers,R.C., Trijbels,J.M., Willems,J.L., Daniels,O., & Stadhouders,A.M. Congenital cataract and mitochondrial myopathy of skeletal and heart muscle associated with lactic acidosis after exercise. *J. Pediatr.* **86,** 873-880 (1975).
103. Wortmann,S.B., Kluijtmans,L.A., Engelke,U.F., Wevers,R.A., & Morava,E. The 3-methylglutaconic acidurias: what's new? *J. Inherit. Metab Dis.* **35,** 13-22 (2012).
104. Morava,E. *et al.* Dystonia and deafness due to SUCLA2 defect; Clinical course and biochemical markers in 16 children. *Mitochondrion.* **9,** 438-442 (2009).
105. Vreken,P. *et al.* Defective remodeling of cardiolipin and phosphatidylglycerol in Barth syndrome. *Biochem. Biophys. Res. Commun.* **279,** 378-382 (2000).

106. Orstavik,K.H. *et al.* X chromosome inactivation in carriers of Barth syndrome. *Am. J. Hum. Genet.* **63,** 1457-1463 (1998).
107. Gibson,K.M., Elpeleg,O.N., Jakobs,C., Costeff,H., & Kelley,R.I. Multiple syndromes of 3-methylglutaconic aciduria. *Pediatr. Neurol.* **9,** 120-123 (1993).
108. Bakkeren,J.A., Sengers,R.C., Ruitenbeek,W., & Trijbels,J.M. 3-Methylglutaconic aciduria in a patient with a disturbed mitochondrial energy metabolism. *Eur. J. Pediatr.* **151,** 313 (1992).
109. Smeitink,J., Sengers,R., Trijbels,F., & Van Den,H.L. Human NADH:ubiquinone oxidoreductase. *J. Bioenerg. Biomembr.* **33,** 259-266 (2001).
110. Muller-Hocker,J. *et al.* Fatal infantile mitochondrial cardiomyopathy and myopathy with heterogeneous tissue expression of combined respiratory chain deficiencies. *Virchows Arch. A Pathol. Anat. Histopathol.* **419,** 355-362 (1991).
111. Broide,E., Elpeleg,O., & Lahat,E. Type IV 3-methylglutaconic (3-MGC) aciduria: a new case presenting with hepatic dysfunction. *Pediatr. Neurol.* **17,** 353-355 (1997).
112. al Aqeel A. *et al.* 3-Methylglutaconic aciduria: ten new cases with a possible new phenotype. *Brain Dev.* **16 Suppl,** 23-32 (1994).
113. Hullin-Matsuda,F. *et al.* De novo biosynthesis of the late endosome lipid, bis(monoacylglycero)phosphate. *J. Lipid Res.* **48,** 1997-2008 (2007).
114. Schlame,M., Rua,D., & Greenberg,M.L. The biosynthesis and functional role of cardiolipin. *Prog. Lipid Res.* **39,** 257-288 (2000).
115. Kobayashi,T. *et al.* Late endosomal membranes rich in lysobisphosphatidic acid regulate cholesterol transport. *Nat. Cell Biol.* **1,** 113-118 (1999).
116. Schlame,M. & Ren,M. The role of cardiolipin in the structural organization of mitochondrial membranes. *Biochim. Biophys. Acta* **1788,** 2080-2083 (2009).
117. Schug,Z.T. & Gottlieb,E. Cardiolipin acts as a mitochondrial signalling platform to launch apoptosis. *Biochim. Biophys. Acta* **1788,** 2022-2031 (2009).
118. Gilissen,C. *et al.* Exome sequencing identifies WDR35 variants involved in Sensenbrenner syndrome. *Am. J. Hum. Genet.* **87,** 418-423 (2010).
119. Derewenda,Z.S. & Sharp,A.M. News from the interface: the molecular structures of triacylglyceride lipases. *Trends Biochem. Sci.* **18,** 20-25 (1993).
120. Ng,P.C. & Henikoff,S. Predicting deleterious amino acid substitutions. *Genome Res.* **11,** 863-874 (2001).
121. Adzhubei,I.A. *et al.* A method and server for predicting damaging missense mutations. *Nat. Methods* **7,** 248-249 (2010).
122. Chevallier,J. *et al.* Lysobisphosphatidic acid controls endosomal cholesterol levels. *J. Biol. Chem.* **283,** 27871-27880 (2008).
123. Reiners,J.J., Jr., Kleinman,M., Kessel,D., Mathieu,P.A., & Caruso,J.A. Nonesterified cholesterol content of lysosomes modulates susceptibility to oxidant-induced permeabilization. *Free Radic. Biol. Med.* **50,** 281-294 (2011).
124. Hayashi,T. & Su,T.P. Sigma-1 receptor chaperones at the ER-mitochondrion interface regulate Ca(2+) signaling and cell survival. *Cell* **131,** 596-610 (2007).
125. Lewis,J.A. & Tata,J.R. A rapidly sedimenting fraction of rat liver endoplasmic reticulum. *J. Cell Sci.* **13,** 447-459 (1973).
126. Vance,J.E. Phospholipid synthesis in a membrane fraction associated with mitochondria. *J. Biol. Chem.* **265,** 7248-7256 (1990).

127. Miller,S.A., Dykes,D.D., & Polesky,H.F. A simple salting out procedure for extracting DNA from human nucleated cells. *Nucleic Acids Res.* **16,** 1215 (1988).
128. Purcell,S. *et al.* PLINK: a tool set for whole-genome association and population-based linkage analyses. *Am. J. Hum. Genet.* **81,** 559-575 (2007).
129. Houtkooper,R.H. *et al.* Cardiolipin and monolysocardiolipin analysis in fibroblasts, lymphocytes, and tissues using high-performance liquid chromatography-mass spectrometry as a diagnostic test for Barth syndrome. *Anal. Biochem.* **387,** 230-237 (2009).
130. Ledvinova,J. & Elleder,M. Filipin test for diagnosis of Niemann-Pick disease type C. *Sb Lek.* **94,** 137-143 (1993).
131. Rozen,S. & Skaletsky,H. Primer3 on the WWW for general users and for biologist programmers. *Methods Mol. Biol.* **132,** 365-386 (2000).
132. Oetting,W.S. *et al.* Linkage analysis with multiplexed short tandem repeat polymorphisms using infrared fluorescence and M13 tailed primers. *Genomics* **30,** 450-458 (1995).
133. Brownstein,M.J., Carpten,J.D., & Smith,J.R. Modulation of non-templated nucleotide addition by Taq DNA polymerase: primer modifications that facilitate genotyping. *Biotechniques* **20,** 1004-1010 (1996).
134. de Brouwer,A.P., van,B.H., & Kremer,H. Comparison of 12 reference genes for normalization of gene expression levels in Epstein-Barr virus-transformed lymphoblastoid cell lines and fibroblasts. *Mol. Diagn. Ther.* **10,** 197-204 (2006).
135. Livak,K.J. & Schmittgen,T.D. Analysis of relative gene expression data using real-time quantitative PCR and the 2(-Delta Delta C(T)) Method. *Methods* **25,** 402-408 (2001).
136. Pfaffl,M.W. A new mathematical model for relative quantification in real-time RT-PCR. *Nucleic Acids Res.* **29,** e45 (2001).
137. Sistermans,E.A. *et al.* Tissue- and cell-specific distribution of creatine kinase B: a new and highly specific monoclonal antibody for use in immunohistochemistry. *Cell Tissue Res.* **280,** 435-446 (1995).
138. Rodenburg,R.J. Biochemical diagnosis of mitochondrial disorders. *J. Inherit. Metab Dis.* **34,** 283-292 (2011).
139. Jonckheere,A.I. *et al.* A novel mitochondrial ATP8 gene mutation in a patient with apical hypertrophic cardiomyopathy and neuropathy. *BMJ Case. Rep.* **2009,** (2009).
140. Jonckheere,A.I. *et al.* High-throughput assay to measure oxygen consumption in digitonin-permeabilized cells of patients with mitochondrial disorders. *Clin. Chem.* **56,** 424-431 (2010).
141. Furlong,I.J., Lopez,M.C., Ascaso,R., Lopez,R.A., & Collins,M.K. Induction of apoptosis by valinomycin: mitochondrial permeability transition causes intracellular acidification. *Cell Death. Differ.* **5,** 214-221 (1998).
142. Rakovic,A. *et al.* Mutations in PINK1 and Parkin impair ubiquitination of Mitofusins in human fibroblasts. *PLoS. One.* **6,** e16746 (2011).
143. Derewenda,Z.S. & Derewenda,U. Relationships among serine hydrolases: evidence for a common structural motif in triacylglyceride lipases and esterases. *Biochem. Cell Biol.* **69,** 842-851 (1991).
144. Karkucinska-Wieckowska,A. *et al.* Increased reactive oxygen species (ROS) production and low catalase level in fibroblasts of a girl with MEGDEL

association (Leigh syndrome, deafness, 3-methylglutaconic aciduria). *Folia Neuropathol.* **49,** 56-63 (2011).

145. Naess,K. *et al.* MtDNA mutations are a common cause of severe disease phenotypes in children with Leigh syndrome. *Biochim. Biophys. Acta* **1787,** 484-490 (2009).
146. Schwab,M.A. *et al.* Secondary mitochondrial dysfunction in propionic aciduria: a pathogenic role for endogenous mitochondrial toxins. *Biochem. J.* **398,** 107-112 (2006).
147. de Keyzer Y. *et al.* Multiple OXPHOS deficiency in the liver, kidney, heart, and skeletal muscle of patients with methylmalonic aciduria and propionic aciduria. *Pediatr. Res.* **66,** 91-95 (2009).
148. Felipo,V. & Butterworth,R.F. Neurobiology of ammonia. *Prog. Neurobiol.* **67,** 259-279 (2002).
149. Onopiuk,M. *et al.* Mutation in dystrophin-encoding gene affects energy metabolism in mouse myoblasts. *Biochem. Biophys. Res. Commun.* **386,** 463-466 (2009).
150. Acsadi,G. *et al.* Mitochondrial dysfunction in a neural cell model of spinal muscular atrophy. *J. Neurosci. Res.* **87,** 2748-2756 (2009).
151. Aldahmesh,M.A., Khan,A.O., Mohamed,J.Y., Alghamdi,M.H., & Alkuraya,F.S. Identification of a truncation mutation of acylglycerol kinase (AGK) gene in a novel autosomal recessive cataract locus. *Hum. Mutat.* **33,** 960-962 (2012).
152. Knerr,I. *et al.* Hematologic features and clinical course of an infant with Pearson syndrome caused by a novel deletion of mitochondrial DNA. *J. Pediatr. Hematol. Oncol.* **25,** 948-951 (2003).
153. Krauch,G., Wilichowski,E., Schmidt,K.G., & Mayatepek,E. Pearson marrow-pancreas syndrome with worsening cardiac function caused by pleiotropic rearrangement of mitochondrial DNA. *Am. J. Med. Genet.* **110,** 57-61 (2002).
154. Wortmann,S.B. *et al.* Inborn errors of metabolism with 3-methylglutaconic aciduria as discriminative feature: proper classification and nomenclature. *J. Inherit. Metab Dis.*(2013).
155. Chae,J.H. *et al.* A novel ND3 mitochondrial DNA mutation in three Korean children with basal ganglia lesions and complex I deficiency. *Pediatr. Res.* **61,** 622-624 (2007).
156. Esteitie,N. *et al.* Secondary metabolic effects in complex I deficiency. *Ann. Neurol.* **58,** 544-552 (2005).
157. Gerards,M. *et al.* Defective complex I assembly due to C20orf7 mutations as a new cause of Leigh syndrome. *J. Med. Genet.* **47,** 507-512 (2010).
158. Gerards,M. *et al.* Riboflavin-responsive oxidative phosphorylation complex I deficiency caused by defective ACAD9: new function for an old gene. *Brain* **134,** 210-219 (2011).
159. Gropman,A. *et al.* Variable clinical manifestation of homoplasmic G14459A mitochondrial DNA mutation. *Am. J. Med. Genet. A* **124A,** 377-382 (2004).
160. Haack,T.B. *et al.* Exome sequencing identifies ACAD9 mutations as a cause of complex I deficiency. *Nat. Genet.* **42,** 1131-1134 (2010).

161. Procaccio,V. & Wallace,D.C. Late-onset Leigh syndrome in a patient with mitochondrial complex I NDUFS8 mutations. *Neurology* **62,** 1899-1901 (2004).
162. Spiegel,R. *et al.* Mutated NDUFS6 is the cause of fatal neonatal lactic acidemia in Caucasus Jews. *Eur. J. Hum. Genet.* **17,** 1200-1203 (2009).
163. Tuppen,H.A. *et al.* The p.M292T NDUFS2 mutation causes complex I-deficient Leigh syndrome in multiple families. *Brain* **133,** 2952-2963 (2010).
164. Zafeiriou,D.I. *et al.* MR spectroscopy and serial magnetic resonance imaging in a patient with mitochondrial cystic leukoencephalopathy due to complex I deficiency and NDUFV1 mutations and mild clinical course. *Neuropediatrics* **39,** 172-175 (2008).
165. Blazquez,A. *et al.* Infantile mitochondrial encephalomyopathy with unusual phenotype caused by a novel BCS1L mutation in an isolated complex III-deficient patient. *Neuromuscul. Disord.* **19,** 143-146 (2009).
166. de Lonlay P. *et al.* A mutant mitochondrial respiratory chain assembly protein causes complex III deficiency in patients with tubulopathy, encephalopathy and liver failure. *Nat. Genet.* **29,** 57-60 (2001).
167. De Meirleir L. *et al.* Clinical and diagnostic characteristics of complex III deficiency due to mutations in the BCS1L gene. *Am. J. Med. Genet. A* **121A,** 126-131 (2003).
168. Karadimas,C.L. *et al.* Recurrent myoglobinuria due to a nonsense mutation in the COX I gene of mitochondrial DNA. *Neurology* **55,** 644-649 (2000).
169. Moran,M. *et al.* Cellular pathophysiological consequences of BCS1L mutations in mitochondrial complex III enzyme deficiency. *Hum. Mutat.* **31,** 930-941 (2010).
170. Wong,L.J. *et al.* Severe lactic acidosis caused by a novel frame-shift mutation in mitochondrial-encoded cytochrome c oxidase subunit II. *Am. J. Med. Genet.* **102,** 95-99 (2001).
171. Antonicka,H. *et al.* Mutations in COX10 result in a defect in mitochondrial heme A biosynthesis and account for multiple, early-onset clinical phenotypes associated with isolated COX deficiency. *Hum. Mol. Genet.* **12,** 2693-2702 (2003).
172. Ghezzi,D. *et al.* FASTKD2 nonsense mutation in an infantile mitochondrial encephalomyopathy associated with cytochrome c oxidase deficiency. *Am. J. Hum. Genet.* **83,** 415-423 (2008).
173. Massa,V. *et al.* Severe infantile encephalomyopathy caused by a mutation in COX6B1, a nucleus-encoded subunit of cytochrome c oxidase. *Am. J. Hum. Genet.* **82,** 1281-1289 (2008).
174. Oquendo,C.E., Antonicka,H., Shoubridge,E.A., Reardon,W., & Brown,G.K. Functional and genetic studies demonstrate that mutation in the COX15 gene can cause Leigh syndrome. *J. Med. Genet.* **41,** 540-544 (2004).
175. Salviati,L. *et al.* Cytochrome c oxidase deficiency due to a novel SCO2 mutation mimics Werdnig-Hoffmann disease. *Arch. Neurol.* **59,** 862-865 (2002).
176. Tay,S.K. *et al.* Unusual clinical presentations in four cases of Leigh disease, cytochrome C oxidase deficiency, and SURF1 gene mutations. *J. Child Neurol.* **20,** 670-674 (2005).

177. Valnot,I. *et al.* Mutations of the SCO1 gene in mitochondrial cytochrome c oxidase deficiency with neonatal-onset hepatic failure and encephalopathy. *Am. J. Hum. Genet.* **67,** 1104-1109 (2000).
178. Valnot,I. *et al.* A mutation in the human heme A:farnesyltransferase gene (COX10) causes cytochrome c oxidase deficiency. *Hum. Mol. Genet.* **9,** 1245-1249 (2000).
179. Verdijk,R.M. *et al.* Phenotypic consequences of a novel SCO2 gene mutation. *Am. J. Med. Genet. A* **146A,** 2822-2827 (2008).
180. Cameron,J.M. *et al.* Complex V TMEM70 deficiency results in mitochondrial nucleoid disorganization. *Mitochondrion.* **11,** 191-199 (2011).
181. Shchelochkov,O.A. *et al.* Milder clinical course of Type IV 3-methylglutaconic aciduria due to a novel mutation in TMEM70. *Mol. Genet. Metab* **101,** 282-285 (2010).
182. Spiegel,R. *et al.* TMEM70 mutations are a common cause of nuclear encoded ATP synthase assembly defect: further delineation of a new syndrome. *J. Med. Genet.* **48,** 177-182 (2011).
183. Torraco,A. *et al.* TMEM70: a mutational hot spot in nuclear ATP synthase deficiency with a pivotal role in complex V biogenesis. *Neurogenetics.* **13,** 375-386 (2012).
184. Tort,F. *et al.* Screening for nuclear genetic defects in the ATP synthase-associated genes TMEM70, ATP12 and ATP5E in patients with 3-methylglutaconic aciduria. *Clin. Genet.* **80,** 297-300 (2011).
185. Acham-Roschitz,B. *et al.* A novel mutation of the RRM2B gene in an infant with early fatal encephalomyopathy, central hypomyelination, and tubulopathy. *Mol. Genet. Metab* **98,** 300-304 (2009).
186. Bakker,H.D. *et al.* Depletion of mitochondrial deoxyribonucleic acid in a family with fatal neonatal liver disease. *J. Pediatr.* **128,** 683-687 (1996).
187. Bao,X. *et al.* Alpers syndrome with prominent white matter changes. *Brain Dev.* **30,** 295-300 (2008).
188. Baris,Z., Eminoglu,T., Dalgic,B., Tumer,L., & Hasanoglu,A. Mitochondrial neurogastrointestinal encephalomyopathy (MNGIE): case report with a new mutation. *Eur. J. Pediatr.* **169,** 1375-1378 (2010).
189. Bekheirnia,M.R. *et al.* POLG mutation in a patient with cataracts, early-onset distal muscle weakness and atrophy, ovarian dysgenesis and 3-methylglutaconic aciduria. *Gene* **499,** 209-212 (2012).
190. Bornstein,B. *et al.* Mitochondrial DNA depletion syndrome due to mutations in the RRM2B gene. *Neuromuscul. Disord.* **18,** 453-459 (2008).
191. Burusnukul,P. & de los Reyes,E.C. Phenotypic variations in 3 children with POLG1 mutations. *J. Child Neurol.* **24,** 482-486 (2009).
192. Ferrari,G. *et al.* Infantile hepatocerebral syndromes associated with mutations in the mitochondrial DNA polymerase-gammaA. *Brain* **128,** 723-731 (2005).
193. Ji,J.Q. *et al.* A novel c.592-4_c.592-3delTT mutation in DGUOK gene causes exon skipping. *Mitochondrion.* **10,** 188-191 (2010).
194. Kollberg,G. *et al.* A novel homozygous RRM2B missense mutation in association with severe mtDNA depletion. *Neuromuscul. Disord.* **19,** 147-150 (2009).

195. Kurt,B. *et al.* A novel POLG gene mutation in 4 children with Alpers-like hepatocerebral syndromes. *Arch. Neurol.* **67,** 239-244 (2010).
196. Lesko,N. *et al.* Two novel mutations in thymidine kinase-2 cause early onset fatal encephalomyopathy and severe mtDNA depletion. *Neuromuscul. Disord.* **20,** 198-203 (2010).
197. Lutz,R.E. *et al.* De novo mutations in POLG presenting with acute liver failure or encephalopathy. *J. Pediatr. Gastroenterol. Nutr.* **49,** 126-129 (2009).
198. Maaswinkel-Mooij,P.D. *et al.* Depletion of mitochondrial DNA in the liver of a patient with lactic acidemia and hypoketotic hypoglycemia. *J. Pediatr.* **128,** 679-683 (1996).
199. Mazziotta,M.R. *et al.* Fatal infantile liver failure associated with mitochondrial DNA depletion. *J. Pediatr.* **121,** 896-901 (1992).
200. Muller-Hocker,J. *et al.* Depletion of mitochondrial DNA in the liver of an infant with neonatal giant cell hepatitis. *Hum. Pathol.* **33,** 247-253 (2002).
201. Navarro-Sastre,A. *et al.* Lethal hepatopathy and leukodystrophy caused by a novel mutation in MPV17 gene: description of an alternative MPV17 spliced form. *Mol. Genet. Metab* **94,** 234-239 (2008).
202. Ostergaard,E. *et al.* A novel missense mutation in SUCLG1 associated with mitochondrial DNA depletion, encephalomyopathic form, with methylmalonic aciduria. *Eur. J. Pediatr.* **169,** 201-205 (2010).
203. Randolph,L.M. *et al.* Fatal infantile lactic acidosis and a novel homozygous mutation in the SUCLG1 gene: a mitochondrial DNA depletion disorder. *Mol. Genet. Metab* **102,** 149-152 (2011).
204. Rivera,H. *et al.* Marked mitochondrial DNA depletion associated with a novel SUCLG1 gene mutation resulting in lethal neonatal acidosis, multi-organ failure, and interrupted aortic arch. *Mitochondrion.* **10,** 362-368 (2010).
205. Salviati,L. *et al.* Mitochondrial DNA depletion and dGK gene mutations. *Ann. Neurol.* **52,** 311-317 (2002).
206. Valayannopoulos,V. *et al.* New SUCLG1 patients expanding the phenotypic spectrum of this rare cause of mild methylmalonic aciduria. *Mitochondrion.* **10,** 335-341 (2010).
207. Van Hove,J.L. *et al.* Succinyl-CoA ligase deficiency: a mitochondrial hepatoencephalomyopathy. *Pediatr. Res.* **68,** 159-164 (2010).
208. Weiss,M.D. & Saneto,R.P. Sensory ataxic neuropathy with dysarthria and ophthalmoparesis (SANDO) in late life due to compound heterozygous POLG mutations. *Muscle Nerve* **41,** 882-885 (2010).
209. Wiltshire,E. *et al.* Juvenile Alpers disease. *Arch. Neurol.* **65,** 121-124 (2008).
210. Wong,L.J. *et al.* Mutations in the MPV17 gene are responsible for rapidly progressive liver failure in infancy. *Hepatology* **46,** 1218-1227 (2007).
211. Edvardson,S. *et al.* Deleterious mutation in the mitochondrial arginyl-transfer RNA synthetase gene is associated with pontocerebellar hypoplasia. *Am. J. Hum. Genet.* **81,** 857-862 (2007).
212. Kishnani,P.S. *et al.* Acute pancreatitis in an infant with lactic acidosis and a mutation at nucleotide 3243 in the mitochondrial DNA tRNALeu(UUR) gene. *Eur. J. Pediatr.* **155,** 898-903 (1996).

213. Lin,J. *et al.* Leukoencephalopathy with brainstem and spinal cord involvement and normal lactate: a new mutation in the DARS2 gene. *J. Child Neurol.* **25,** 1425-1428 (2010).
214. Lindberg,C., Moslemi,A.R., & Oldfors,A. MELAS syndrome in a patient with a point mutation in MTTS1. *Acta Neurol. Scand.* **117,** 128-132 (2008).
215. Linnankivi,T. *et al.* Five new cases of a recently described leukoencephalopathy with high brain lactate. *Neurology* **63,** 688-692 (2004).
216. Ogle,R.F. *et al.* Mitochondrial myopathy with tRNA(Leu(UUR)) mutation and complex I deficiency responsive to riboflavin. *J. Pediatr.* **130,** 138-145 (1997).
217. Schara,U. *et al.* Acute liver failure with subsequent cirrhosis as the primary manifestation of TRMU mutations. *J. Inherit. Metab Dis.* **34,** 197-201 (2011).
218. Seneca,S. *et al.* A new mitochondrial point mutation in the transfer RNA(Leu) gene in a patient with a clinical phenotype resembling Kearns-Sayre syndrome. *Arch. Neurol.* **58,** 1113-1118 (2001).
219. Serkov,S.V. *et al.* Five patients with a recently described novel leukoencephalopathy with brainstem and spinal cord involvement and elevated lactate. *Neuropediatrics* **35,** 1-5 (2004).
220. Valente,L. *et al.* Infantile encephalopathy and defective mitochondrial DNA translation in patients with mutations of mitochondrial elongation factors EFG1 and EFTu. *Am. J. Hum. Genet.* **80,** 44-58 (2007).
221. Van der Knaap,M.S. *et al.* A new leukoencephalopathy with brainstem and spinal cord involvement and high lactate. *Ann. Neurol.* **53,** 252-258 (2003).
222. Zeharia,A. *et al.* Mitochondrial myopathy, sideroblastic anemia, and lactic acidosis: an autosomal recessive syndrome in Persian Jews caused by a mutation in the PUS1 gene. *J. Child Neurol.* **20,** 449-452 (2005).
223. Zeharia,A. *et al.* Acute infantile liver failure due to mutations in the TRMU gene. *Am. J. Hum. Genet.* **85,** 401-407 (2009).
224. Ojala,T. *et al.* New mutation of mitochondrial DNAJC19 causing dilated and noncompaction cardiomyopathy, anemia, ataxia, and male genital anomalies. *Pediatr. Res.* **72,** 432-437 (2012).
225. Aljishi,E. & Ali,F. Barth syndrome: an X-linked cardiomyopathy with a novel mutation. *Indian J. Pediatr.* **77,** 1432-1433 (2010).
226. D'Adamo,P. *et al.* The X-linked gene G4.5 is responsible for different infantile dilated cardiomyopathies. *Am. J. Hum. Genet.* **61,** 862-867 (1997).
227. Momoi,N. *et al.* Differing clinical courses and outcomes in two siblings with Barth syndrome and left ventricular noncompaction. *Eur. J. Pediatr.* **171,** 515-520 (2012).
228. McCanta,A.C., Chang,A.C., & Weiner,K. Cardiomyopathy in a child with neutropenia and motor delay. *Curr. Opin. Pediatr.* **20,** 605-607 (2008).
229. Rugolotto,S. *et al.* Long-term treatment of Barth syndrome with pantothenic acid: a retrospective study. *Mol. Genet. Metab* **80,** 408-411 (2003).
230. Sakamoto,O., Kitoh,T., Ohura,T., Ohya,N., & Iinuma,K. Novel missense mutation (R94S) in the TAZ (G4.5) gene in a Japanese patient with Barth syndrome. *J. Hum. Genet.* **47,** 229-231 (2002).
231. Sweeney,R.T., Davis,G.J., & Noonan,J.A. Cardiomyopathy of unknown etiology: Barth syndrome unrecognized. *Congenit. Heart Dis.* **3,** 443-448 (2008).

232. Wortmann,S.B. *et al.* Mutations in the phospholipid remodeling gene SERAC1 impair mitochondrial function and intracellular cholesterol trafficking and cause dystonia and deafness. *Nat. Genet.* **44,** 797-802 (2012).
233. Bleyl,S.B. *et al.* Xq28-linked noncompaction of the left ventricular myocardium: prenatal diagnosis and pathologic analysis of affected individuals. *Am. J. Med. Genet.* **72,** 257-265 (1997).
234. Bleyl,S.B. *et al.* Neonatal, lethal noncompaction of the left ventricular myocardium is allelic with Barth syndrome. *Am. J. Hum. Genet.* **61,** 868-872 (1997).
235. Brady,A.N., Shehata,B.M., & Fernhoff,P.M. X-linked fetal cardiomyopathy caused by a novel mutation in the TAZ gene. *Prenat. Diagn.* **26,** 462-465 (2006).
236. Chang,B. *et al.* Gonadal mosaicism of a TAZ (G4.5) mutation in a Japanese family with Barth syndrome and left ventricular noncompaction. *Mol. Genet. Metab* **100,** 198-203 (2010).
237. Cosson,L. *et al.* Barth syndrome in a female patient. *Mol. Genet. Metab* **106,** 115-120 (2012).
238. Donati,M.A. *et al.* Barth syndrome presenting with acute metabolic decompensation in the neonatal period. *J. Inherit. Metab Dis.* **29,** 684 (2006).
239. Ichida,F. *et al.* Novel gene mutations in patients with left ventricular noncompaction or Barth syndrome. *Circulation* **103,** 1256-1263 (2001).
240. Katsushima,Y. *et al.* Normal pituitary function in a Japanese patient with Barth syndrome. *Eur. J. Pediatr.* **161,** 67-68 (2002).
241. Ronghe,M.D., Foot,A.B., Martin,R., Ashworth,M., & Steward,C.G. Non-Epstein-Barr virus-associated T-cell lymphoma following cardiac transplantation for Barth syndrome. *Acta Paediatr.* **90,** 584-586 (2001).
242. Sakamoto,O. *et al.* A novel intronic mutation of the TAZ (G4.5) gene in a patient with Barth syndrome: creation of a 5' splice donor site with variant GC consensus and elongation of the upstream exon. *Hum. Genet.* **109,** 559-563 (2001).
243. Steward,C.G. *et al.* Barth syndrome: an X-linked cause of fetal cardiomyopathy and stillbirth. *Prenat. Diagn.* **30,** 970-976 (2010).
244. Takeda,A. *et al.* Barth syndrome diagnosed in the subclinical stage of heart failure based on the presence of lipid storage myopathy and isolated noncompaction of the ventricular myocardium. *Eur. J. Pediatr.* **170,** 1481-1484 (2011).
245. Vesel,S. *et al.* A novel mutation in the G4.5 (TAZ) gene in a kindred with Barth syndrome. *Eur. J. Hum. Genet.* **11,** 97-101 (2003).
246. Xing,Y. *et al.* Genetic analysis in patients with left ventricular noncompaction and evidence for genetic heterogeneity. *Mol. Genet. Metab* **88,** 71-77 (2006).
247. Calvo,S.E. *et al.* Molecular diagnosis of infantile mitochondrial disease with targeted next-generation sequencing. *Sci. Transl. Med.* **4,** 118ra10 (2012).
248. Ho,G., Walter,J.H., & Christodoulou,J. Costeff optic atrophy syndrome: New clinical case and novel molecular findings. *J. Inherit. Metab Dis.*(2008).
249. Mayr,J.A. *et al.* Lack of the mitochondrial protein acylglycerol kinase causes Sengers syndrome. *Am. J. Hum. Genet.* **90,** 314-320 (2012).

250. Yu-Wai-Man,P. *et al.* Multi-system neurological disease is common in patients with OPA1 mutations. *Brain* **133,** 771-786 (2010).
251. Barshop,B.A. *et al.* Kearns-Sayre syndrome presenting as 2-oxoadipic aciduria. *Mol. Genet. Metab* **69,** 64-68 (2000).
252. Bruno,C. *et al.* Primary adrenal insufficiency in a child with a mitochondrial DNA deletion. *J. Inherit. Metab Dis.* **21,** 155-161 (1998).
253. Lacbawan,F. *et al.* Clinical heterogeneity in mitochondrial DNA deletion disorders: a diagnostic challenge of Pearson syndrome. *Am. J. Med. Genet.* **95,** 266-268 (2000).
254. Lee,H.F. *et al.* The neurological evolution of Pearson syndrome: case report and literature review. *Eur. J. Paediatr. Neurol.* **11,** 208-214 (2007).
255. Morel,A.S. *et al.* Early neurological impairment and severe anemia in a newborn with Pearson syndrome. *Eur. J. Pediatr.* **168,** 311-315 (2009).
256. Ribes,A. *et al.* Pearson syndrome: altered tricarboxylic acid and urea-cycle metabolites, adrenal insufficiency and corneal opacities. *J. Inherit. Metab Dis.* **16,** 537-540 (1993).
257. Seneca,S. *et al.* Pearson marrow pancreas syndrome: a molecular study and clinical management. *Clin. Genet.* **51,** 338-342 (1997).
258. Shanske,S. *et al.* Identical mitochondrial DNA deletion in a woman with ocular myopathy and in her son with pearson syndrome. *Am. J. Hum. Genet.* **71,** 679-683 (2002).
259. Superti-Furga,A. *et al.* Pearson bone marrow-pancreas syndrome with insulin-dependent diabetes, progressive renal tubulopathy, organic aciduria and elevated fetal haemoglobin caused by deletion and duplication of mitochondrial DNA. *Eur. J. Pediatr.* **152,** 44-50 (1993).
260. Yau,E.K., Chan,K.Y., Au,K.M., Chow,T.C., & Chan,Y.W. A novel mitochondrial DNA deletion in a Chinese girl with Kearns-Sayre syndrome. *Hong. Kong. Med. J.* **15,** 374-377 (2009).
261. Beresford,M.W., Pourfarzam,M., & Davidson,J.E. "So doctor, what exactly is wrong with my muscles? Glutaric aciduria type II presenting in a teenager". *Neuromuscul. Disord.* **16,** 613 (2006).
262. Curcoy,A. *et al.* Late-onset form of beta-electron transfer flavoprotein deficiency. *Mol. Genet. Metab* **78,** 247-249 (2003).
263. Ishii,K. *et al.* Central nervous system and muscle involvement in an adolescent patient with riboflavin-responsive multiple acyl-CoA dehydrogenase deficiency. *Brain Dev.* **32,** 669-672 (2010).
264. Olsen,R.K. *et al.* ETFDH mutations as a major cause of riboflavin-responsive multiple acyl-CoA dehydrogenation deficiency. *Brain* **130,** 2045-2054 (2007).
265. Diomedi-Camassei,F. *et al.* COQ2 nephropathy: a newly described inherited mitochondriopathy with primary renal involvement. *J. Am. Soc. Nephrol.* **18,** 2773-2780 (2007).
266. Salviati,L. *et al.* Infantile encephalomyopathy and nephropathy with CoQ10 deficiency: a CoQ10-responsive condition. *Neurology* **65,** 606-608 (2005).
267. Wen,B. *et al.* Riboflavin-responsive lipid-storage myopathy caused by ETFDH gene mutations. *J. Neurol. Neurosurg. Psychiatry* **81,** 231-236 (2010).

268. Cameron,J.M. *et al.* Pyruvate dehydrogenase phosphatase 1 (PDP1) null mutation produces a lethal infantile phenotype. *Hum. Genet.* **125,** 319-326 (2009).
269. Head,R.A. *et al.* Pyruvate dehydrogenase deficiency presenting as dystonia in childhood. *Dev. Med. Child Neurol.* **46,** 710-712 (2004).
270. Bourgeron,T. *et al.* Mutation of the fumarase gene in two siblings with progressive encephalopathy and fumarase deficiency. *J. Clin. Invest* **93,** 2514-2518 (1994).
271. Guffon,N. *et al.* 2-Ketoglutarate dehydrogenase deficiency, a rare cause of primary hyperlactataemia: report of a new case. *J. Inherit. Metab Dis.* **16,** 821-830 (1993).
272. Kohlschutter,A. *et al.* A familial progressive neurodegenerative disease with 2-oxoglutaric aciduria. *Eur. J. Pediatr.* **138,** 32-37 (1982).
273. Wortmann,S.B. *et al.* 3-Methylglutaconic aciduria-lessons from 50 genes and 977 patients. *J. Inherit. Metab Dis.*(2013).

Dankwoord (Acknowledgements)

After having completed this thesis I have indeed learned a lot about doing science, writing articles and the importance of impact factor points. Still I am convinced that this and the following chapter have the highest social impact factor and will be read by more people than all the articles together. Please do forgive me if you do not read your name below. So many people were part of my life during the six years of work on this thesis, that I will surely forget someone with no ill intent.

First of all I want to thank my mentors Ron Wevers and Eva Morava. Ron and Eva, during this long period of six years we did not only work together, but we also became friends. Both of you were always enthusiastic and interested in the progress of our work. But besides working, we did also spent substantial time on *"borrelen"* (having drinks) on meetings around the world or with diet coke in Ron's office. I will also never forget your compassion during the time my life was upside-down due to the illness of my father.

Jan Smeitink, dear Jan, you are my third promotor. I am grateful for this. As in the daily clinical practice you allow me to develop with the good feeling that I can always count on you.

Co-promotor Richard Rodenburg, *"de stille kracht"*. From the beginning you were continuously interested in the progress of my thesis. I really appreciate our discussions, your deep knowledge about mitochondria and your critical reading of the manuscripts. But most of all, I like your attitude: always calm and always positive.

I would like to thank all national and international collaborators and coauthors for their efforts. My special thanks go to Arjan de Brouwer and Fred Vaz for their collaboration on MEGDEL syndrome.

My colleagues from the Nijmegen metabolic micro cosmos. There are quite a lot of people I would like to thank. My (former) clinical colleagues Maaike de Vries, Mirian Janssen, An Jonckheere and our nurse practitioner Marion Hermans. Our metabolic dieticians, in particular Annemiek Wegberg who is more a friend than a colleague. The colleagues from the laboratory of genetic, endocrine and metabolic diseases (LGEM), in particular Leo Kluijtmans for always and once more being helpful. And all the hard working people behind the scenes: the technicians of the different metabolic investigations, the colleagues from the "cell culture group", the "muscle group", the "DNA group" and the beating heart: Inge Konijnenberg and her colleagues from the "*monsterontvangst"* Francien, Wilma and Riette. Could you count how many overseas parcels with fibroblasts or other tissues you received for me and how many DNA samples had to be prepared? Thank you all, this work would have been impossible without your valuable help. And there are some more very important

ladies: Sandra van Kolck-Hoenderop and her colleagues from the LGEM secretariat. Last, not least my fellow phD students: Thatjana Gardeitchik (queen of cell culture and Western Blotting, thank you so much), Miski Mohamed (dear friend, always bringing me back in balance), Saskia Koene and Paul de Laat.

Furthermore, I would like to thank all my (former) colleagues (doctors, nurses, administrative staff) from our children's hospital for the pleasant collaboration in daily clinical practice. Of course, this also includes the colleagues from the Pediatric Neurology and the Pediatric Intensive Care. Some of you are friends and not only colleagues: Chantal Liebrand, Annette Reimer, Ad Backx and Zina Fejzic. Furthermore I don't want to forget Annette de Boer, Anita Kerkhof and her colleagues from our secretariat.

I am also grateful to Ulrike Schara, Ursula Felderhoff-Müser, Adela Della-Marina, Sören Lutz, Katja Schaaf, Astrid Bertsche and the other colleagues from the Department of Pediatric Neurology/ *Klinik für Kinderheilkunde I* of the University of Essen, Essen, Germany. It was a hard time, but you were colleagues to rely on!

I would like to thank the doctors and nurses of the Streekziekenhuis Koningin Beatrix in Winterswijk for giving me the feeling of being a general paediatrician.

My friends, Britta Hohlwegler, Mark Muijrers & Tobi Verbeet, Antje Simmert, Adela Della Marina, Carolin Scheffler, Mone & Jens Lehwald, Nadja Lehwald, Andrea Kutsche, Steffi Gerhardy, Michaela Sanderhoff. Though miles may lie between us, we are never far apart.

Papa en mama, jullie hebben voor een warm nest gezorgd en onder jullie liefdevolle ogen hebben we leren vliegen. Papa, ik mis je. Mama, Nicole & Marc, Frank: samen komen we er wel!

Florian,
Es ist was es ist
sagt die Liebe (Erich Fried)

Curriculum Vitae

Saskia was born on Februari 28, 1978 in Hamm, Germany. She grew up in Langscheid and finished secondary school at the Gymnasium in Sundern in 1997.
In the same year she started Medical School at the RWTH Aachen University, Aachen, Germany. From September 2000 onwards she interrupted her studies for one year of research on interleukine 6 (IL-6) signalling at the Institute of Biochemistry of the same university. Later she continued the research beside her medical studies. She performed clinical electives in the Seychelles and in Malaysia. After having finished her practical year (Maastricht, the Netherlands; Aachen, Germany; Zurich, Switzerland) she obtained her medical degree in May 2004.
In June of the same year she started her residency in Paediatrics at the Radboud University Medical Center. In November 2004 she defended her medical thesis "Characterisation of fluorescent variants of the cytokine-receptor gp 130 concerning activity and dimerisation with molecular biological and fluorescence spectroscopy methods" (magna cum laude; Prof. dr. P.C: Heinrich, Prof. dr. G. Muller-Newen) at the RWTH Aachen University. She interrupted her residency for voluntary work in Kolkata, India (2006) and Pisco, Peru (2007). Winning the Sengers stipendium in 2007 for her research proposal "Clinical, biochemical and genetic investigations in children with 3–methylglutaconic aciduria" enabled her to deepen her studies on metabolic diseases and finally resulted in this thesis. She finished her residency with 1.5 years of working in the department of Paediatric Neurology at the University of Essen (head: Prof. dr. U. Schara) and passed the paediatric board examination in March 2010.
Between July 2010 and June 2011 she worked as a clinical researcher at the Nijmegen Centre for Mitochondrial Disorders. Since July 2011 she is a fellow in metabolic diseases at the same department (head: Prof. dr. J.A.M. Smeitink).
She has won the prize for the best article of the Dutch society for metabolic diseases (ESN) in 2009 and for the best abstract in 2012. She was granted a travel award of the society for the study of inborn errors of metabolism (SSIEM) in 2010. Furthermore she received the Wadman-van Gennip Price of the ESN and the young investigators award of the Dutch society of Pediatrics (NVK) in 2012. She is the ambassador for metabolic diseases of the journal '*Kinderarts en Wetenschap*'.
Saskia enjoys her life together with Florian. They are expecting their first child in autum 2013.

List of publications

In relation with 3–methylglutaconic aciduria

1. Wortmann S, Kluijtmans L, Rodenburg R, Sass J, Nouws J, van Kaauwen E, Kleefstra T, Tranebjaerg L, de Vries M, Isohanni P, Walter K, Alkuraya F, Smuts S, Reinecke C, van der Westhuizen F, Thorburn D, Smeitink J, Morava E, Wevers R. 3–methylglutaconic aciduria - lessons from nearly 50 genes and more than 900 patients. J Inherit Metab Dis. 2013, DOI 10.1007/s10545-012-9579-6.

2. Wortmann S, Duran M, Anikster Y, Barth P, Sperl W, Zschocke J, Morava E, Wevers R. Inborn errors of metabolism with 3–methylglutaconic aciduria as discriminative feature: proper classification and nomenclature. J Inherit Metab Dis. 2013, DOI 10.1007/s10545-012-9580-0.

3. Wortmann S, Vaz F, Gardeitchik T, Vissers L, Renkema G, Schuurs-Hoeijmakers J, Kulik W, Lammens M, Christin C, Kluijtmans L, Rodenburg R, Nijtmans L, Grünewald A, Klein C, Gerhold J, Kozicz T, van Hasselt P, Harakalova M, Kloosterman W, Barić I, Pronicka E, Ucar S, Naess K, Singhal K, Krumina Z, Gilissen C, van Bokhoven H, Veltman J, Smeitink J, Lefeber D, Spelbrink J, Wevers R, Morava E, de Brouwer A. Mutations in the phospholipid remodeling gene SERAC1 impair mitochondrial function and intracellular cholesterol trafficking and cause dystonia and deafness. Nat Genet. 2012 Jun 10;44(7):797-802.

4. Wortmann S, Morava E. 3–methylglutaconic aciduria type IV: a syndrome with an evolving phenotype. Clin Dysmorphol. 2011 Jul;20(3):168-9.

5. Wortmann S, Kluijtmans L, Engelke U, Wevers R, Morava E. The 3–methylglutaconic acidurias: what's new? J Inherit Metab Dis. 2012;35(1):13-22.

6. Wortmann S, Kremer B, Graham A, Willemsen M, Loupatty F, Hogg S, Engelke U, Kluijtmans L, Wanders R, Illsinger S, Wilcken B, Cruysberg J, Das A, Morava E, Wevers R. 3–methylglutaconic aciduria type I redefined: a syndrome with late-onset leukoencephalopathy. Neurology. 2010 Sep 21;75(12):1079-83.

7. Wortmann S, Rodenburg R, Jonckheere A, de Vries M, Huizing M, Heldt K, van den Heuvel L, Wendel U, Kluijtmans L, Engelke U, Wevers R, Smeitink J, Morava E. Biochemical and genetic analysis of 3–methylglutaconic aciduria type IV: a diagnostic strategy. Brain. 2009 Jan;132(Pt 1):136-46.

8. Wortmann S, Rodenburg R, Huizing M, Loupatty F, de Koning T, Kluijtmans L, Engelke U, Wevers R, Smeitink J, Morava E. Association of 3–methylglutaconic aciduria with sensori-neural deafness, encephalopathy, and Leigh-like syndrome (MEGDEL association) in four patients with a disorder of the oxidative phosphorylation. Mol Genet Metab. 2006 May;88(1):47-52.

Other publications

10. Koene S, Wortmann S, de Vries M, Jonckheere A, Morava E, de Groot I, Smeitink J. Developing outcome measures for pediatric mitochondrial disorders: Which complaints

and limitations are most burdensome to patients and their parents? Mitochondrion. 2012 Nov 17. doi:pii: S1567-7249(12)00247-4.

11. Horvers M, Anttonen A, Lehesjoki A, Morava E, Wortmann S, Vermeer S, van de Warrenburg B, Willemsen M. Marinesco-Sjögren syndrome due to SIL1 mutations with a comment on the clinical phenotype. Eur J Paediatr Neurol. 2012 Oct 10. doi:pii: S1090-3798(12)00199-7. 10.1016/j.ejpn.2012.09.007.

12. Wortmann S, Champion M, van den Heuvel L, Barth H, Trutnau B, Craig K, Lammens M, Schreuder M, Taylor R, Smeitink J, Wevers R, Rodenburg R, Morava E. Mitochondrial DNA m.3242G>A mutation, an under diagnosed cause of hypertrophic cardiomyopathy and renal tubular dysfunction? Eur J Med Genet. 2012 Oct;55(10):552-6.

13. Binkhorst M, Wortmann S, Funke S, Kozicz T, Wevers R, Morava E. Glycosylation defects underlying fetal alcohol spectrum disorder: a novel pathogenetic model : "When the wine goes in, strange things come out" - S.T. Coleridge, The Piccolomini. J Inherit Metab Dis. 2012 May;35(3):399-405.

14. Wortmann S, Mitchell A, Ruzhensova U, Hoyer P, Neudorf U. Fieber, Schüttelfrost und schwarze Finger. Monatsschr Kinderheilkd 2011 159:612–615.

15. Achouitar S, Goldstein J, Mohamed M, Austin S, Boyette K, Blanpain F, Rehder C, Kishnani P, Wortmann S, den Heijer M, Lefeber D, Wevers R, Bali D, Morava E. Common mutation in the PHKA2 gene with variable phenotype in patients with liver phosphorylase b kinase deficiency. Mol Genet Metab. 2011 Dec;104(4):691-4.

16. Achouitar S, Mohamed M, Gardeitchik T, Wortmann S, Sykut-Cegielska J, Ensenauer R, de Baulny H, Õunap K, Martinelli D, de Vries M, McFarland R, Kouwenberg D, Theodore M, Wijburg F, Grünewald S, Jaeken J, Wevers R, Nijtmans L, Elson J, Morava E. Nijmegen paediatric CDG rating scale: a novel tool to assess disease progression. J Inherit Metab Dis. 2011 Aug;34(4):923-7.

17. Mohamed M, Guillard M, Wortmann S, Cirak S, Marklova E, Michelakakis H, Korsch E, Adamowicz M, Koletzko B, van Spronsen F, Niezen-Koning K, Matthijs G, Gardeitchik T, Kouwenberg D, Lim B, Zeevaert R, Wevers R, Lefeber D, Morava E. Clinical and diagnostic approach in unsolved CDG patients with a type 2 transferrin pattern. Biochim Biophys Acta. 2011 Jun;1812(6):691-8.

18. Smits P, Saada A, Wortmann S, Heister A, Brink M, Pfundt R, Miller C, Haas D, Hantschmann R, Rodenburg R, Smeitink J, van den Heuvel L. Mutation in mitochondrial ribosomal protein MRPS22 leads to Cornelia de Lange-like phenotype, brain abnormalities and hypertrophic cardiomyopathy. Eur J Hum Genet. 2011 Apr;19(4):394-9

19. Kleefstra T, Wortmann S, Rodenburg R, Bongers E, Hadzsiev K, Noordam C, van den Heuvel L, Nillesen W, Hollody K, Gillessen-Kaesbach G, Lammens M, Smeitink J, van der Burgt I, Morava E. Mitochondrial dysfunction and organic aciduria in five patients carrying mutations in the Ras-MAPK pathway. Eur J Hum Genet. 2011 Feb;19(2):138-44.

20. Albrecht B, de Brouwer A, Lefeber D, Cremer K, Hausser I, Rossen N, Wortmann S, Wevers R, Kornak U, Morava E. MACS syndrome: A combined collagen and elastin disorder due to abnormal Golgi trafficking. Am J Med Genet A. 2010 Nov;152A(11):2916-8.

21. Schreuder L, Nijhuis-van der Sanden M, de Hair A, Peters G, Wortmann S, Bok LA, Morava E. Successful use of albuterol in a patient with central core disease and mitochondrial dysfunction. J Inherit Metab Dis. 2010 May 5.
22. Wortmann S, Lefeber D, Dekomien G, Willemsen M, Wevers R, Morava E. Substrate deprivation therapy in juvenile Sandhoff disease. J Inherit Metab Dis. 2009 Nov 4.
23. Wortmann S, Zweers-van Essen H, Rodenburg R, van den Heuvel L, de Vries M, Rasmussen-Conrad E, Smeitink J, Morava E. Mitochondrial energy production correlates with the age-related BMI. Pediatr Res. 2009 Jan;65(1):103-8.
24. Koene S, Kozicz T, Rodenburg R, Verhaak C, de Vries M, Wortmann S, van de Heuvel L, Smeitink J, Morava E. Major depression in adolescent children consecutively diagnosed with mitochondrial disorder. J Affect Disord. 2009 Apr;114(1-3):327-32.
25. Wortmann S, Reimer A, Creemers J, Mullaart R. Prenatal diagnosis of cerebral lesions in Tuberous sclerosis complex (TSC). Case report and review of the literature. Eur J Paediatr Neurol. 2008 Mar;12(2):123-6.
26. Wortmann S, Rodenburg R, Schwahn B, Smeitink J, Morava E. Distal joint contractures, mental retardation, characteristic face and growth retardation: Chitayat syndrome revisited. Genet Couns. 2007;18(1):119-23.
27. Wortmann S, Rodenburg R, Backx A, Schmitt E, Smeitink J, Morava E. Early cardiac involvement in children carrying the A3243G mtDNA mutation. Acta Paediatr. 2007 Mar;96(3):450-1.
28. Wortmann S, Fiselier T, Van De Kar N, Aarts R, Warris A, Draaisma J. Refractory severe intestinal vasculitis due to Henoch-Schönlein purpura: successful treatment with plasmapheresis. Acta Paediatr. 2006 May;95(5):622-3.
29. Giese B, Roderburg C, Sommerauer M, Wortmann S, Metz S, Heinrich P, Müller-Newen G. Dimerization of the cytokine receptors gp130 and LIFR analysed in single cells. J Cell Sci. 2005 Nov 1;118(Pt 21):5129-40.
30. Morava E, Wortmann S, van Essen H, Liebrand van Sambeek R, Wevers R, van Diggelen O. Biochemical characteristics and increased tetraglucoside excretion in patients with phosphorylase kinase deficiency. J Inherit Metab Dis. 2005;28(5):703-6.
31. Giese B, Au-Yeung C, Herrmann A, Diefenbach S, Haan C, Küster A, Wortmann S, Roderburg C, Heinrich P, Behrmann I, Müller-Newen G. Long term association of the cytokine receptor gp130 and the Janus kinase Jak1 revealed by FRAP analysis. J Biol Chem. 2003 Oct 3;278(40):39205-13.

Thesis series of the Institute for Genetic and Metabolic Disease

Radboud University Medical Centre

1. Guillard, M. (2012). Biochemical and clinical investigations in the diagnosis of congenital disorders of glycosylation.
   Radboud University Nijmegen, Nijmegen, The Netherlands.

3. Jonckheere, A. (2013). Mitochondrial Medicine: assay development and application with special emphasis on human complex V.
   Radboud University Nijmegen, Nijmegen, The Netherlands

4. Wessels, J. (2013). Mitochondrial proteomics: method development and application.
   Radboud University Nijmegen, Nijmegen, The Netherlands

5. Vries de, H. (2012). Risk assessment of biological treatment in inflammatory bowel disease & analysis of genetic susceptibility factors.
   Radboud University Nijmegen, Nijmegen, The Netherlands

6. Brom, M. (2013). Development of a tracer to image pancreatic beta cells.
   Radboud University Nijmegen, Nijmegen, The Netherlands.

7. Schuurs-Hoeijmakers, J.H.M. (2012). Gene identification in intellectual disability.
   Radboud University Nijmegen, Nijmegen, The Netherlands.

8. Esch van, A. (2012). Genetic and clinical aspects of chronic pancreatitis.
   Radboud University Nijmegen, The Netherlands.

9. Calvaruso, M. (2013). Mitochondrial complex I assembly in man and mouse.
   Radboud University Nijmegen, The Netherlands.


IGMD
Institute for Genetic
and Metabolic Disease